Supporting Information

For

Beta-ketoacyl-ACP substrate mimics for 3-oxoacyl-ACP utilizing AHL synthases

Contents

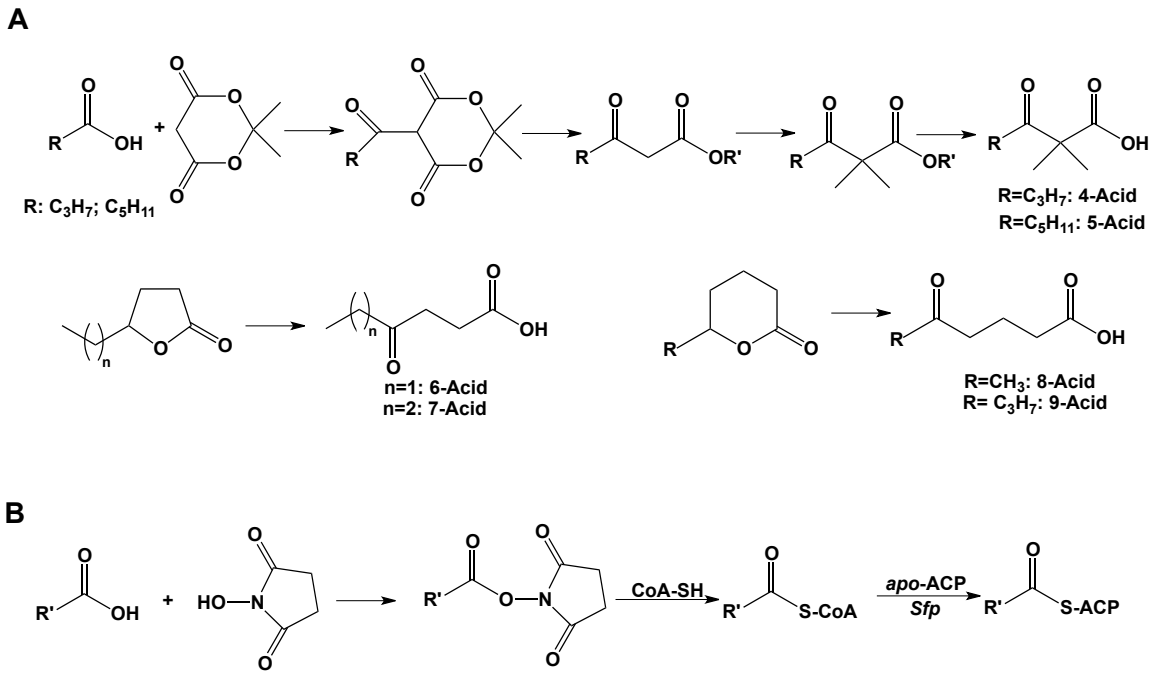

Scheme S1. Synthetic scheme for β-ketoacyl-ACP mimics. The numbers correspond to substrates listed in Figure 2 (main text). A) Synthesis of carboxylic acid starting materials used to synthesize substrates **4-9**. Meldrum's acid procedure was used to introduce the beta-keto moiety in substrate **4** and **5**. Ring opening of gamma and delta-lactones yielded the corresponding carboxylic acids for substrates **6-9**. B) General synthetic procedure for acyl-ACP synthesis. The carboxylic acids were first activated to a succinimide ester or an imidazole amide, which was coupled with CoA to synthesize acyl-CoA. *Bacillus subtilis* sfp phosphopantetheinyl transferase was used to enzymatically couple acyl-CoAs and apo-ACP to make the corresponding acyl-ACPs (**1-ACP**-**15-ACP**) described in this study.

General Information

All chemical reagents and solvents were purchased from commercial sources and used without further purification, except where indicated. The acyl-CoA compounds (**1-CoA**, **2-CoA** and **3-CoA**) were commercially available from Sigma-Aldrich. Ethyl-3-oxohexanoate was purchased from Acros Organics and used to make **4-DM-Ester**. Methyl 3-oxooctanoate was prepared according to the procedure described by D'Oca *et al.*[1] Ni^{+}-NTA resin was purchased from Qiagen. Silica gel 230-400 mesh from Fisher was used in flash column chromatography. A Thermo Scientific Evolution 260 Bio UV-Vis spectrophotometer was used to measure the concentration of analytes. HPLC data was analyzed by Chromeleon 7.2 software on a Thermo Scientific Dionex UltiMate-3000 HPLC system. Thermo Scientific Hypersil Gold C18 reverse-phase analytical UHPLC column (25002-054630) and preparative HPLC column (25005-159070) were used in acyl-ACP and acyl-CoA syntheses, respectively. Deuterated chloroform and methanol solvent were obtained commercially through Cambridge Isotope Laboratories, Inc. NMR spectra were recorded at 298 K using BRUKER AVANCE III 300 MHz and 600 MHz spectrometers. Chemical shifts were expressed in parts per million (ppm) and referenced to residual solvent as the internal reference for ^{1}H ($CDCl_3$: δ = 7.24 ppm or CD_3OD: δ = 3.31 ppm) and ^{13}C ($CDCl_3$: δ = 77.16 ppm and CD_3OD: δ = 49.00 ppm). We are grateful to the following PI's for providing plasmids for the following proteins: *Pantoea Stewartii* EsaI (Prof. Mair Churchill, University of Colorado-Denver), *Bacillus subtilis* Sfp (Prof. Michael D. Burkart, University of California-San Diego), *Yersinia pestis* YspI (Prof. E. P. Greenberg, University of Washington-Seattle) and *Escherichia coli* ACPg (Prof. John Cronan, University of Illinois-Urbana Champaign).

Experimental Procedures

General procedure for the preparation of 2,2-dimethyl β-ketoesters (4-DM-Ester and 5-DM-Ester). To a dry THF solution (60 mL) containing a suspension of NaH (1 equiv, 60% wt. dispersion in mineral oil) under a nitrogen atmosphere, was added the appropriate β-ketoester (1 equiv). The solution was stirred at room temperature until hydrogen gas evolution stopped (~30 minutes), then methyl iodide (1 equiv) was added and the solution heated to reflux for 12 h. After cooling to room temperature, additional NaH (1 equiv, 60% wt. dispersion in mineral oil) and methyl iodide (1 equiv) were added, and the solution refluxed for another 12 h. The completion of the reaction was checked using TLC (5% ethyl acetate: 95% hexane). To this solution, was added a saturated solution of ammonium chloride until all the white precipitate dissolved, which was extracted with dichloromethane (3 x 70 mL). The organic layer was separated, dried with anhydrous sodium sulfate, filtered and the solvent removed under reduced pressure. The products were purified by column chromatography on silica gel (99:1 hexanes/EtOAc).

Ethyl 2,2-dimethyl-3-oxohexanoate (4-DM-Ester).

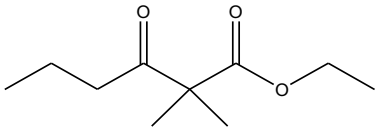

Yield from 2.0 g of ethyl-3-oxohexanoate: 2.13 g (91%). ^{1}H NMR (600 MHz, $CDCl_3$): δ 4.15 (q, J = 7.2 Hz, 2H), 2.40 (t, J = 7.2 Hz, 2H), 1.59 (sextet, J = 7.3 Hz, 2H), 1.33 (s, 6H), 1.23 (t, J = 7.1 Hz, 3H), 0.87 (t, J = 7.4 Hz, 3H).

Methyl 2,2-dimethyl-3-oxooctanoate (5-DM-Ester).

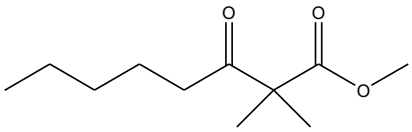

Yield from 0.714 g of methyl 3-oxooctanoate[1] : 0.6 g (72%). ^{1}H NMR (600 MHz, $CDCl_3$): δ 3.69 (s, 3H), 2.40 (t, *J* = 7.3 Hz, 2H), 1.55 (quintet, *J* = 7.5 Hz, 2H), 1.34 (s, 6H), 1.27 (sextet, *J* = 7.5 Hz, 2H), 1.24-1.18 (m, 2H), 0.86 (t, *J* = 7.2 Hz, 3H). ^{13}C NMR (600 MHz, $CDCl_3$): δ 208.3, 174.5, 55.8, 52.6, 38.1, 31.5, 23.7, 22.7, 22.2, 14.1. The NMR spectra for **5-DM-Ester** were identical to data obtained for the product by an alternate procedure.[2]

General procedure for the preparation of 2,2'-dimethyl β-ketoacids (4-Acid and 5-Acid). The appropriate 2,2-dimethyl ketoester (1 equiv) was added to a 1 N NaOH (4.3 mL) solution and stirred overnight. The aqueous solution was then washed twice with ethyl acetate (2 x 8 mL), and cooled to 0 ºC using an ice bath. 2 N HCl was added slowly to adjust the pH to 2, resulting in the formation of a cloudy solution. The workup for acids **4-Acid** and **5-Acid** differ and the details are discussed below.

2,2-Dimethyl-3-oxohexanoic acid (4-Acid).

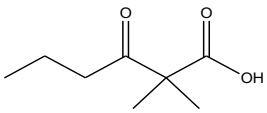

For **4-Acid**, the solution was then washed with petroleum ether (10 mL) and the aqueous phase was collected and lyophilized to afford **4-Acid** as a white solid. Yield from 0.2 g of ethyl 2,2-dimethyl-3-oxohexanoate: 0.12 g (74%). ^{1}H NMR (300 MHz, CD_3OD): δ 2.53

(t, J = 7.2 Hz, 2H), 1.59 (sextet, J = 7.3 Hz, 2H), 1.26 (s, 6H), 0.90 (t, J = 7.4 Hz, 3H). ^{13}C NMR (300 MHz, CD_3OD): δ 209.1, 175.6, 55.1, 39.3, 21.0, 16.9, 12.5.

2,2-Dimethyl-3-oxooctanoic acid (5-Acid).

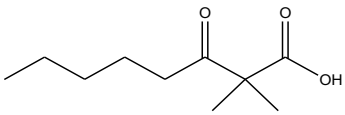

For **5-Acid**, petroleum ether (10 mL) was used to extract the product from the aqueous solution. The organic layer was collected and the solvent removed under reduced pressure to afford **5-Acid** as a white solid. Yield from 0.6 g of methyl 2,2-dimethyl-3-oxooctanoate: 0.54 g (97%). ^{1}H NMR (600 MHz, $CDCl_3$): δ 2.51 (t, J = 7.3 Hz, 2H), 1.57 (quintet, J = 7.4 Hz, 2H), 1.39 (s, 6H), 1.35-1.23 (m, 4H), 0.86 (t, J = 7.3 Hz, 3H). ^{13}C NMR (600 MHz, $CDCl_3$): δ 208.4, 178.9, 55.6, 38.2, 31.5, 23.7, 22.7, 22.3, 14.1.

General procedure for preparation of 4-oxocarboxylic acids (6-Acid and 7-Acid).

Compounds **6-Acid** and **7-Acid** were prepared similar to the protocol described by Ambrosio *et al.*[3] The appropriate alkyl-substituted γ-lactone (1 equiv) was hydrolyzed overnight with 0.5 M NaOH in EtOH (2 equiv). The solvent was removed using reduced pressure and the residue dissolved in ~40 mL of a phosphate buffer (5.5 g NaH_2PO_4 and 1.6 g Na_2HPO_4). Concentrated 10-15% NaOCl (2.4 equiv) was added and the solution stirred for 20 h at room temperature. Concentrated HCl was added to adjust the pH to 3 before the product was extracted using diethyl ether (2 x 20 mL). The organic layer was washed with brine (40 mL), dried with anhydrous $MgSO_4$, filtered and the solvent removed to afford the 4-oxocarboxylic acid.

4-Oxohexanoic acid (6-Acid).

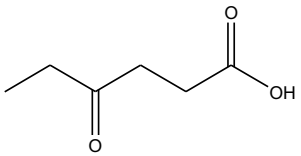

Yield from 0.24 g of γ-hexalactone: 0.21 g (81%). ^{1}H NMR (600 MHz, $CDCl_3$): δ 2.71 (t, *J* = 6.4 Hz, 2H), 2.62 (t, *J* = 6.4 Hz, 2H), 2.46 (q, *J* = 7.4 Hz, 2H), 1.06 (t, *J* = 7.4 Hz, 3H). The ^{13}C NMR spectrum for **6-Acid** was identical to data obtained for the product by Ambrosio and co-workers.[3]

4-Oxooctanoic acid (7-Acid).

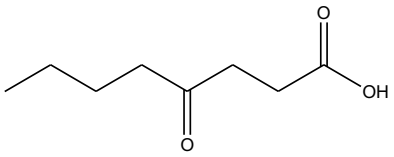

Yield from 0.50 g of γ-octalactone: 0.26 g (48%). ^{1}H NMR (300 MHz, $CDCl_3$): δ 2.69 (t, *J* = 6.2 Hz, 2H), 2.60 (t, *J* = 6.2 Hz, 2H), 2.42 (t, *J* = 7.5 Hz, 2H), 1.55 (quint, *J* = 7.5 Hz, 2H), 1.29 (sextet, *J* = 7.5 Hz, 2H), 0.88 (t, *J* = 7.3 Hz, 3H). ^{13}C NMR (300 MHz, $CDCl_3$): δ 209.3, 178.8, 42.6, 36.9, 27.9, 26.1, 22.5, 14.0.

General procedure for preparation of 5-oxocarboxylic acids (8-Acid and 9-Acid).

Compounds **8-Acid** and **9-Acid** were prepared similar to the protocol described by Ambrosio *et al.*[3] The appropriate alkyl-substituted δ-lactone (1 equiv) was hydrolyzed overnight with 0.5 M NaOH in EtOH (2 equiv). The solvent was removed using reduced pressure and the residue dissolved in ~40 mL of a phosphate buffer (5.5 g NaH_2PO_4 and

1.6 g Na_2HPO_4). Concentrated 10-15% NaOCl (2.4 equiv) was added and the solution stirred for 20 h at room temperature. Concentrated HCl was added to adjust the pH to 3 before the product was extracted using diethyl ether (2 x 20 mL). The organic layer was washed with brine (40 mL), dried with anhydrous $MgSO_4$, filtered and the solvent removed to afford the 5-oxocarboxylic acid.

5-Oxohexanoic acid (8-Acid).

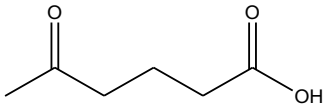

Yield from 0.104 g of δ-hexalactone: 0.15 g (29%). ^{1}H NMR (300 MHz, $CDCl_3$): δ 2.51 (t, *J* = 7.2 Hz, 2H), 2.38 (t, *J* = 7.2 Hz, 2H), 2.13 (s, 3H), 1.88 (quint, *J* = 7.2 Hz, 2H). The ^{13}C NMR spectrum for **8-Acid** was identical to data obtained for the product by Ambrosio and co-workers.[3]

5-Oxooctanoic acid (9-Acid).

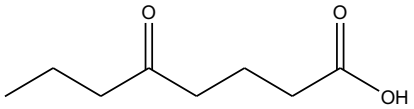

Yield from 0.11 g, 0.79 mmol) of δ-octalactone: 0.084 g (67%). ^{1}H NMR (600 MHz, $CDCl_3$): δ 2.47 (t, *J* = 7.2 Hz, 2H), 2.37 (t, *J* = 7.1 Hz, 2H), 2.36 (t, *J* = 7.2 Hz, 2H), 1.88 (quint, *J* = 7.2 Hz, 2H), 1.58 (sextet, *J* = 7.4 Hz, 2H), 0.88 (t, *J* = 7.4 Hz, 3H). ^{13}C NMR (600 MHz, $CDCl_3$): δ 210.5, 178.8, 45.0, 41.5, 33.1, 18.8, 17.5, 13.9.

General Procedure for the preparation of *N*-hydroxysuccinimide esters (4-Succ – 15-Succ). To a 1,4-dioxane (3 mL) solution of the appropriate carboxylic acid (1 equiv), *N*-hydroxysuccinimide (1 equiv) and *N,N'*-dicyclohexylcarbodiimide (1 equiv) were added and stirred for 24 hours. Diethyl ether (2 mL) was added to the reaction mixture and the white cloudy solution was filtered through Celite and the solvent removed under reduced pressure. Warm methanol (2 mL) was used to dissolve the residue and, upon precipitation of the urea by-product upon cooling to room temperature, the solution was filtered through Celite and the solvent removed. The residue was then titurated with 1,4-dioxane (3 mL), filtered with Celite and the filtrate collected and the solvent removed under reduced pressure to give the product.

2,2-Dimethyl-3-oxohexanoyl *N*-hydroxysuccinimide ester (4-Succ).

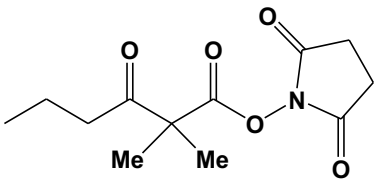

Further purification by column chromatography on silica gel (1:1 hexanes/EtOAc) was necessary. Yield from 0.15 g of 2,2-dimethyl-3-oxohexanoic acid: 0.062 g (26%). ^{1}H NMR (600 MHz, $CDCl_3$): δ 2.81 (d, J = 6.5 Hz, 4H), 2.64 (t, J = 7.1 Hz, 2H), 1.63 (sextet, J = 7.3 Hz, 2H), 1.48 (s, 6H), 0.89 (t, J = 7.4 Hz, 3H). ^{13}C NMR (600 MHz, $CDCl_3$): δ 205.5, 169.7, 168.9, 54.7, 40.3, 25.6, 22.1, 17.3, 13.6. HRMS (ESI-TOF) *m/z* calculated for $[M+Na]^+$: 278.0999, observed: 278.1107.

2,2-Dimethyl-3-oxooctanoyl *N*-hydroxysuccinimide ester (5-Succ).

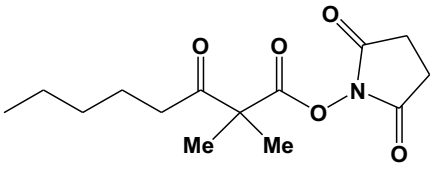

Further purification by column chromatography on silica gel (1:1 hexanes/EtOAc) was necessary. Yield from 0.027 g of 2,2-dimethyl-3-oxooctanoic acid: 0.035 g (83%). ^{1}H NMR (600 MHz, $CDCl_3$): δ 2.81 (d, J = 6.1 Hz, 4H), 2.65 (t, J = 7.3 Hz, 2H), 1.59 (quint, J = 7.4 Hz, 2H), 1.48 (s, 6H), 1.32-1.21 (m, 4H), 0.85 (t, J = 7.1 Hz, 3H). ^{13}C NMR (600 MHz, $CDCl_3$): δ 205.6, 169.7, 168.9, 54.7, 38.5, 31.3, 25.8, 23.5, 22.6, 22.2, 14.1. HRMS (ESI-TOF) *m/z* calculated for $[M+Na]^+$: 306.1312, observed: 306.1333.

4-Oxohexanoyl *N*-hydroxysuccinimide ester (6-Succ).

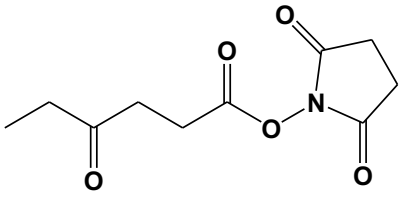

Yield from 0.21 g of 4-oxohexanoic acid: 0.15 g (41%). ^{1}H NMR (600 MHz, $CDCl_3$): δ 2.89 (t, J = 6.4 Hz, 2H), 2.84 (t, J = 6.4 Hz, 2H), 2.82 (d, J = 6.5 Hz, 4H), 2.47 (q, J = 7.3 Hz, 2H), 1.07 (t, J = 7.3 Hz, 3H). ^{13}C NMR (600 MHz, $CDCl_3$): δ 207.9, 169.2, 168.5, 36.4, 35.9, 25.8, 25.3, 7.9. HRMS (ESI-TOF) *m/z* calculated for $[M+Na]^+$: 250.0686, observed: 250.0700.

4-Oxooctanoyl *N*-hydroxysuccinimide ester (7-Succ).

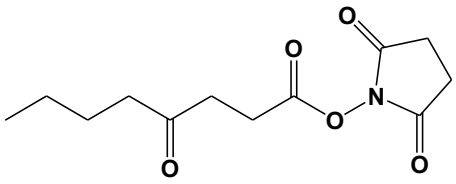

Yield from 0.078 g of 4-oxooctanoic acid: 0.11 g (88%). ^{1}H NMR (300 MHz, $CDCl_3$): δ 2.90-2.75 (m, 4H), 2.79 (s, 4H), 2.42 (t, *J* = 7.4 Hz, 2H), 1.54 (quint, *J* = 7.5 Hz, 2H), 1.27 (sextet, *J* = 7.5 Hz, 2H), 0.86 (t, *J* = 7.3 Hz, 3H). ^{13}C NMR (300 MHz, $CDCl_3$): δ 207.6, 169.2, 168.4, 42.5, 36.8, 26.0, 25.7, 25.2, 22.4, 13.9. HRMS (ESI-TOF) *m/z* calculated for $[M+Na]^+$: 278.0999, observed: 278.1009.

5-Oxohexanoyl *N*-hydroxysuccinimide ester (8-Succ).

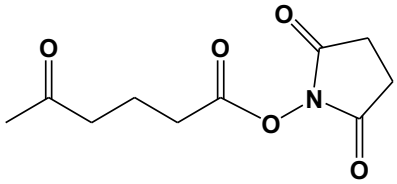

Yield from 0.15 g of 5-oxohexanoic acid: 0.15 g (56%). ^{1}H NMR (600 MHz, $CDCl_3$): δ 2.82 (s, 4H), 2.64 (t, *J* = 7.1 Hz, 2H), 2.59 (t, *J* = 7.1 Hz, 2H), 2.14 (s, 3H), 1.98 (quint, *J* = 7.1 Hz, 2H). ^{13}C NMR (600 MHz, $CDCl_3$): δ 207.6, 169.3, 168.5, 41.7, 30.2, 30.1, 25.8, 18.7. HRMS (ESI-TOF) *m/z* calculated for $[M+Na]^+$: 250.0686, observed: 250.0700.

5-Oxooctanoyl *N*-hydroxysuccinimide ester (9-Succ).

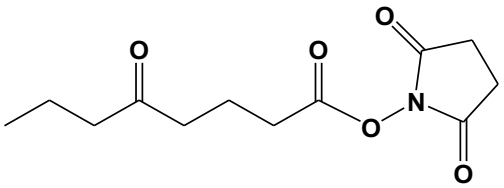

Yield from 0.028 g of 5-oxooctanoic acid: 0.038 g, (84%). ^{1}H NMR (600 MHz, $CDCl_3$): δ 2.81 (s, 4H), 2.64 (t, *J* = 7.1 Hz, 2H), 2.55 (t, *J* = 7.1 Hz, 2H), 2.37 (t, *J* = 7.4 Hz, 2H), 1.99 (quint, *J* = 7.1 Hz, 2H), 1.66-1.48 (m, 2H), 0.89 (t, *J* = 7.4 Hz, 3H). ^{13}C NMR (600 MHz, $CDCl_3$): δ 209.7, 169.0, 168.3, 44.8, 40.5, 30.0, 25.6, 18.6, 17.3, 13.7. HRMS (ESI-TOF) *m/z* calculated for $[M+Na]^+$: 278.0999, observed: 278.1012.

2-Furanacetyl *N*-hydroxysuccinimide ester (10-Succ).

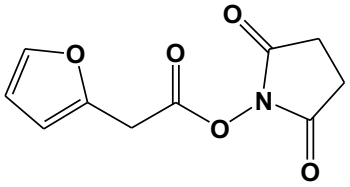

Yield from 0.20 g of 2-furanacetic acid: 0.19 g (54%). ^{1}H NMR (300 MHz, $CDCl_3$) δ 7.38 (t, *J* = 1.3 Hz, 1H), 6.38-6.32 (m, 2H), 3.99 (s, 2 H), 2.82 (s, 4H). ^{13}C NMR (300 MHz, $CDCl_3$): δ 169.0, 164.8, 144.9, 142.9, 110.9, 109.4, 31.1, 25.8. HRMS (ESI-TOF) *m/z* calculated for $[M+Na]^+$: 246.0373, observed: 246.0389.

2-Tetrahydrofuranacetyl *N*-hydroxysuccinimide ester (11-Succ).

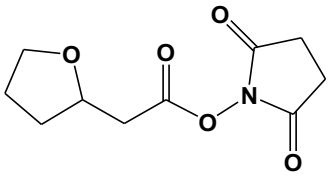

Yield from 0.043 g of 2-tetrahydrofuranylacetic acid: 0.050 g (62%). ^{1}H NMR (600 MHz, $CDCl_3$): δ 4.30 (quint, *J* = 6.7 Hz, 1H), 3.89 (dt, *J* = 8.3, 6.8 Hz, 1H), 3.77 (dt, *J* = 8.3, 6.8 Hz, 1H), 2.90 (dd, *J* = 15.4, 6.4 Hz, 1H), 2.82 (s, 4H), 2.74 (dd, *J* = 15.4, 6.7 Hz, 1H), 2.22-2.09 (m, 1H), 2.01-1.84 (m, 2H), 1.75-1.56 (m, 1H). ^{13}C NMR (600 MHz, $CDCl_3$): δ 169.1, 166.4, 74.8, 68.5, 37.6, 31.4, 25.8, 25.8. HRMS (ESI-TOF) *m/z* calculated for $[M+Na]^+$: 250.0686, observed: 250.0709.

2-Thiopheneacetyl *N*-hydroxysuccinimide ester (12-Succ).

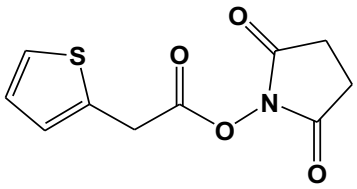

Yield from 0.20 g of 2-thiopheneacetic acid: 0.27 g (82%). ^{1}H NMR (300 MHz, $CDCl_3$): δ 7.25 (dd, *J* = 5.2, 1.2 Hz, 1H), 7.05 (dd, *J* = 3.5, 1.1 Hz, 1H), 6.97 (dd, *J* = 5.2, 3.5 Hz, 1H), 4.14 (s, 2H), 2.82 (s, 4H). ^{13}C NMR (300 MHz, $CDCl_3$): δ 169.0, 165.9, 131.9, 128.1, 127.3, 126.0, 32.2, 25.8. HRMS (ESI-TOF) *m/z* calculated for $[M+Na]^+$: 262.0145, observed: 262.0276.

2-Pyridylacetyl *N*-hydroxysuccinimide ester (13-Succ).

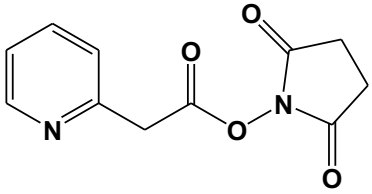

Further purification by column chromatography on silica gel (1:1 hexanes/EtOAc to 1:3 hexanes/EtOAc gradient) was necessary. Yield from 0.50 g of 2-pyridylacetic acid: 0.23 g (29%). ^{1}H NMR (600 MHz, $CDCl_3$): δ 8.55 (ddd, J = 4.7, 1.7, 1.0 Hz, 1H), 7.67 (td, J = 7.7, 1.8 Hz, 1H), 7.37 (dt, J = 7.8, 1.0 Hz, 1H), 7.20 (ddd, J =7.6, 4.9, 1.0 Hz, 1H), 4.12 (s, 2H), 2.79 (s, 4H). ^{13}C NMR (600 MHz, $CDCl_3$): δ 168.9, 165.9, 152.0, 149.7, 137.1, 123.8, 122.8, 40.4, 25.6. HRMS (ESI-TOF) *m/z* calculated for $[M+Na]^+$: 257.0533, observed: 257.0500.

2-Furoyl *N*-hydroxysuccinimide ester (14-Succ).

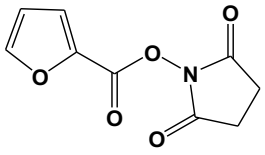

Yield from 0.50 g of 2-furoic acid: 0.71 g (76%). ^{1}H NMR (600 MHz, $CDCl_3$): δ 7.71 (dd, J = 1.7, 0.7 Hz, 1H), 7.47 (dd, J = 3.7, 0.7 Hz, 1H), 6.61 (dd, J = 3.7, 1.7 Hz, 1H), 2.89 (s, 4H). ^{13}C NMR (600 MHz, $CDCl_3$): δ 169.2, 153.7, 148.9, 139.9, 122.4, 112.8, 25.8. HRMS (ESI-TOF) *m/z* calculated for $[M+Na]^+$: 232.0216, observed: 232.0249.

General preparation of acyl-CoA compounds (1-CoA – 14-CoA). Under inert conditions, the appropriate acyl-*N*-hydroxysuccinimide ester (0.2 mmol, 2 equiv) was dissolved in a mixture consisting of water/dimethylformamide (1:1, 3 mL). K_2CO_3 was added to adjust the pH of the solution to 8-9. To this reaction mixture, free CoA (0.1 mmol, 1 equiv) was added with gentle mixing. The reaction was stirred at room temperature overnight under a nitrogen atmosphere. The reaction mixture was washed twice with diethyl ether (2 x 3 mL) to remove any organic contaminants. The aqueous layer was collected and filtered through a 0.22 μm centrifugal spin filter. Acyl-CoA was purified by a preparative C-18 reverse-phase HPLC with gradient beginning at 95% buffer B (25 mM ammonium acetate, pH 5) and ending at 95% solvent D (acetonitrile + 0.1% TFA) at a flow rate of 3 mL/min over a period of 25 minutes.

Mass determination of acyl-CoA compounds (4-CoA – 14-CoA). Acyl-CoA compounds **4-CoA – 14-CoA** were characterized on an ultra-high resolution Bruker maXis Quadrupole Time of Flight (QTOF) instrument using direct injection to the MS. The ESI source was operated under the following conditions: positive ion mode, nebulizer pressure: 0.4 Bar; flow rate of drying gas (N_2): 4L/min; drying gas temperature: 200 ºC; voltage between HV capillary and HV end-plate offset: 3000 V to -500 V; and the quadrupole ion energy was 4.0 eV. Sodium formate was used to calibrate the system in the mass range. All MS data was analyzed using the Compass Data Analysis software package (Bruker Corporation, Billerica, Massachusetts).

2,2-Dimethyl-3-oxohexanoyl-CoA (4-CoA): HRMS (ESI-TOF) *m/z* calculated for $[M+H]^+$: 908.2062, observed: 908.2022.

2,2-Dimethyl-3-oxooctanoyl-CoA (5-CoA): HRMS (ESI-TOF) *m/z* calculated for $[M+H]^+$: 936.2375, observed: 936.2399.

4-Oxohexanoyl-CoA (6-CoA): HRMS (ESI-TOF) *m/z* calculated for $[M+H]^+$: 879.1671, observed: 879.1881.

4-Oxooctanoyl-CoA (7-CoA): HRMS (ESI-TOF) *m/z* calculated for $[M+H]^+$: 907.1984, observed: 907.1887.

5-Oxohexanoyl-CoA (8-CoA): HRMS (ESI-TOF) *m/z* calculated for $[M+H]^+$: 879.1671, observed: 879.1877.

5-Oxooctanoyl-CoA (9-CoA): HRMS (ESI-TOF) *m/z* calculated for $[M+H]^+$: 907.1984, observed: 907.1878.

2-Furanacetyl-CoA (10-CoA): HRMS (ESI-TOF) *m/z* calculated for $[M+H]^+$: 876.1436, observed: 876.1451.

2-Tetrahydrofuranacetyl-CoA (11-CoA): HRMS (ESI-TOF) *m/z* calculated for $[M+H]^+$: 880.1749, observed: 880.1721.

2-Thiopheneacetyl-CoA (12-CoA): HRMS (ESI-TOF) *m/z* calculated for $[M+H]^+$: 892.1208, observed: 892.1194.

2-Pyridylacetyl-CoA (13-CoA): HRMS (ESI-TOF) *m/z* calculated for $[M+H]^+$: 887.1596, observed: 888.0821.

2-Furoyl-CoA (14-CoA): HRMS (ESI-TOF) *m/z* calculated for $[M+H]^+$: 862.1280, observed: 862.1309.

Preparation of 2-Benzofuranacetyl-CoA (15-CoA). To a solution of acetonitrile (3 mL) at -5 ºC, 2-benzofuranacetic acid (10 mg, 0.057 mmol) and 1,1′-carbonyldiimidazole (12 mg, 0.073 mmol) were added. The reaction mixture was stirred at below 0 ºC for 1.5 hours. In a separate flask containing a 1:1 acetonitrile:water solution (2 mL), free CoA (22 mg, 0.037 mmol) was dissolved under a nitrogen atmosphere. The reaction mixture containing the 2-benzofuranacetic acid and 1,1′-carbonyldiimidazole was transferred into the free CoA solution and continued to stir under nitrogen for another 3-5 hours at 0 ºC. The crude product was collected and filtered through a 0.22 μm centrifugal spin filter. Benzofuranacetyl-CoA was purified by a preparative C-18 reverse-phase HPLC with gradient beginning at 95% buffer B (25 mM ammonium acetate, pH 5) and ending at 95% solvent D (acetonitrile + 0.1% TFA) at flow rate of 3 mL/min over a period of 25 minutes. HRMS (ESI-TOF) *m/z* calculated for $[M+H]^+$: 926.1593, observed: 926.1626.

General preparation of acyl-ACP compounds (1-ACP – 15-ACP). Acyl-ACP compounds **1-ACP** – **15-ACP** can be synthesized by enzymatic modification of apo-ACP with acyl-CoA analogs **1-CoA** – **15-CoA** using phosphopantheinyl transferase, *B. subtilis* Sfp. The reaction mixture contained nanopure water, 50 mM Tris-HCl, pH 6.8, 10 mM $MgCl_2$, apo-ACP (1 equiv), acyl-CoA (1.25 equiv), and 3 μM Sfp. The appropriate acyl-CoA was added in three portions over 15 minute intervals. The reaction was incubated at 37 °C and the reaction monitored by removing and adding 10 μL aliquots to 90 μL nanopure water and monitoring the reaction progress using analytical C-18 reverse-phase UHPLC. Acyl-ACP separation using UHPLC began with 75% solvent A (99.9% H_2O + 0.1% TFA) and 25% solvent D (99.9% acetonitrile + 0.1% TFA), and ended with 25% solvent A and 75% solvent D over a period of 10 minutes at flow rate of 600 μL/min. The reaction time varied from 1 hour to 4 hours. Once the reaction went to completion, ammonium sulfate was added to the reaction mixture to 75% saturation to precipitate out Sfp. After at least 1 hour of stirring at 4 °C, the reaction solution was centrifuged to pellet out Sfp at 13,000 xg for 15 minutes. The clear supernatant containing acyl-ACP solution was desalted and concentrated by multiple washes with nanopure water and then 10 mM MES, pH 6 + 20% glycerol buffer using a 3 kD molecular cutoff spin filter column. Concentration of acyl-ACP was determined using UV-Vis (ε_{280} = 1490 M^{-1} cm^{-1}).

Mass determination of Acyl-ACP proteins. Molecular mass of ACP and its derivatives were determined by high performance liquid chromatography mass spectrometry (HPLC-MS) using an ultra-high resolution Quadrupole Time of Flight (QTOF) instrument (Bruker maXis, Bruker Corporation, Billerica, Massachusetts). The electrospray ionization (ESI) source was operated under the following conditions: positive ion mode; nebulizer pressure: 1.2 Bar; flow rate of drying gas (N2): 8 L/min; drying gas temperature: 200 °C; voltage between HV capillary and HV end-plate offset: 3000 V to −500 V; and the quadrupole ion energy was 4.0 eV. Low concentration ESI tuning mix (Agilent Technologies, Santa Clara, California) was used to calibrate the system in the mass range. HPLC separation was achieved using a Dionex UltiMate® 3000 uHPLC system (Dionex Corporation, Sunnyvale, California). Ten microliter of samples were injected onto a Phenomenex Kinetex XB-C18 column (100 x 2.1 mm, 2.6μm) (Phenomenex Corporation, Torrance, California) at a flow rate of 0.3 mL/min followed by a simple linear gradient for sample desalting and separation. The initial eluent was 98% mobile phase A (99.9% water, 0.1% formic acid) and 2% B (99.9% acetonitrile, 0.1% formic acid) for 5 min and then mobile phase B was increased to 50% in 25 min. LC eluent was diverted to the waste during the first five minutes of the gradient to eliminate salts in the sample buffer. The obtained mass spectra were deconvoluted using Bruker Data Analysis 4.0 software to determine the charge state (N) of the protein ions. To calculate the molecular mass of ACP and its derivatives, the measured *m/z* values were multiplied by the corresponding charge state (N) of the protein ions and subtracted by the mass of N protons (N x 1.0079).

Apo-ACP: calculated mass: 8508.1636 Da, observed: 8508.2138 Da.

Hexanoyl-ACP (1-ACP): calculated mass: 8946.8127 Da, observed: 8946.5601 Da.

Octanoyl-ACP (2-ACP): calculated mass: 8974.8667 Da, observed: 8974.5376 Da.

Decanoyl-ACP (3-ACP): calculated mass: 9002.3857 Da, observed mass: 9002.3736 Da.

2,2-Dimethyl-3-oxohexanoyl-ACP (4-ACP): calculated mass: 8988.6773 Da, observed: 8988.9023 Da.

2,2-Dimethyl-3-oxooctanoyl-ACP (5-ACP): calculated mass: 9017.3746 Da, observed: 9017.3185 Da.

4-Oxohexanoyl-ACP (6-ACP): calculated mass: 8960.3228 Da, observed: 8960.4226 Da.

4-Oxooctanoyl-ACP (7-ACP): calculated mass: 8988.3234 Da, observed: 8988.3352 Da.

5-Oxohexanoyl-ACP (8-ACP): calculated mass: 8961.3224 Da, observed: 8960.6268 Da.

5-Oxooctanoyl-ACP (9-ACP): calculated mass: 8988.3225 Da, observed: 8988.4745 Da.

2-Furanacetyl-ACP (10-ACP): calculated mass: 8957.2798 Da, observed: 8957.6844 Da.

2-Tetrahydrofuranacetyl-ACP (11-ACP): calculated mass: 8961.3068 Da, observed: 8961.2978 Da.

2-Thiopheneacetyl-ACP (12-ACP): calculated mass: 8972.5905 Da, observed: 8972.5293 Da.

2-Pyridylacetyl-ACP (13-ACP): calculated mass: 8969.2168 Da, observed: 8969.1140 Da.

2-Furoyl-ACP (14-ACP): calculated mass: 8942.6020 Da, observed: 8942.5198 Da.

2-Benzofuranacetyl-ACP (15-ACP): calculated mass: 9006.2867 Da, observed mass: 9006.0533 Da.

NMR Characterization of Compounds (^{1}H and ^{13}C NMR Spectra)

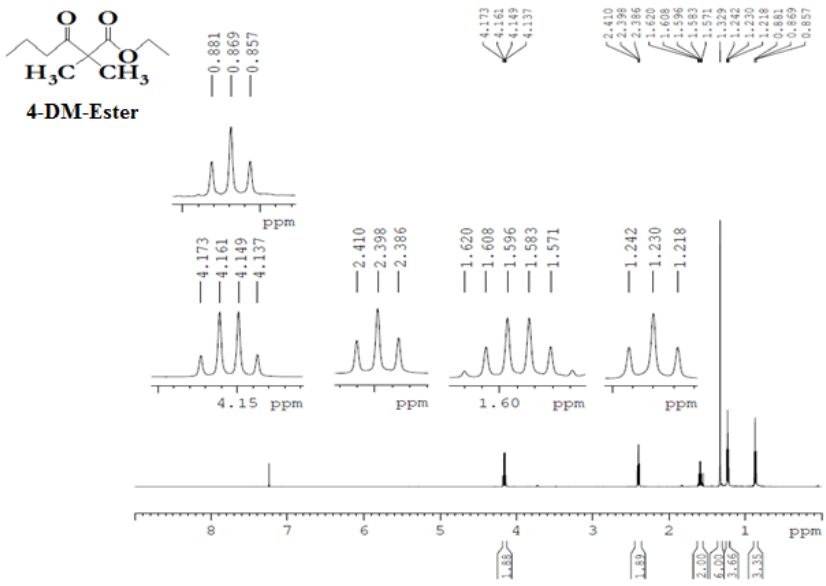

Fig. S1 ^{1}H NMR of **4-DM-Ester** in $CDCl_3$.

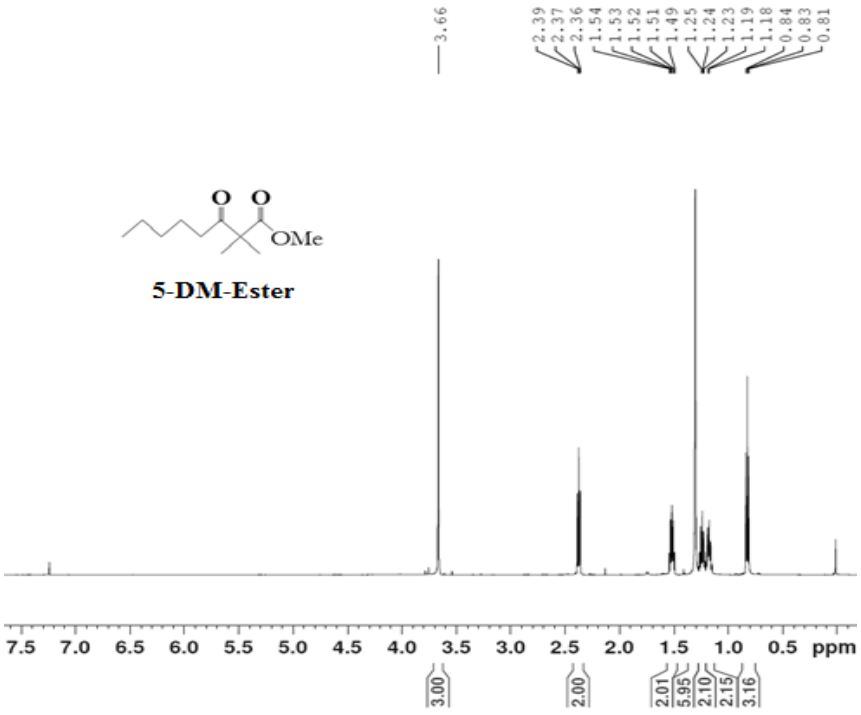

Fig. S2 ^{1}H NMR of **5-DM-Ester** in $CDCl_3$.

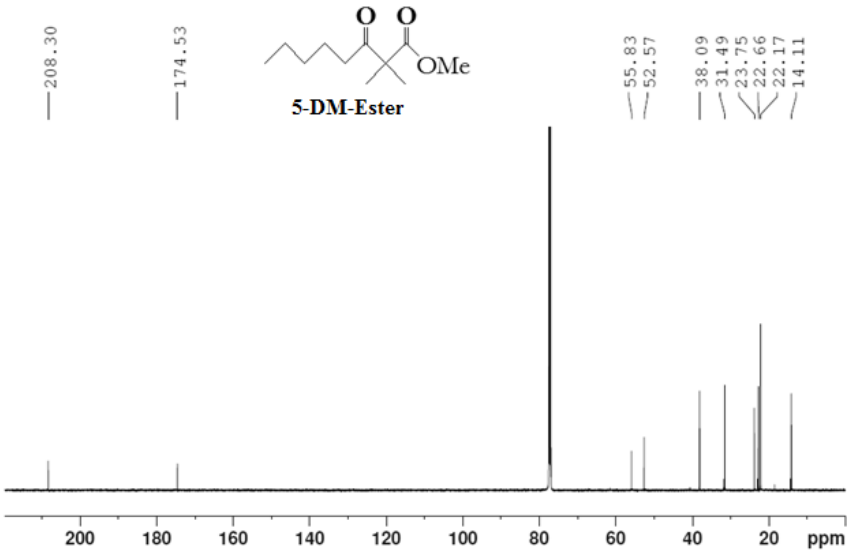

Fig. S3 ^{13}C NMR of **5-DM-Ester** in $CDCl_3$.

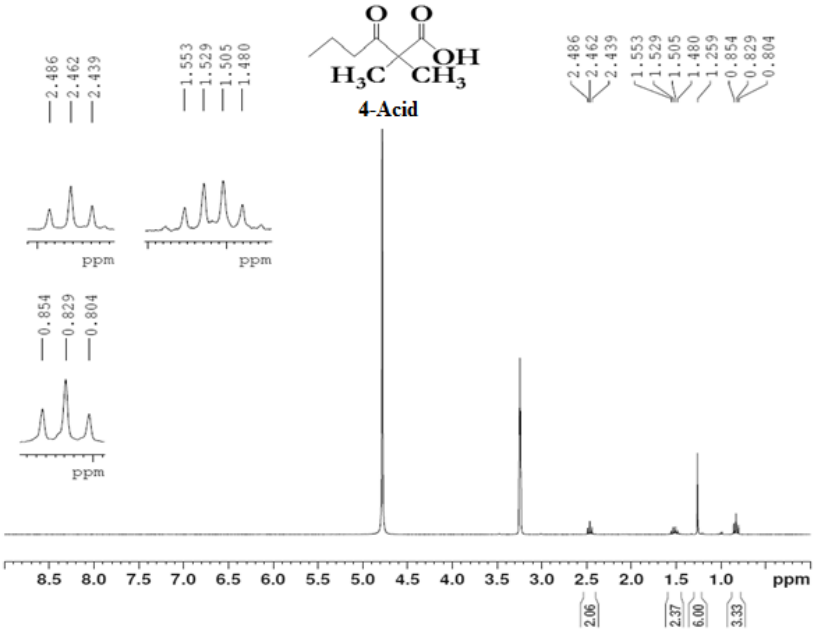

Fig. S4 ^{1}H NMR of **4-Acid** in CD_3OD.

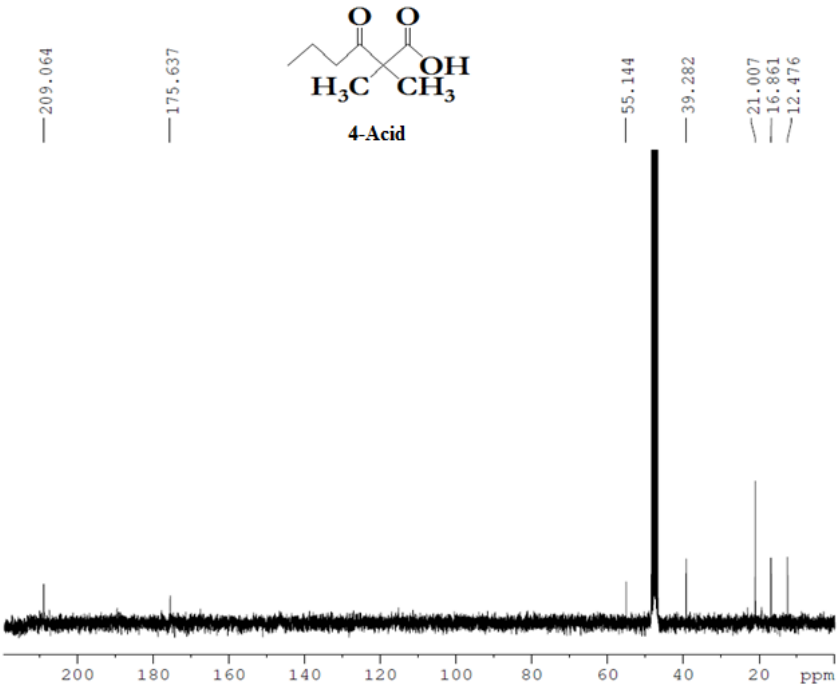

Fig. S5 ^{13}C NMR of **4-Acid** in CD_3OD.

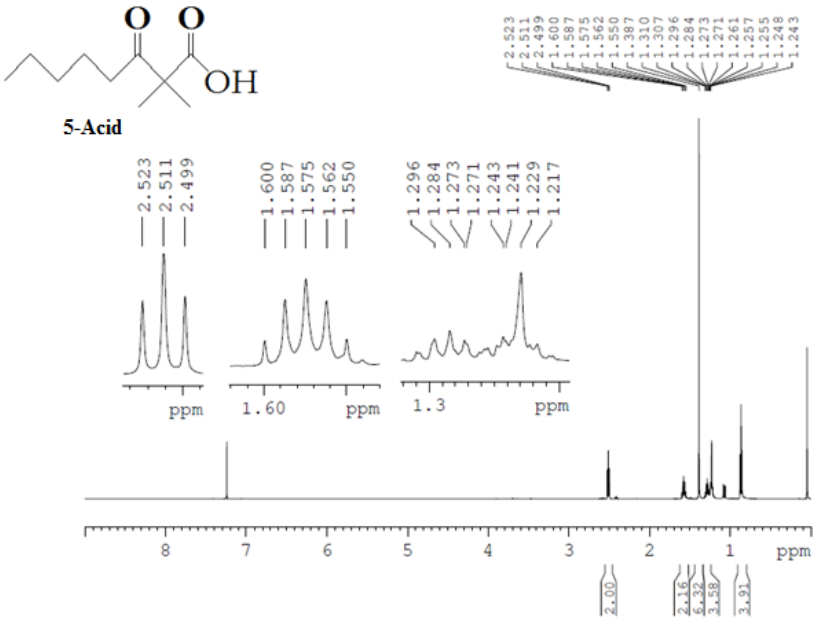

Fig. S6 ^{1}H NMR of **5-Acid** in $CDCl_3$.

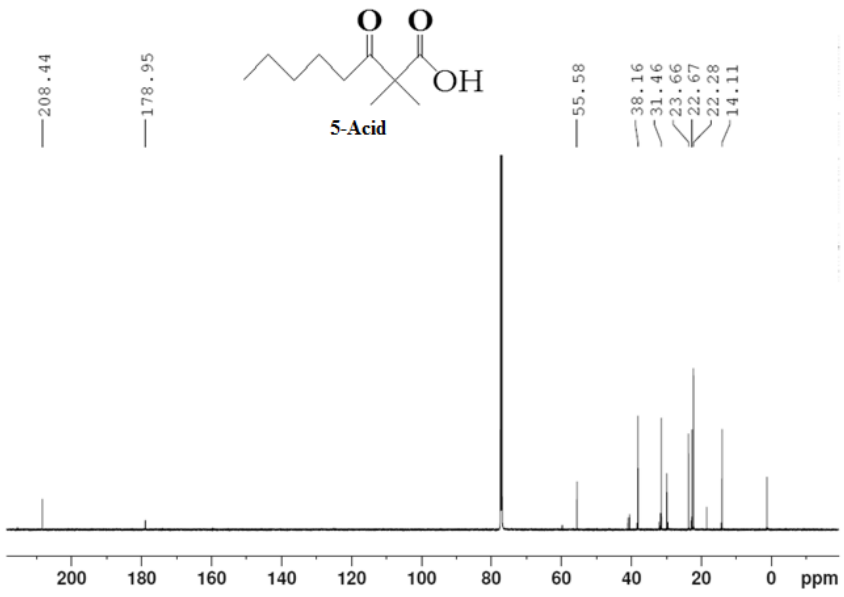

Fig. S7 ^{13}C NMR of **5-Acid** in $CDCl_3$.

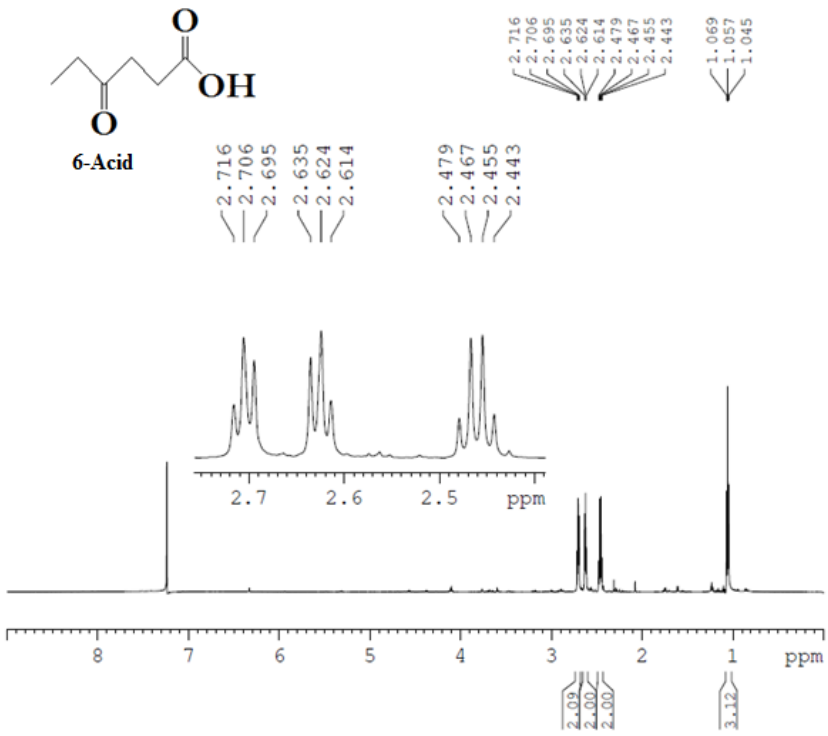

Fig. S8 ^{1}H NMR of **6-Acid** in $CDCl_3$.

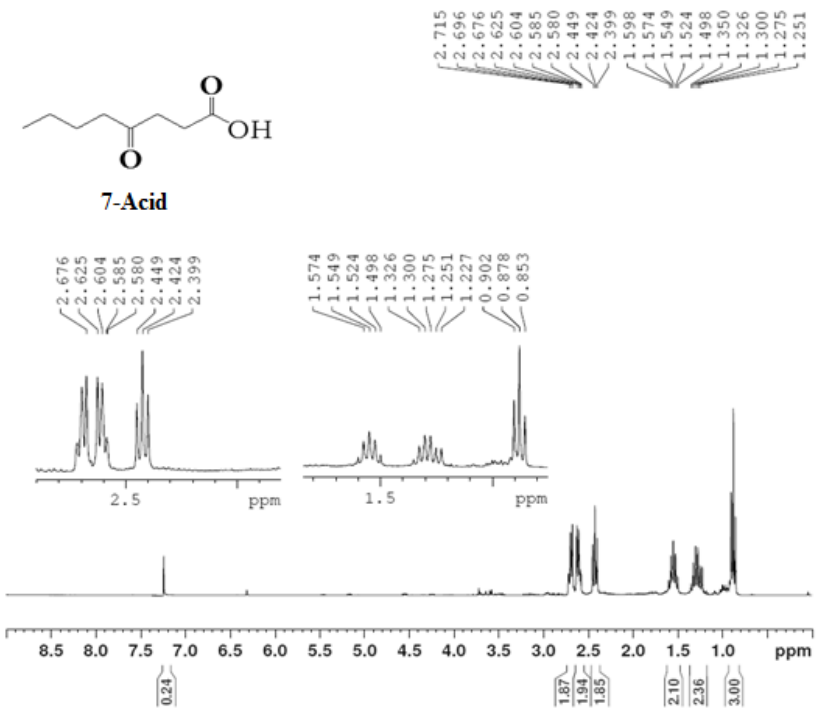

Fig. S9 ^{1}H NMR of **7-Acid** in $CDCl_3$.

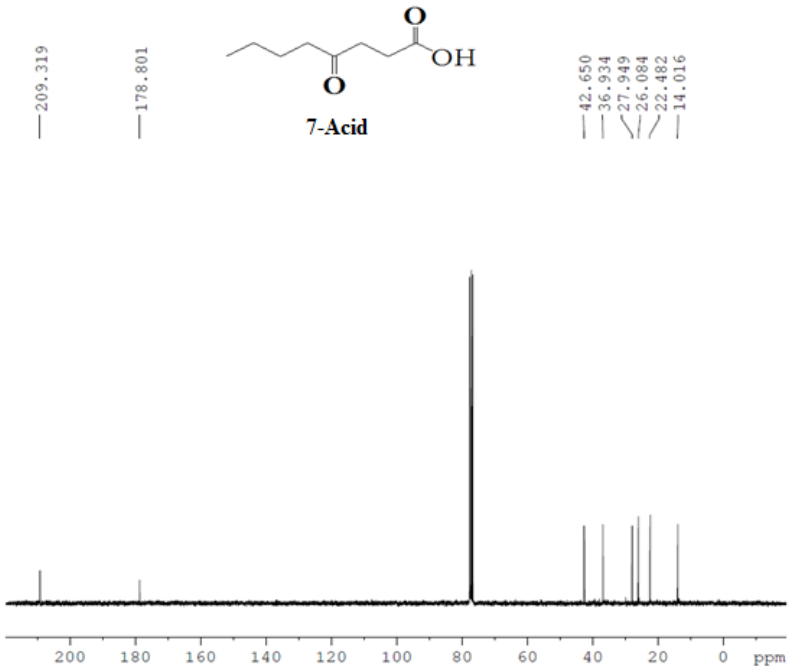

Fig. S10 ^{13}C NMR of **7-Acid** in $CDCl_3$.

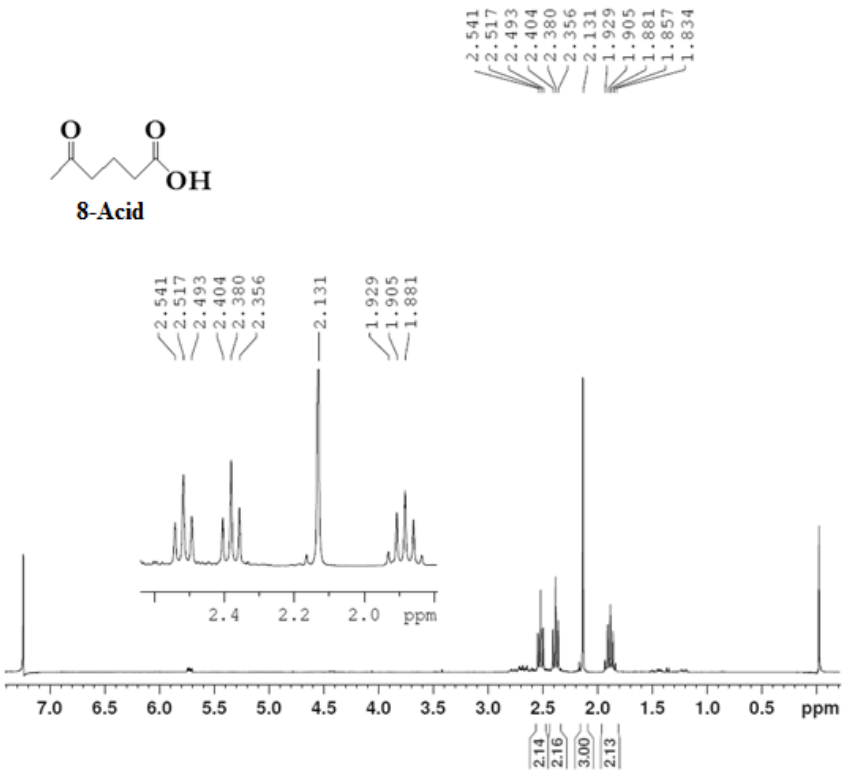

Fig. S11 ^{1}H NMR of **8-Acid** in $CDCl_3$.

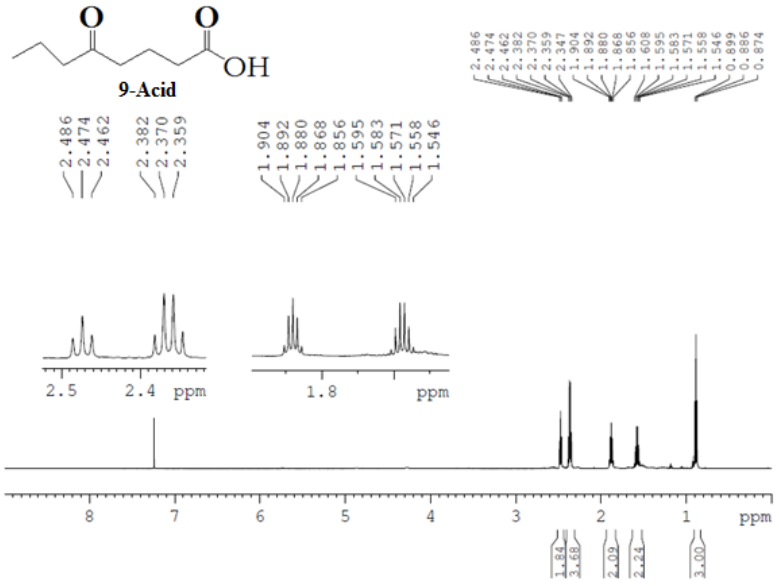

Fig. S12 ^{1}H NMR of **9-Acid** in $CDCl_3$.

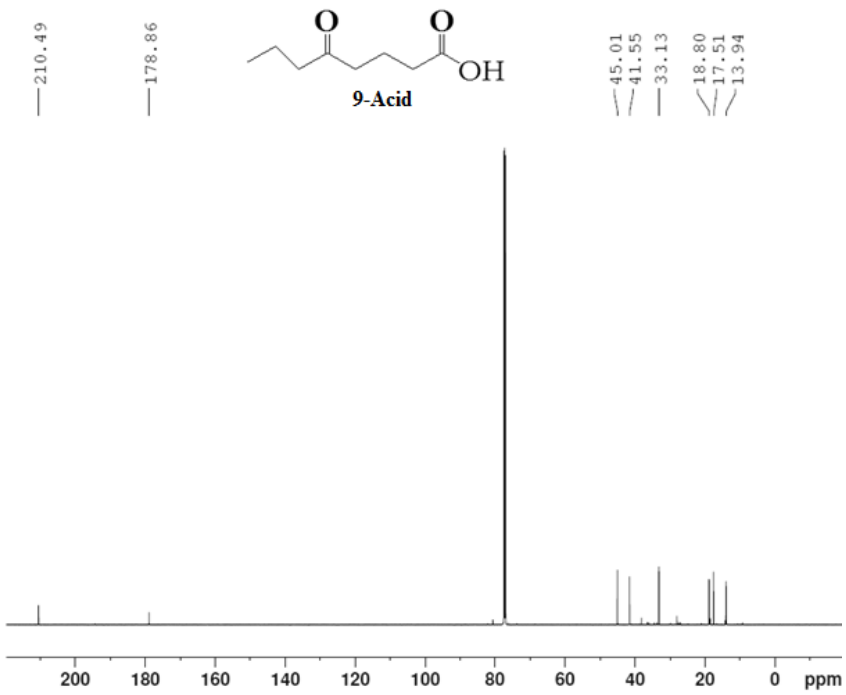

Fig. S13 ^{13}C NMR of **9-Acid** in $CDCl_3$.

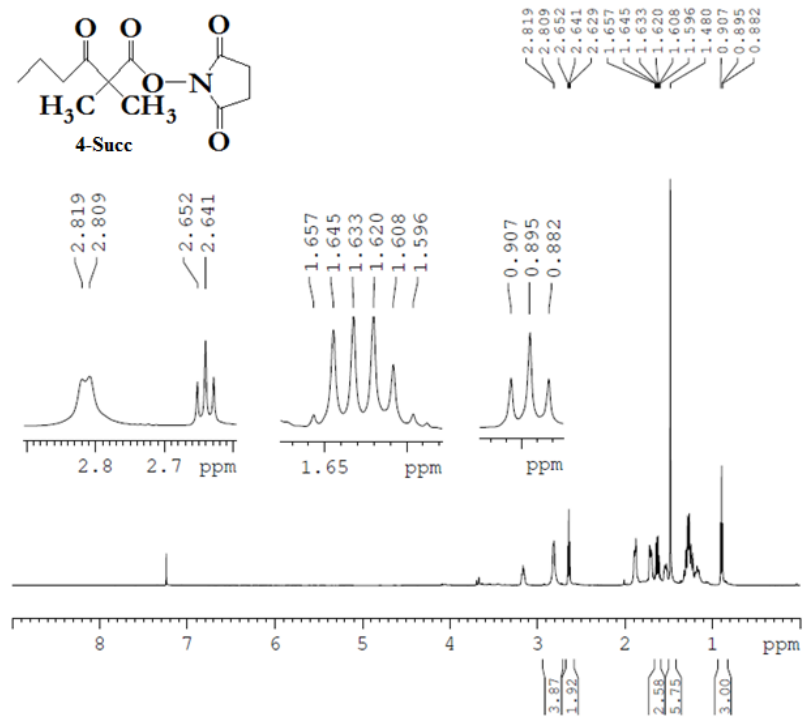

Fig. S14 ^{1}H NMR of **4-Succ** in $CDCl_3$.

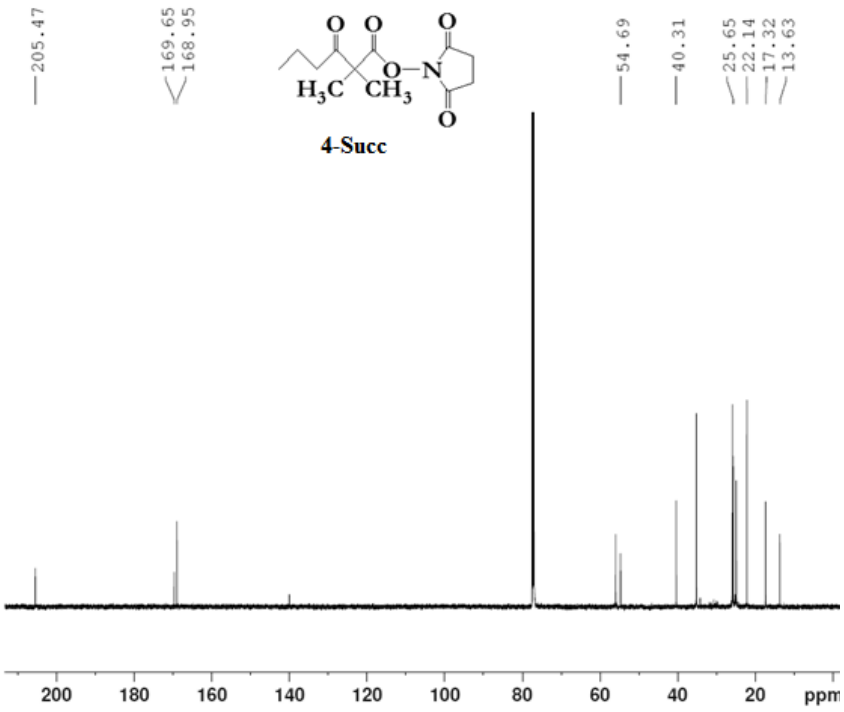

Fig. S15 ^{13}C NMR of **4-Succ** in $CDCl_3$.

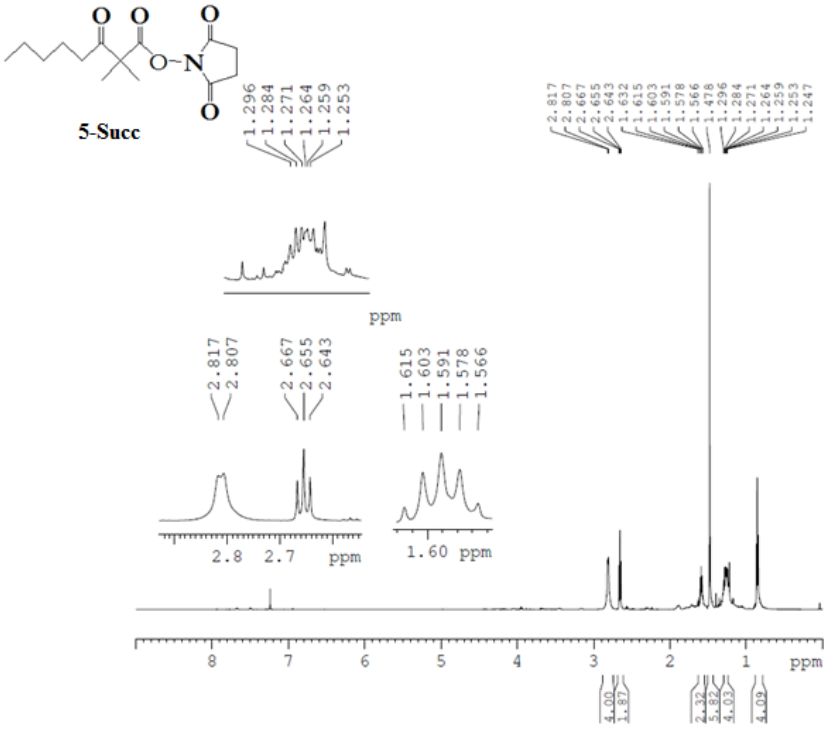

Fig. S16 ^{1}H NMR of **5-Succ** in $CDCl_3$.

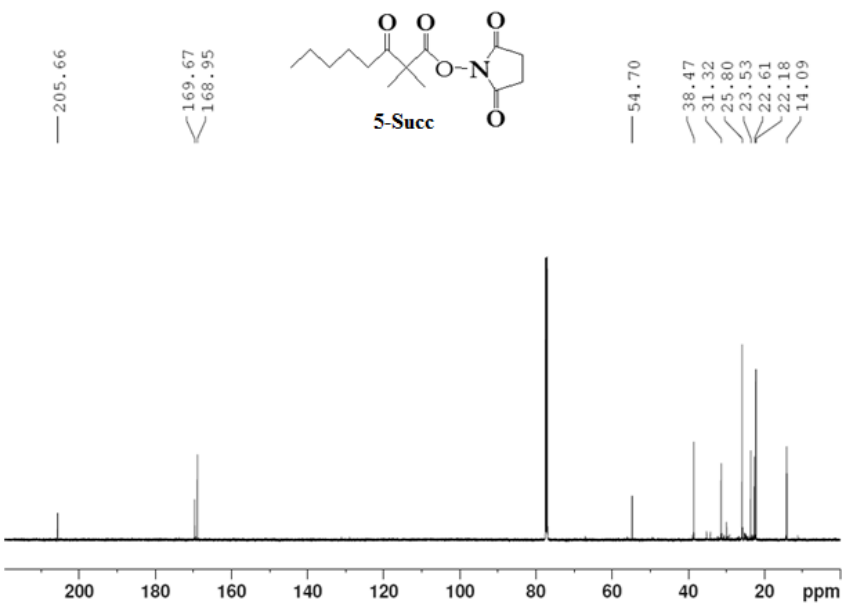

Fig. S17 ^{13}C NMR of **5-Succ** in $CDCl_3$.

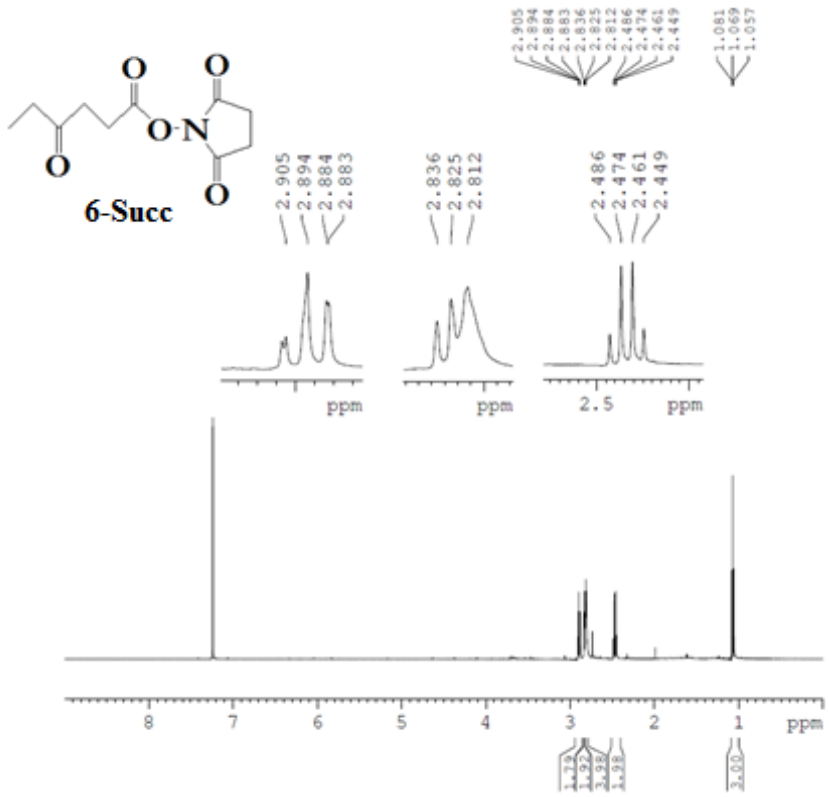

Fig. S18 ^{1}H NMR of **6-Succ** in $CDCl_3$.

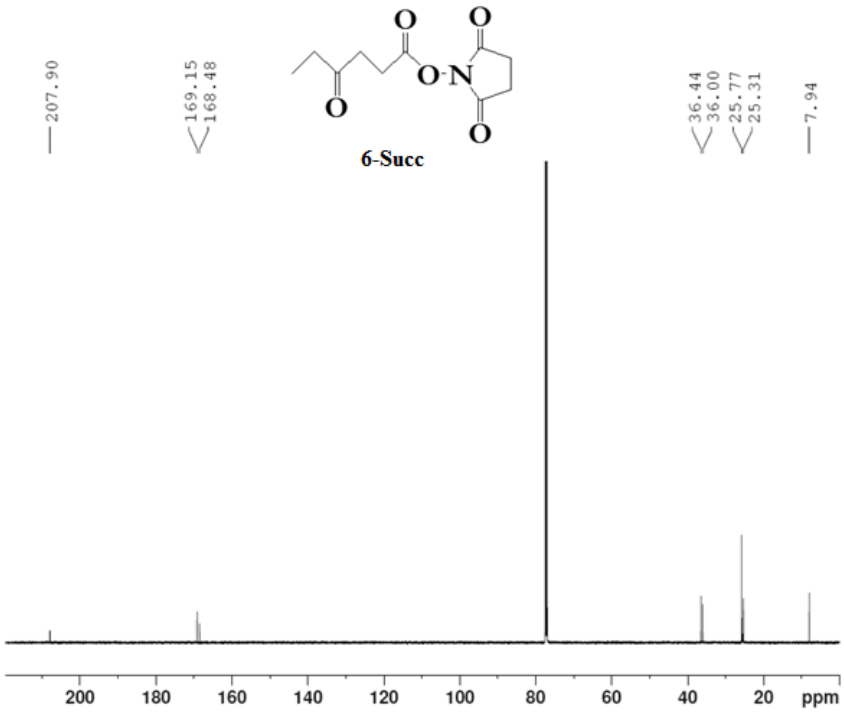

Fig. S19 ^{13}C NMR of **6-Succ** in $CDCl_3$.

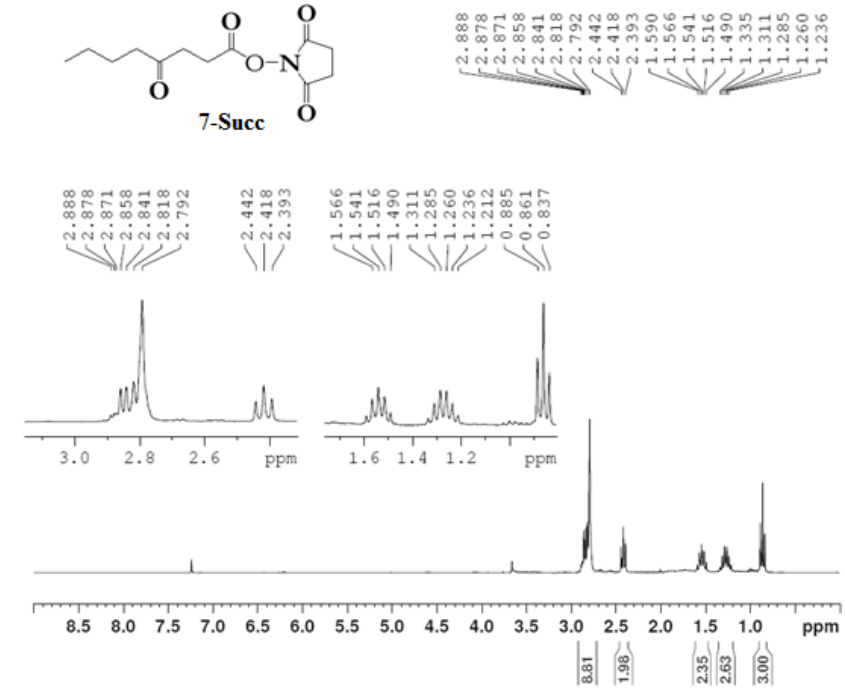

Fig. S20 ^{1}H NMR of **7-Succ** in $CDCl_3$.

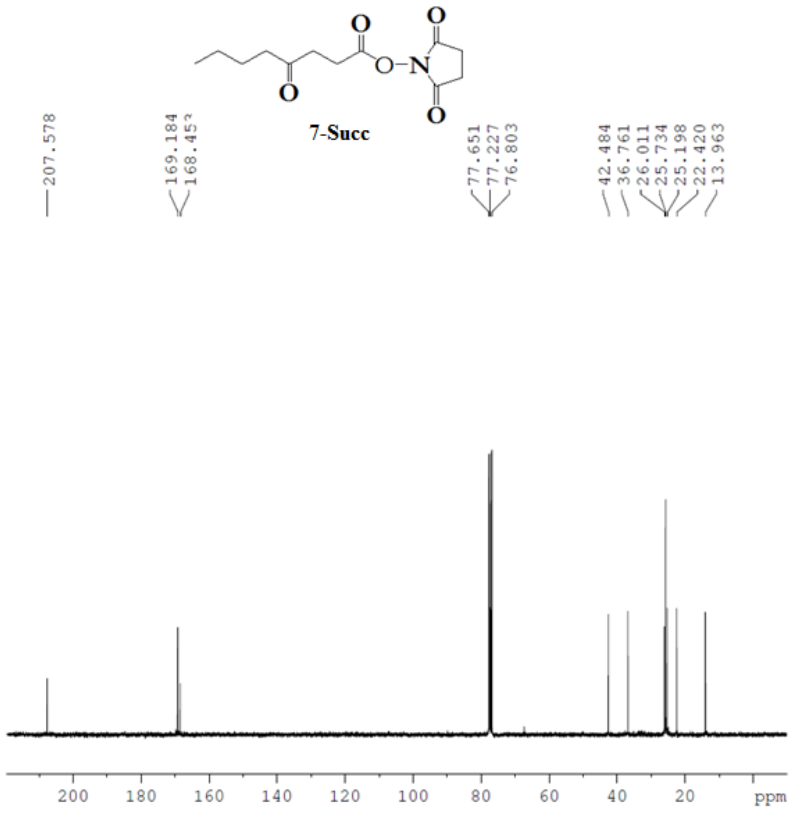

Fig. S21 ^{13}C NMR of **7-Succ** in $CDCl_3$.

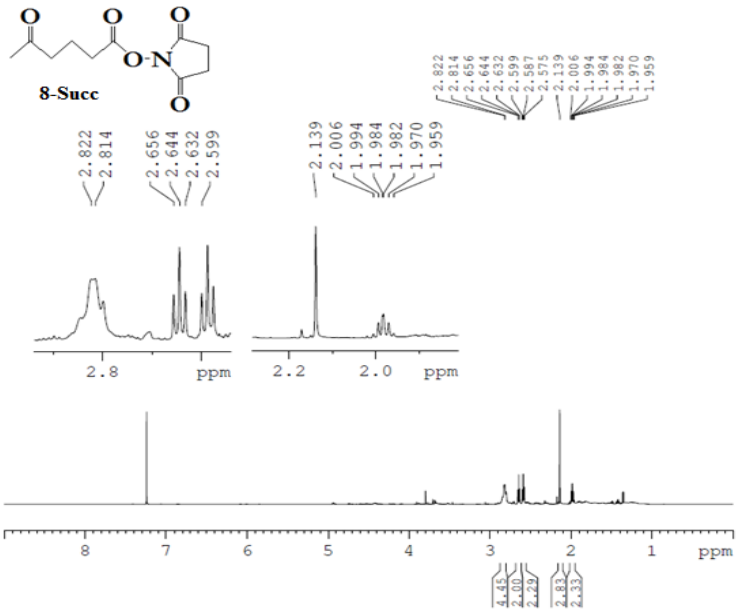

Fig. S22 ^{1}H NMR of **8-Succ** in $CDCl_3$.

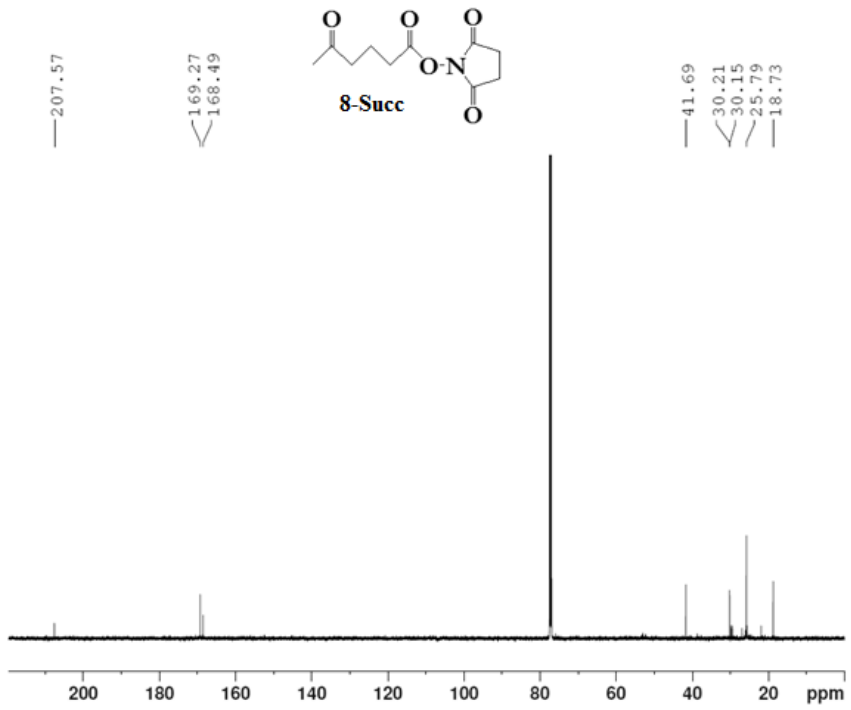

Fig. S23 ^{13}C NMR of **8-Succ** in $CDCl_3$.

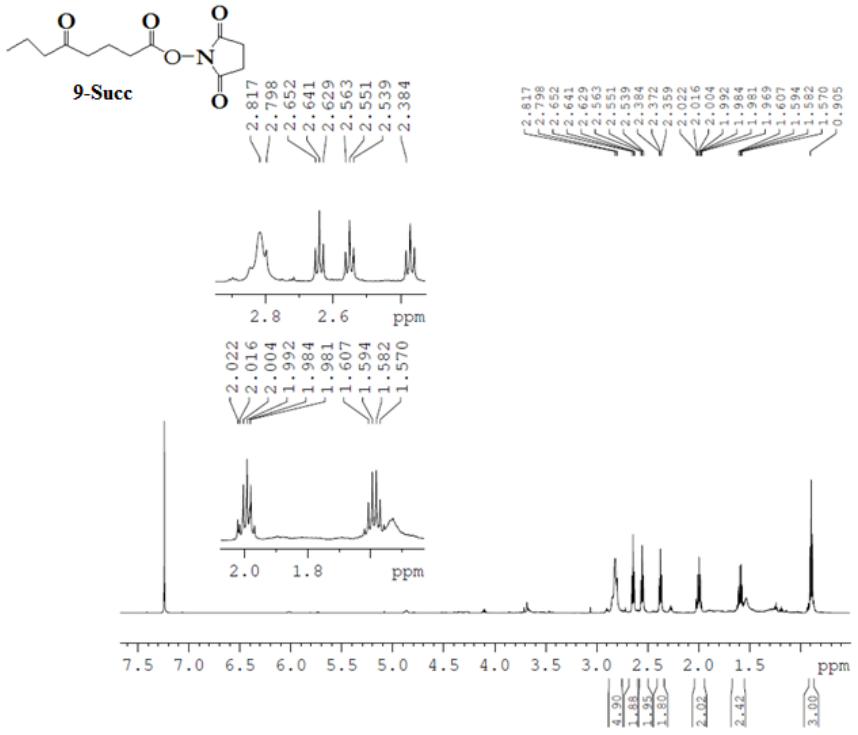

Fig. S24 ^{1}H NMR of **9-Succ** in $CDCl_3$.

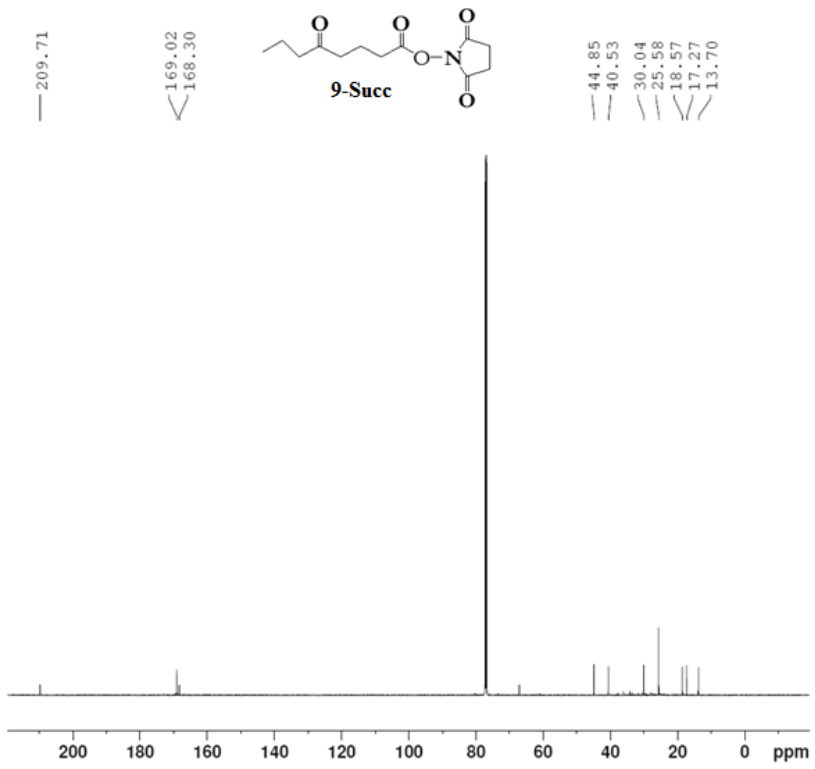

Fig. S25 ^{13}C NMR of **9-Succ** in $CDCl_3$.

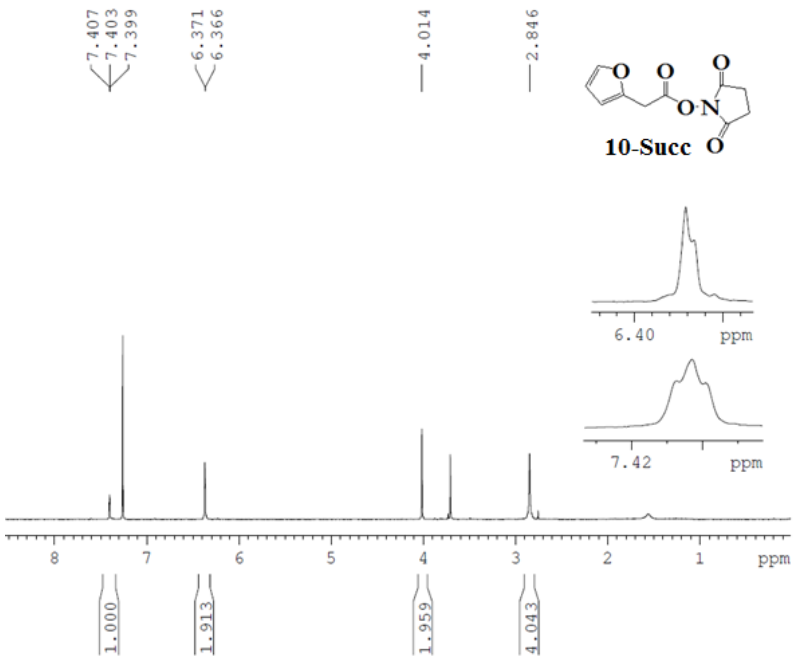

Fig. S26 ^{1}H NMR of **10-Succ** in $CDCl_3$.

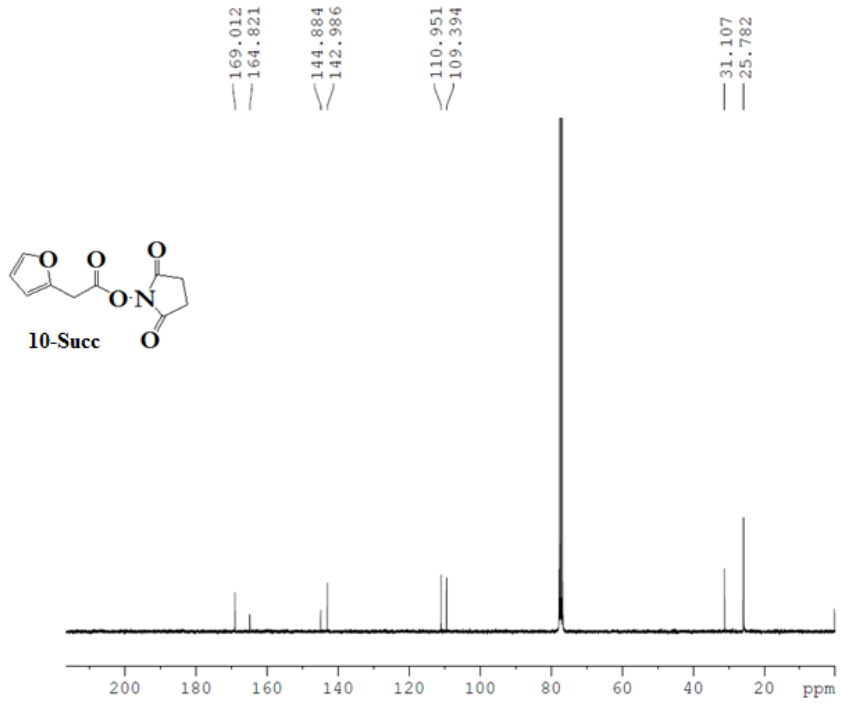

Fig. S27 ^{13}C NMR of **10-Succ** in $CDCl_3$.

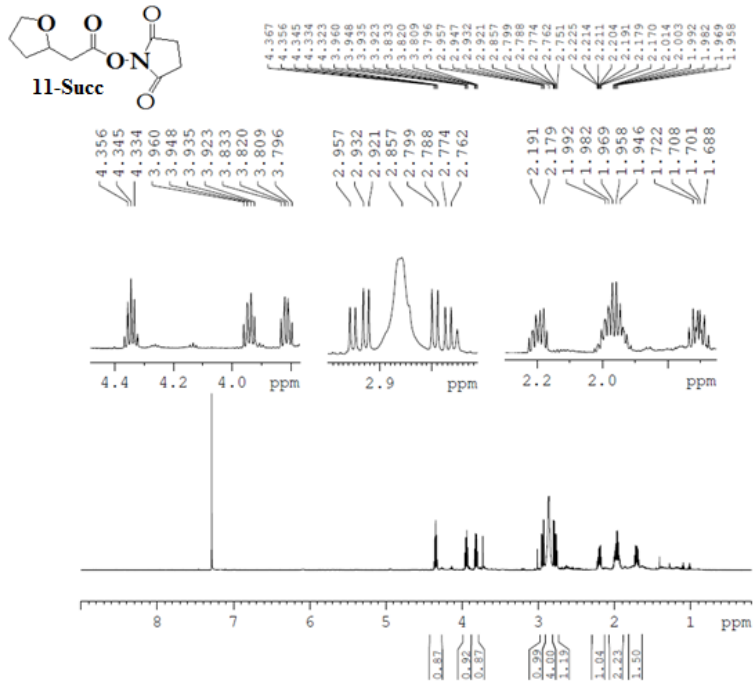

Fig. S28 ^{1}H NMR of **11-Succ** in $CDCl_3$.

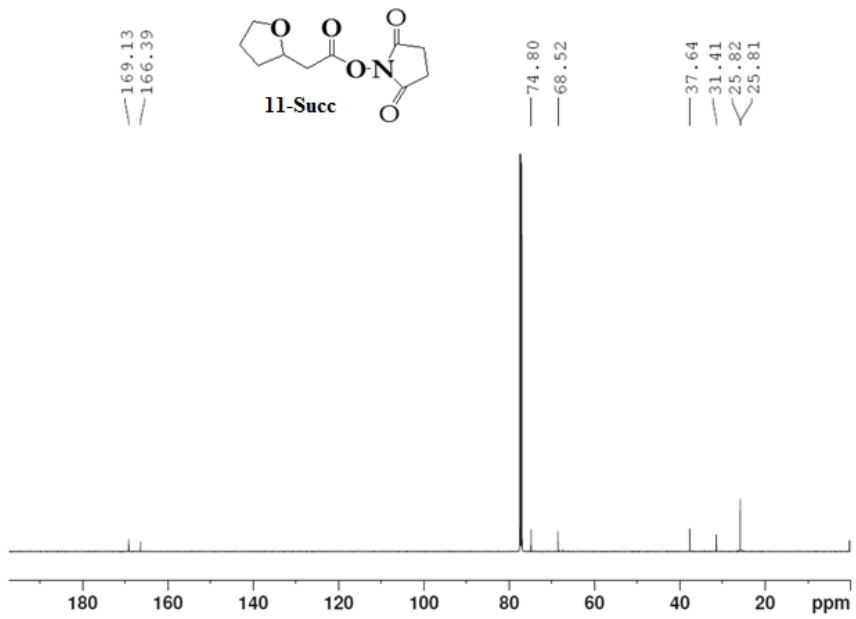

Fig. S29 ^{13}C NMR of **11-Succ** in $CDCl_3$.

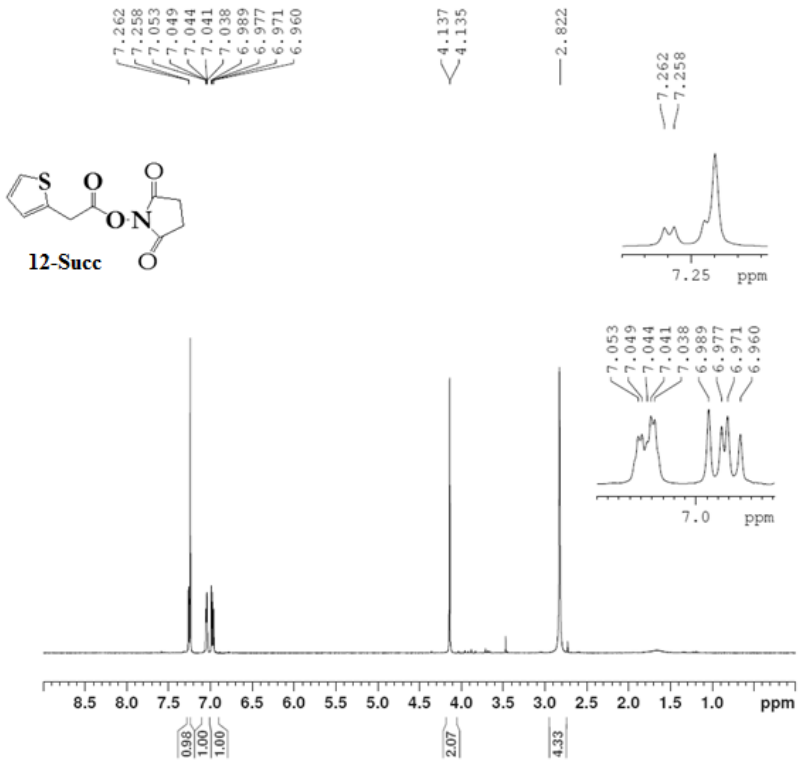

Fig. S30 ^{1}H NMR of **12-Succ** in $CDCl_3$.

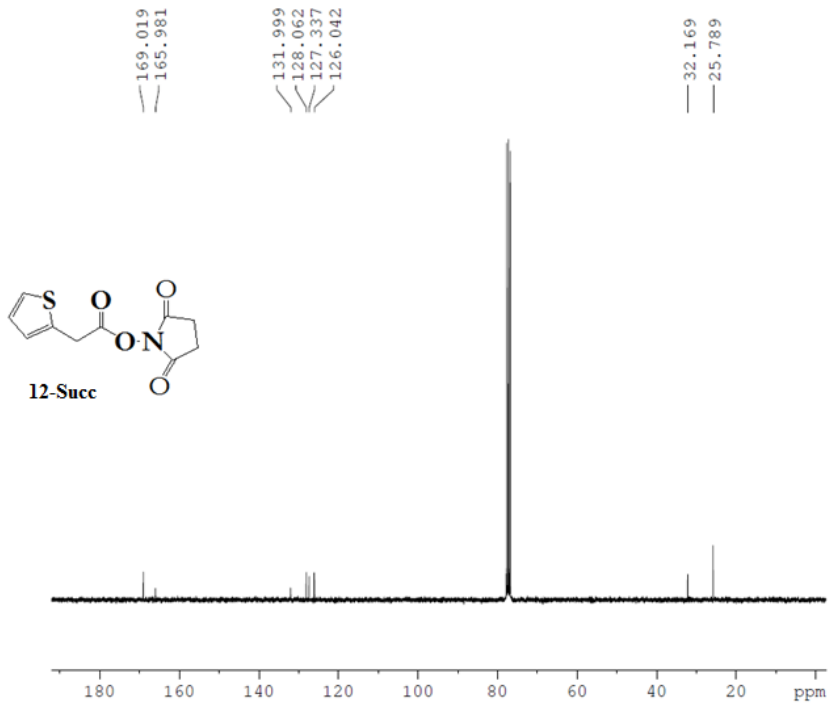

Fig. S31 ^{13}C NMR of **12-Succ** in $CDCl_3$.

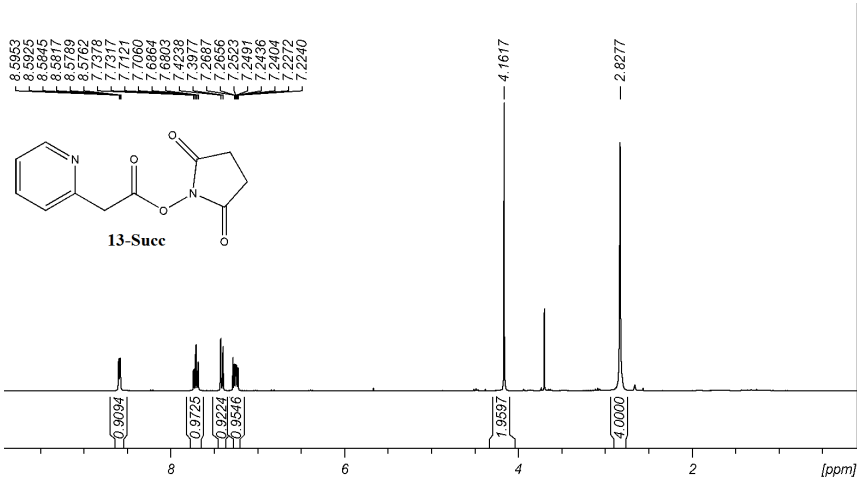

Fig. S32 ^{1}H NMR of **13-Succ** in $CDCl_3$.

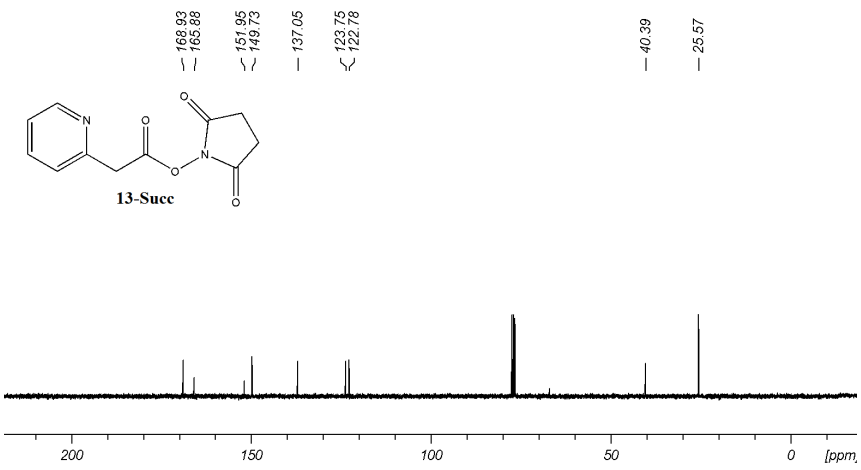

Fig. S33 ^{13}C NMR of **13-Succ** in $CDCl_3$.

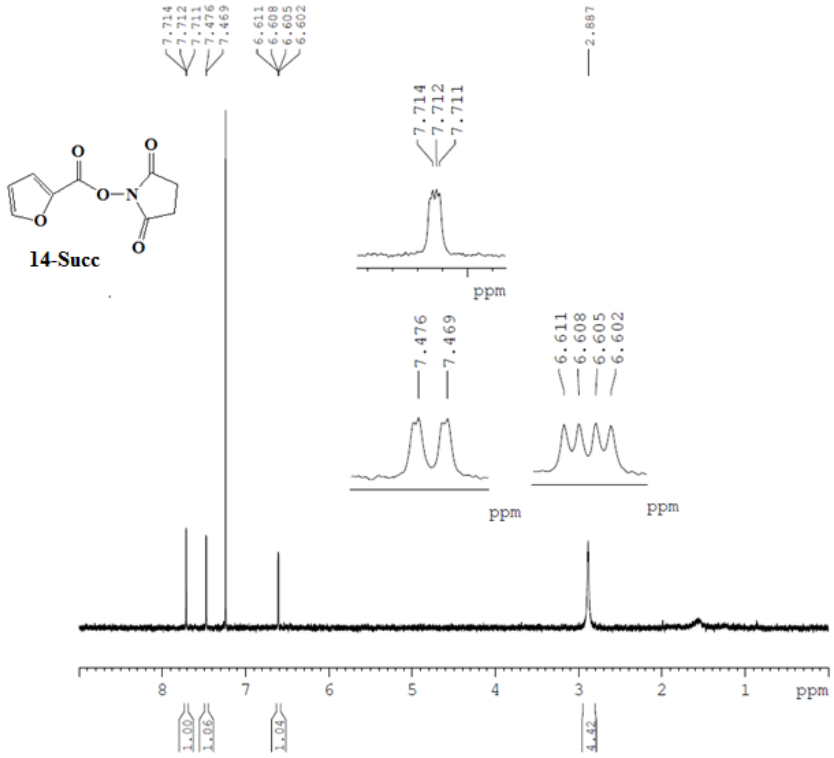

Fig. S34 ^{1}H NMR of **14-Succ** in $CDCl_3$.

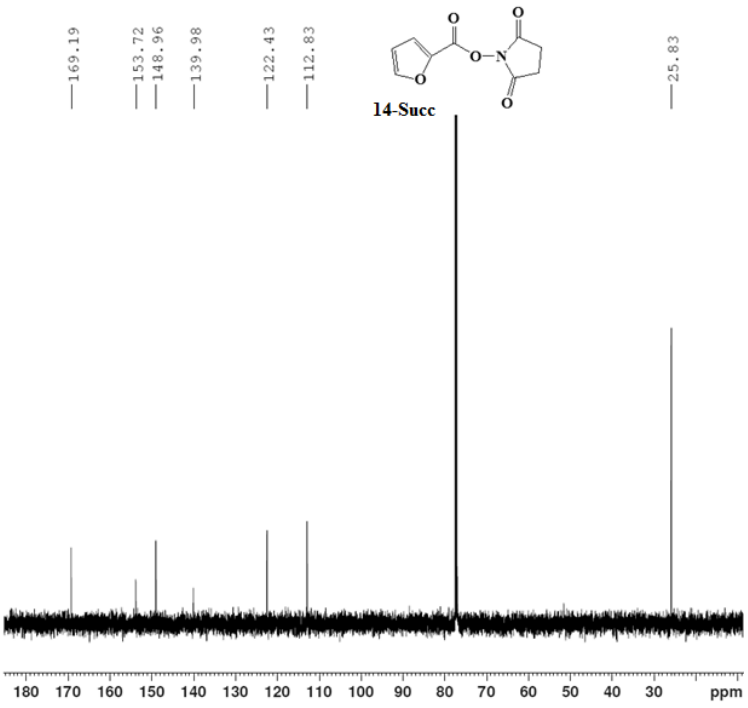

Fig. S35 ^{13}C NMR of **14-Succ** in $CDCl_3$.

HRMS Spectra for 4-Succ - 14-Succ

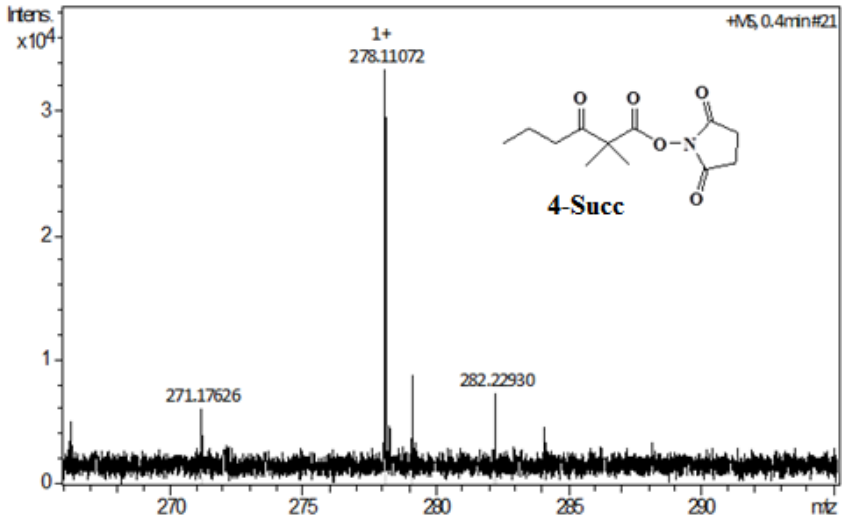

Fig. S36 HRMS spectrum of **4-Succ**.

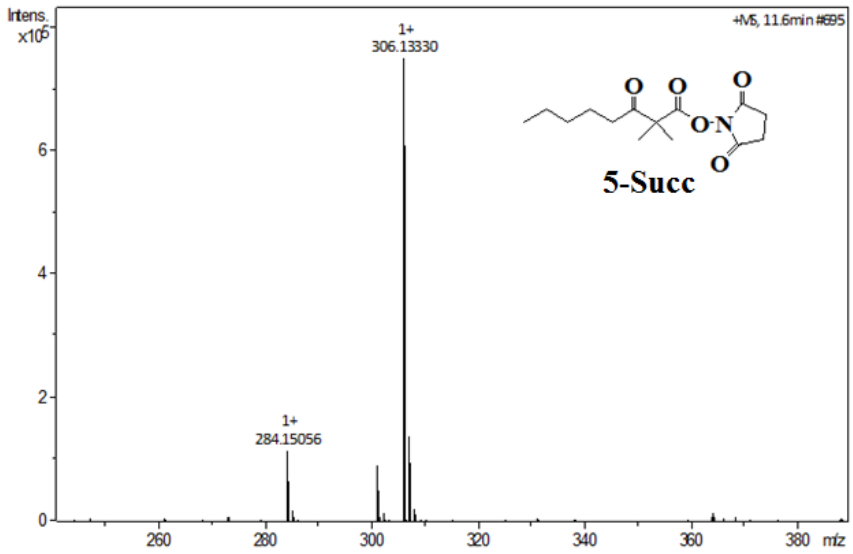

Fig. S37 HRMS spectrum of **5-Succ**.

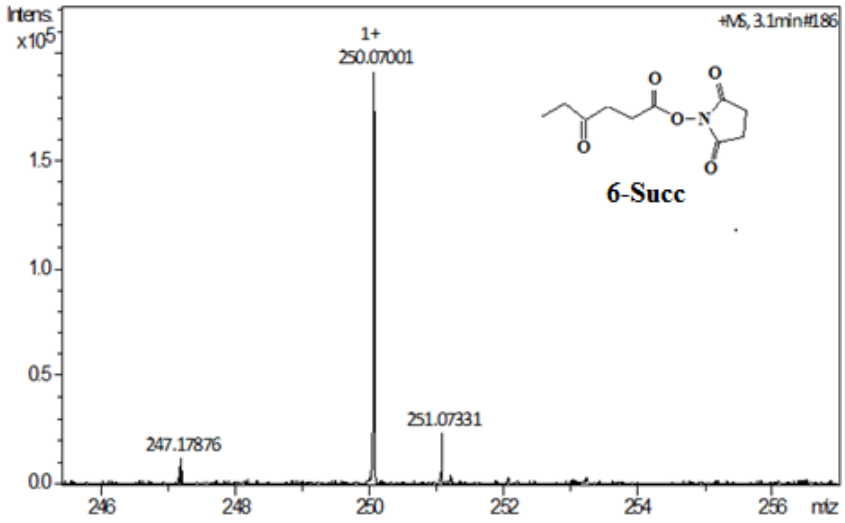

Fig. S38 HRMS spectrum of **6-Succ**.

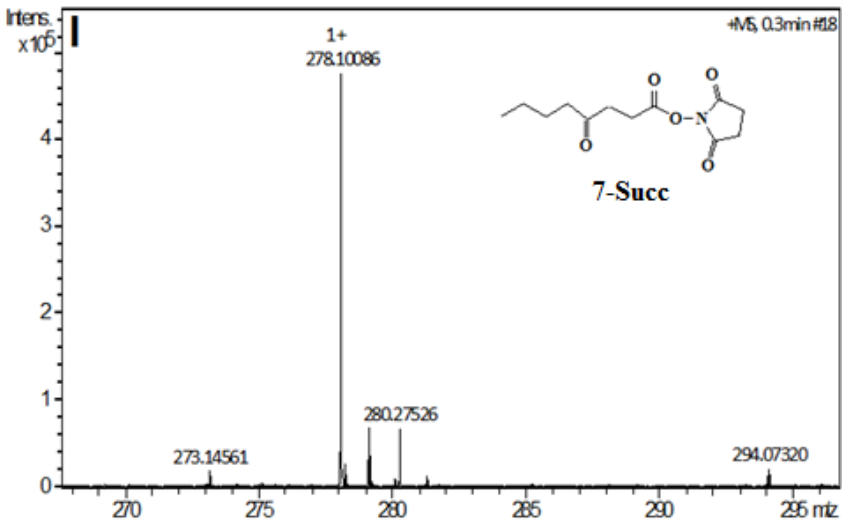

Fig. S39 HRMS spectrum of **7-Succ**.

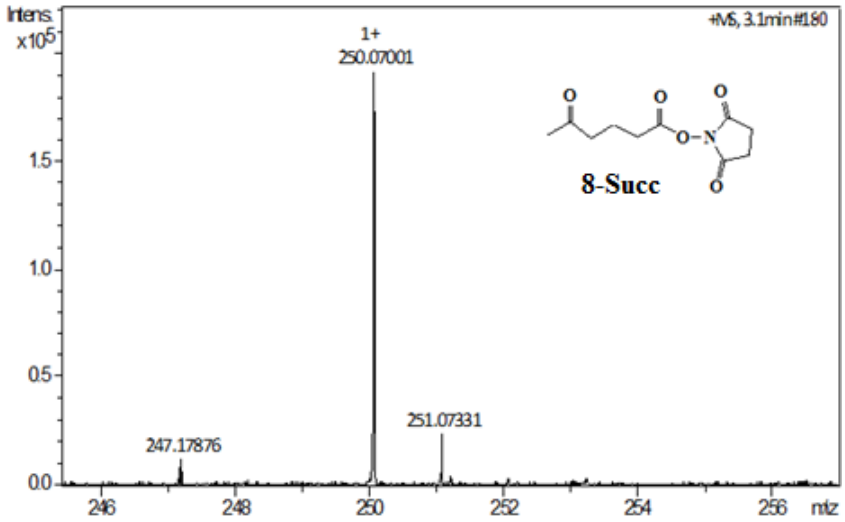

Fig. S40 HRMS spectrum of **8-Succ**.

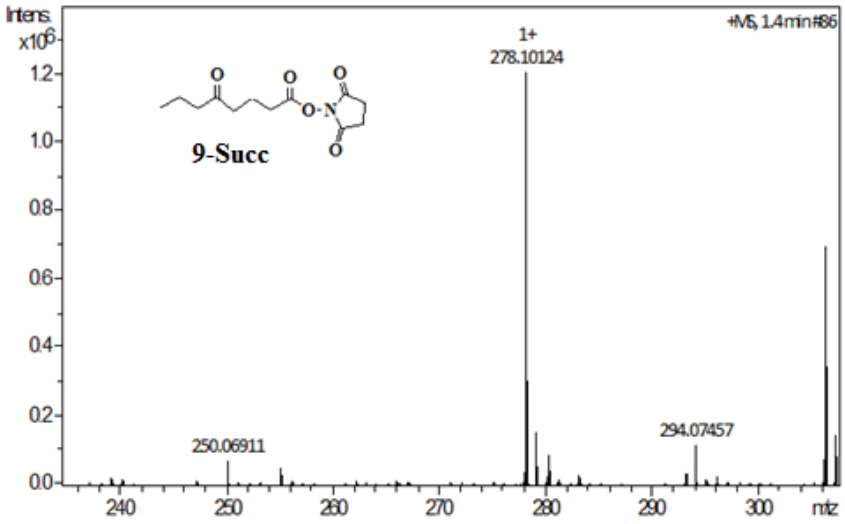

Fig. S41 HRMS spectrum of **9-Succ**.

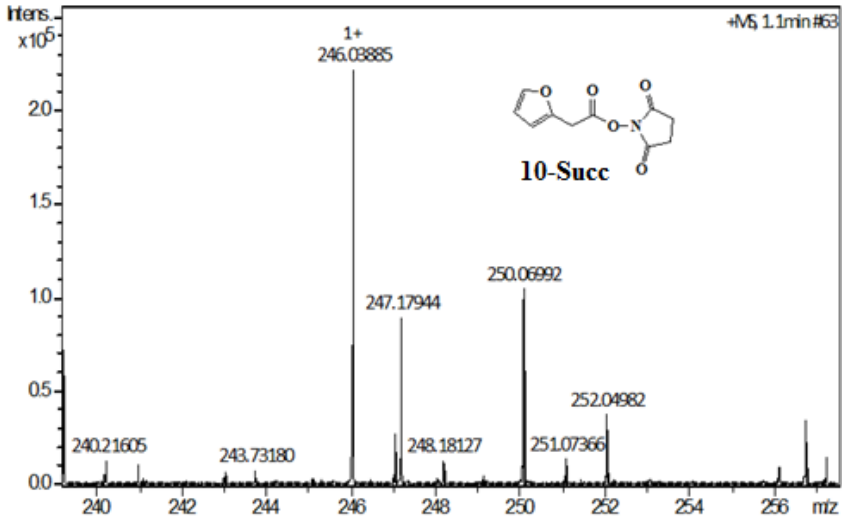

Fig. S42 HRMS spectrum of **10-Succ**.

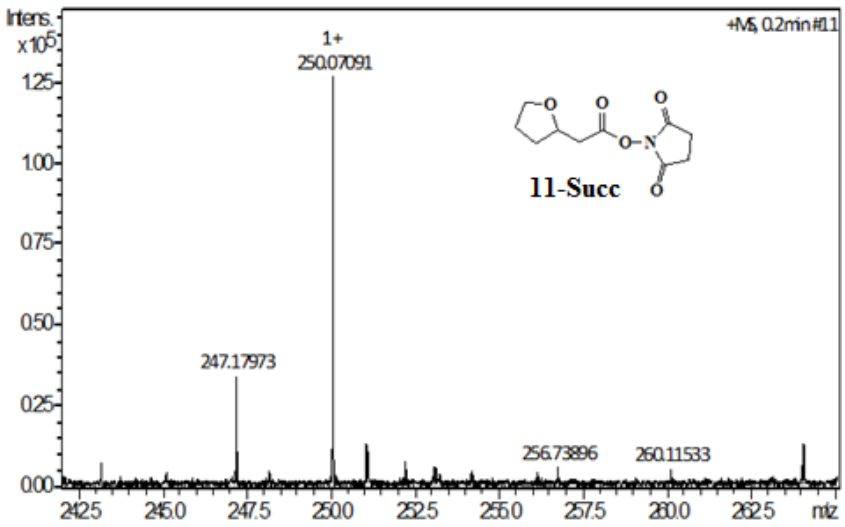

Fig. S43 HRMS spectrum of **11-Succ**.

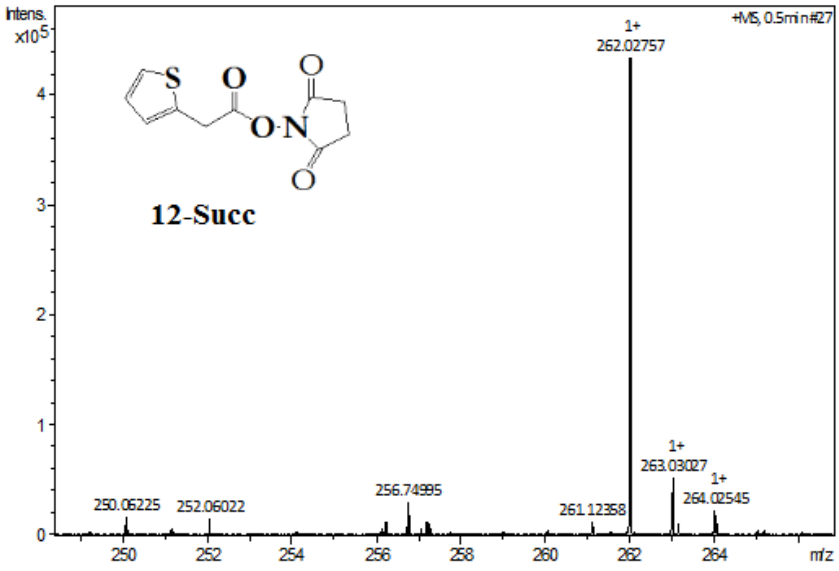

Fig. S44 HRMS spectrum of **12-Succ**.

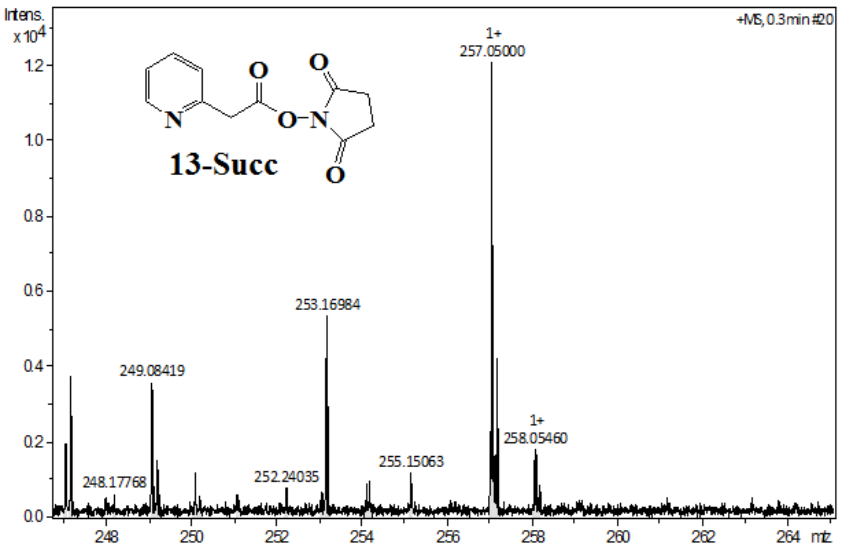

Fig. S45 HRMS spectrum of **13-Succ**.

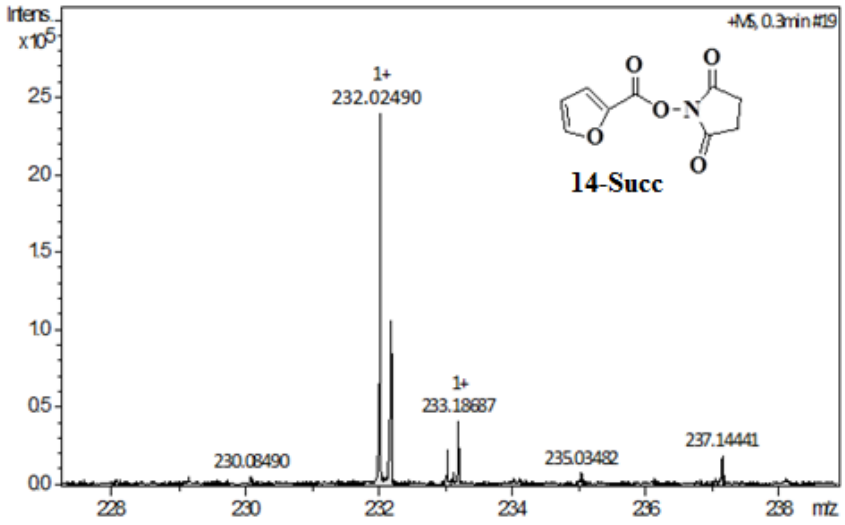

Fig. S46 HRMS spectrum of **14-Succ**.

HRMS Spectra for 4-CoA – 15-CoA

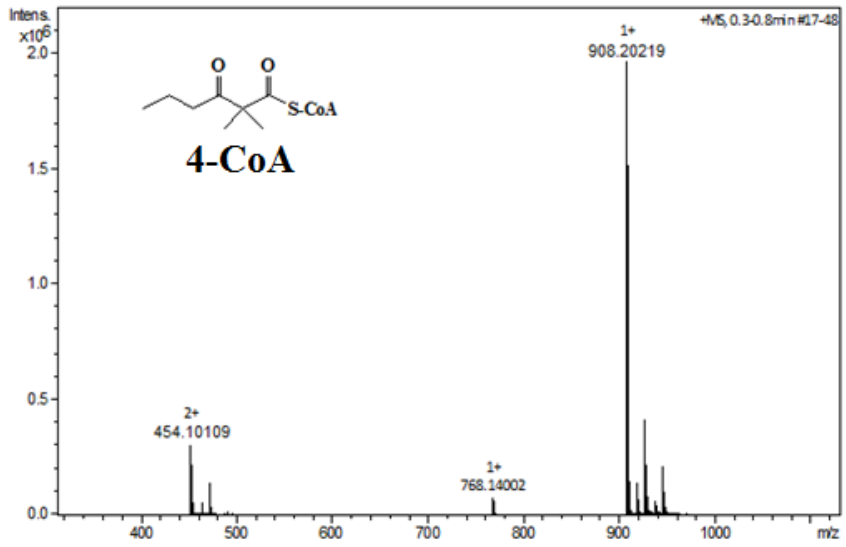

Fig. S47 HRMS spectrum of **4-CoA**.

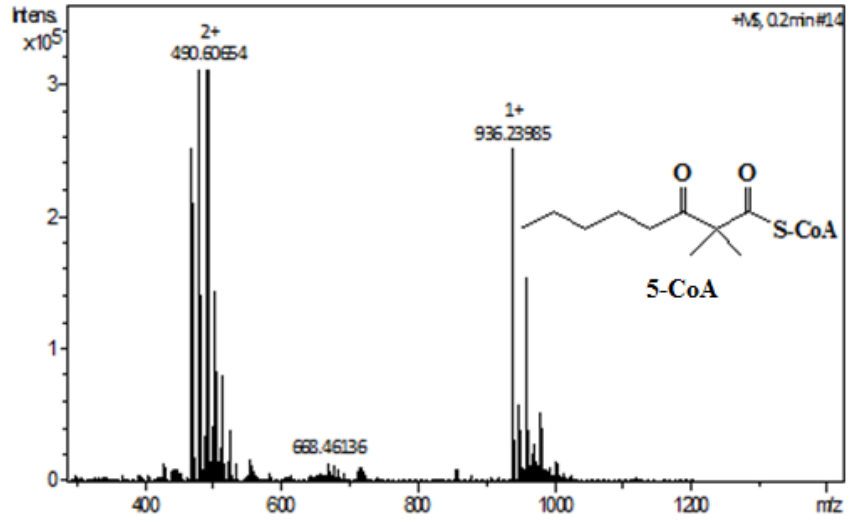

Fig. S48 HRMS spectrum of **5-CoA**.

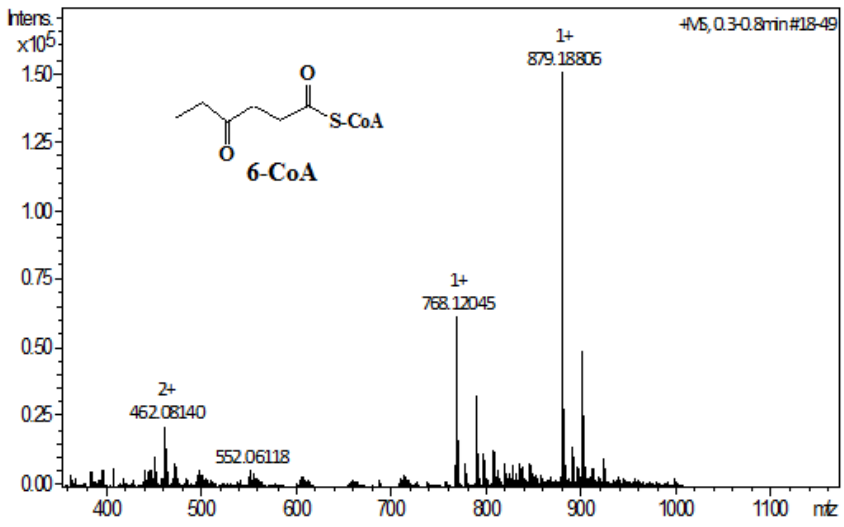

Fig. S49 HRMS spectrum of **6-CoA**.

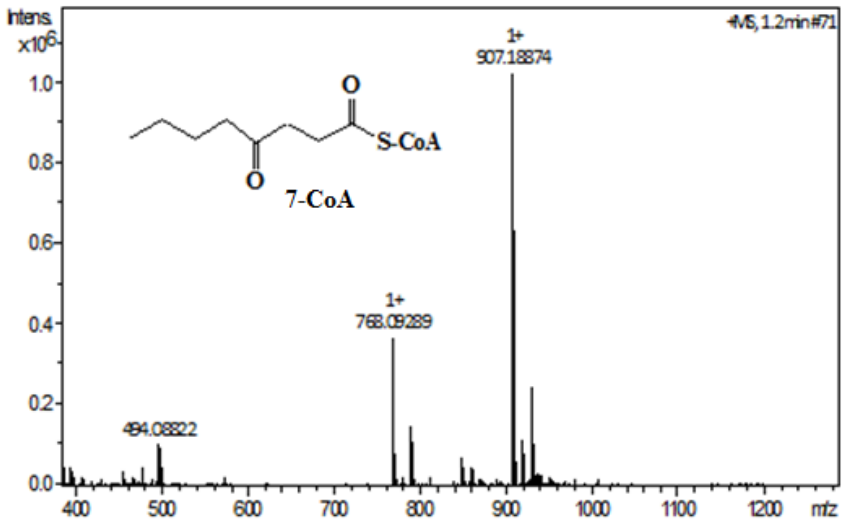

Fig. S50 HRMS spectrum of **7-CoA**.

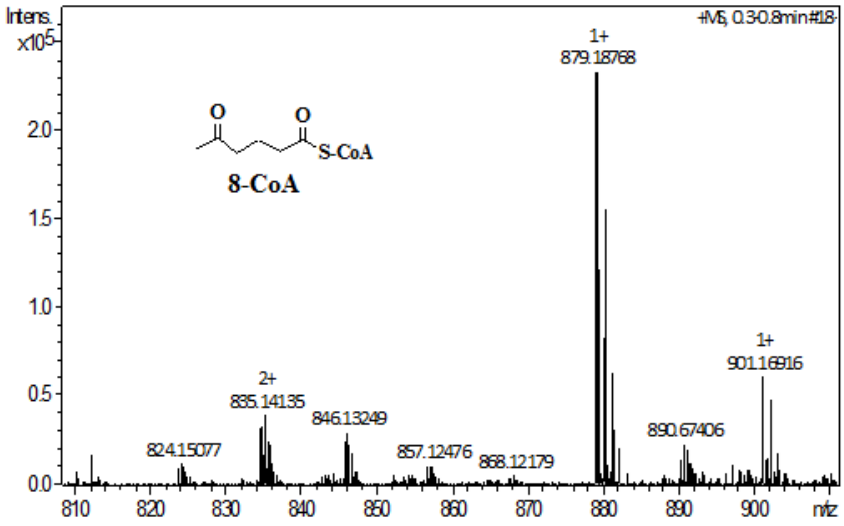

Fig. S51 HRMS spectrum of **8-CoA**.

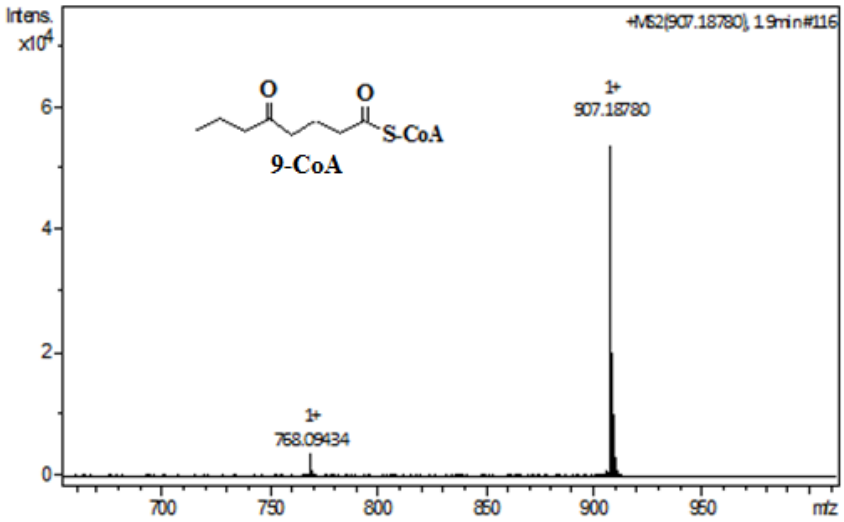

Fig. S52 HRMS spectrum of **9-CoA**.

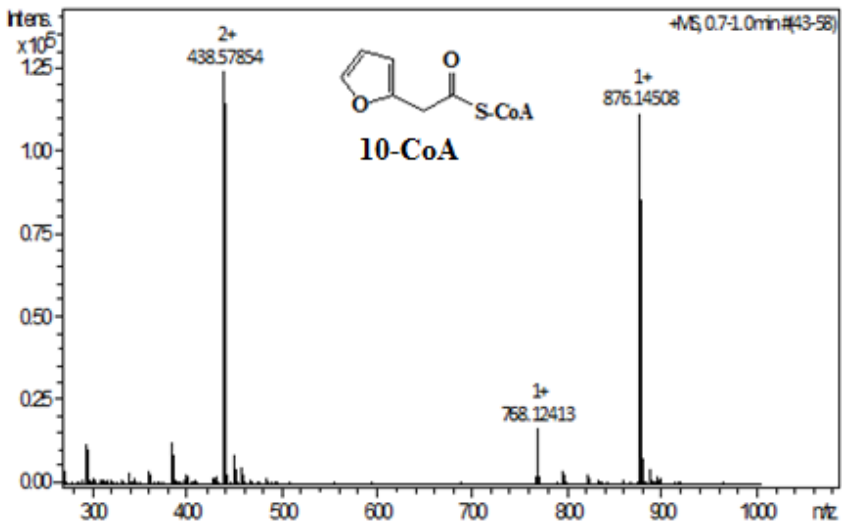

Fig. S53 HRMS spectrum of **10-CoA**.

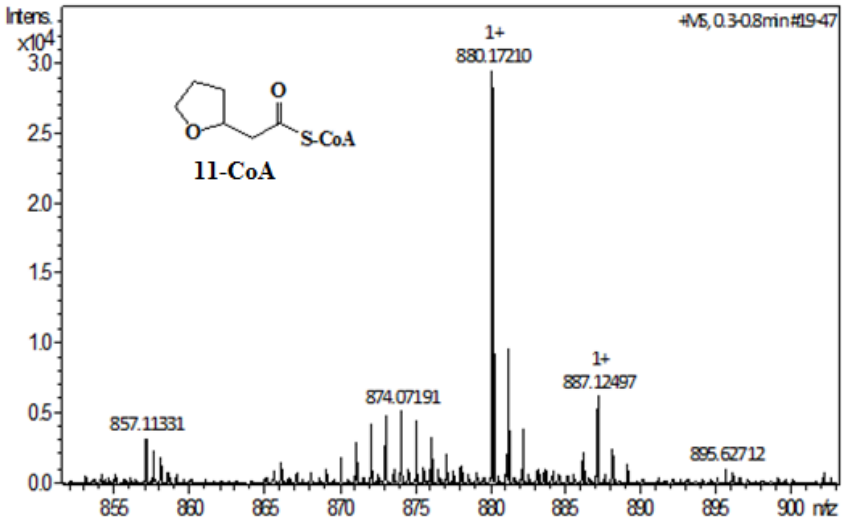

Fig. S54 HRMS spectrum of **11-CoA**.

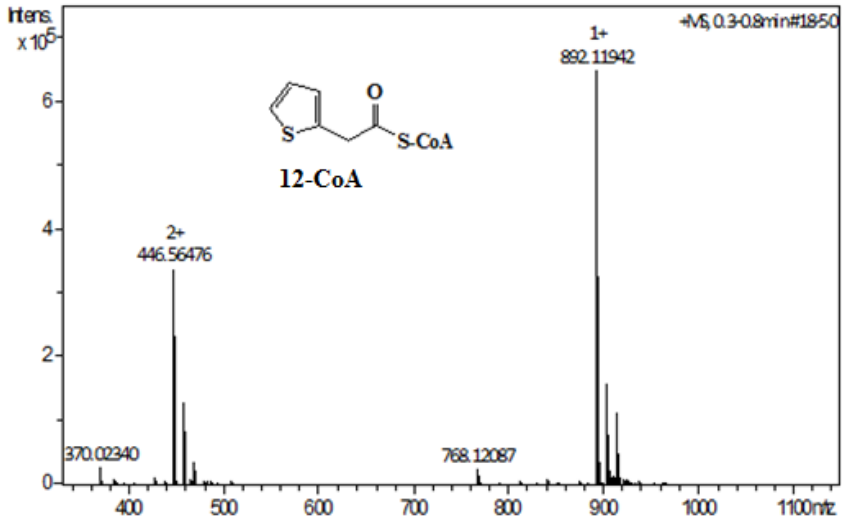

Fig. S55 HRMS spectrum of **12-CoA**.

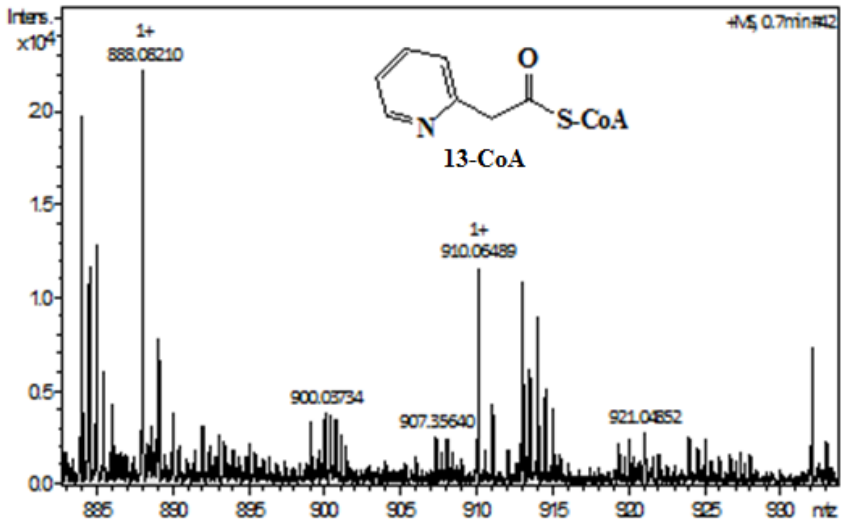

Fig. S56 HRMS spectrum of **13-CoA**.

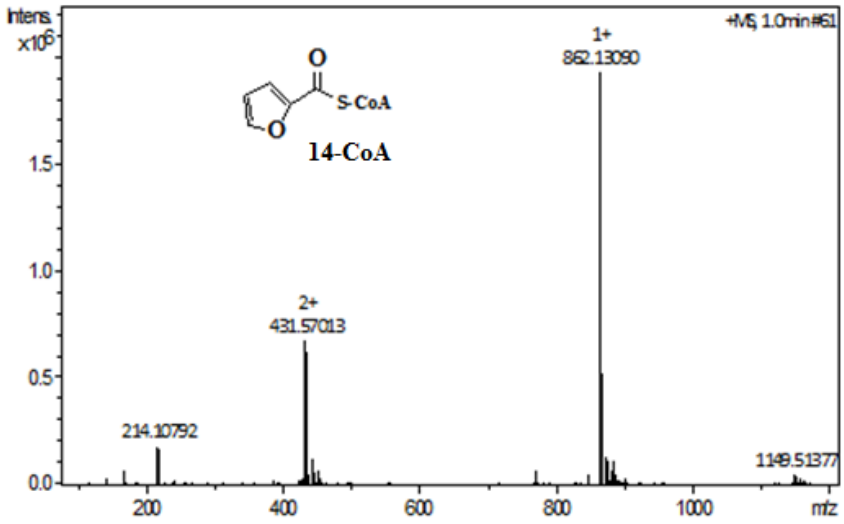

Fig. S57 HRMS spectrum of **14-CoA**.

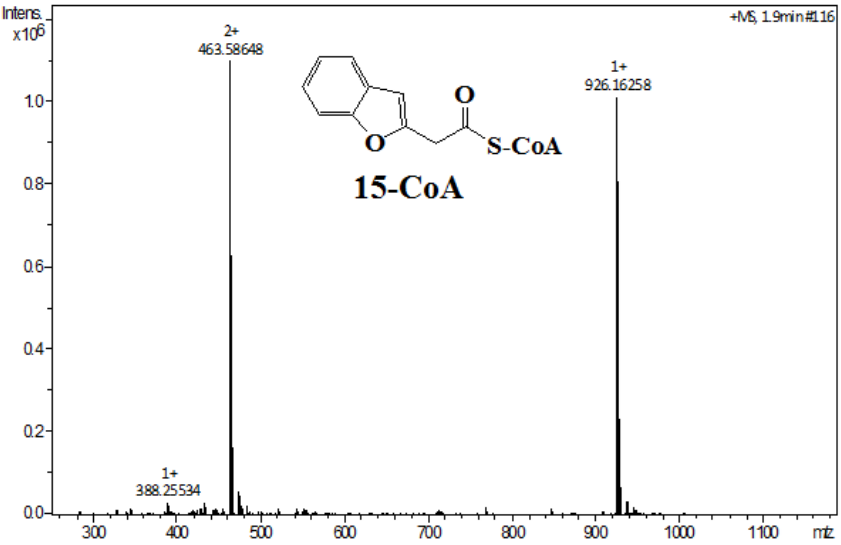

Fig. S58 HRMS spectrum of **15-CoA**.

HRMS Spectra for 1-ACP – 15-ACP

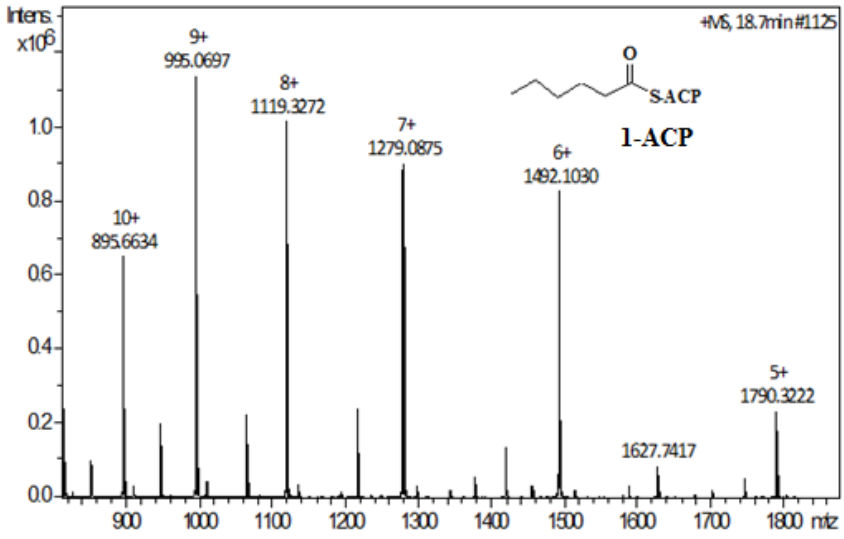

Fig. S59 HRMS spectrum of **1-ACP**.

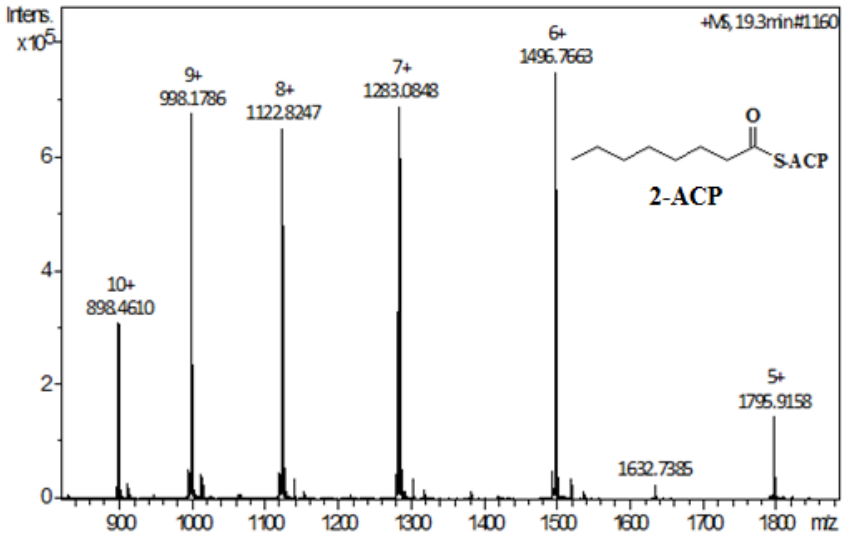

Fig. S60 HRMS spectrum of **2-ACP**.

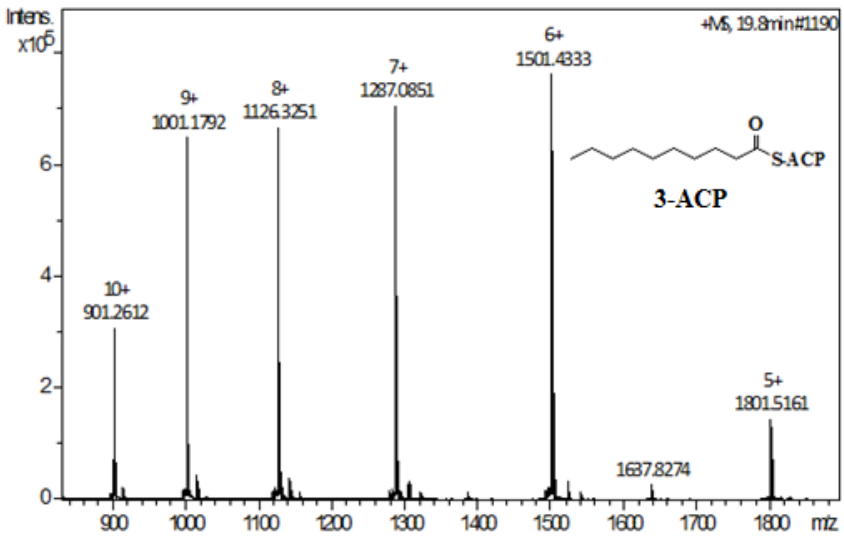

Fig. S61 HRMS spectrum of **3-ACP**.

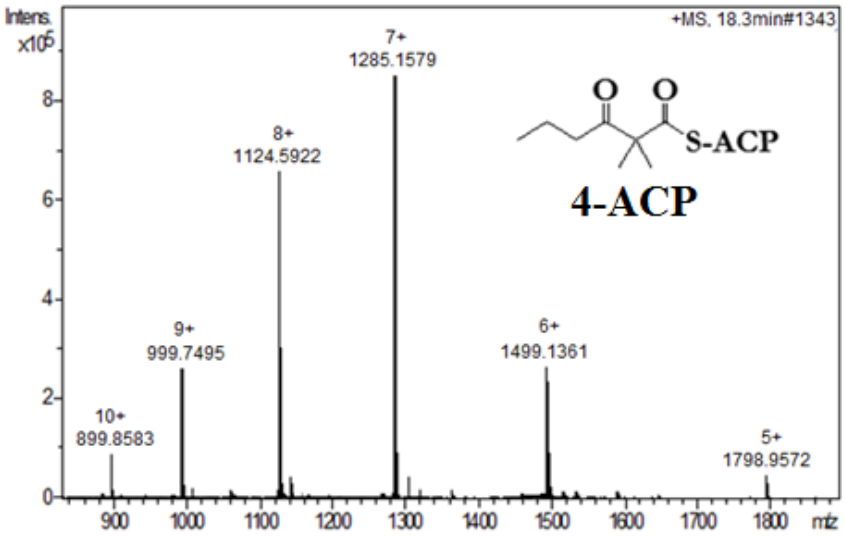

Fig. S62 HRMS spectrum of **4-ACP**.

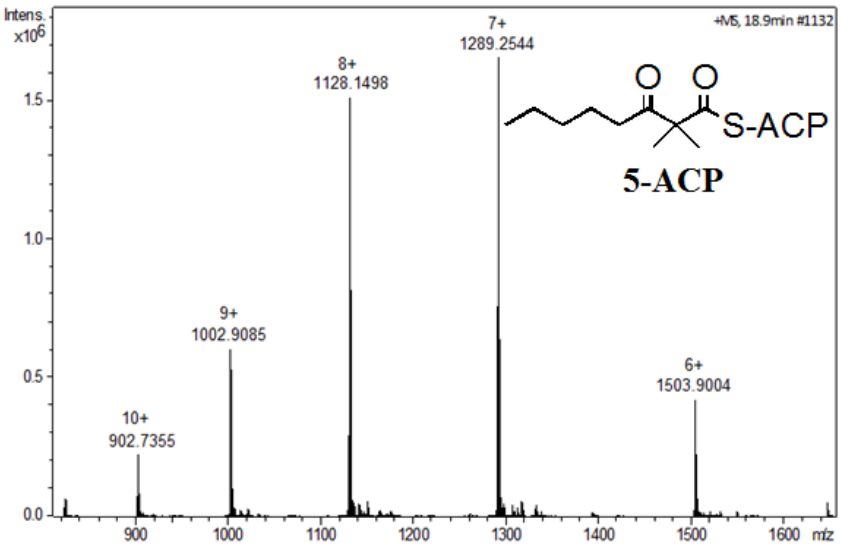

Fig. S63 HRMS spectrum of **5-ACP**.

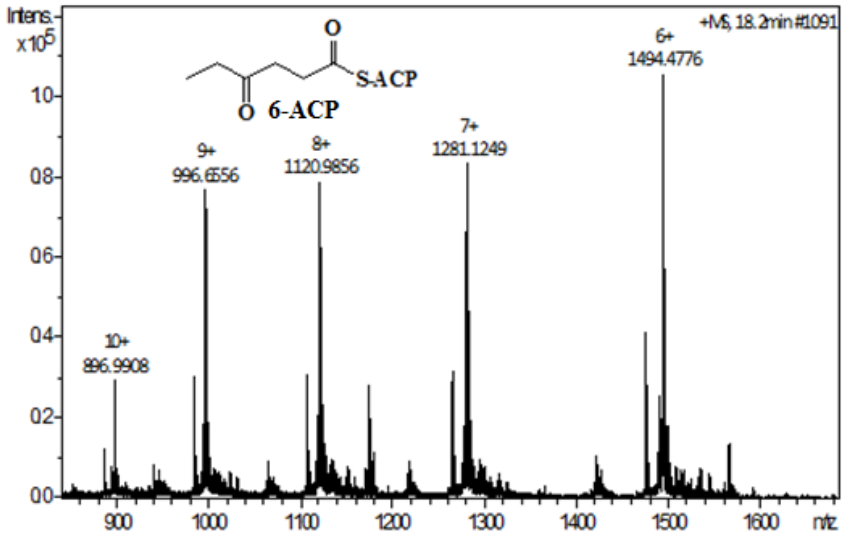

Fig. S64 HRMS spectrum of **6-ACP**.

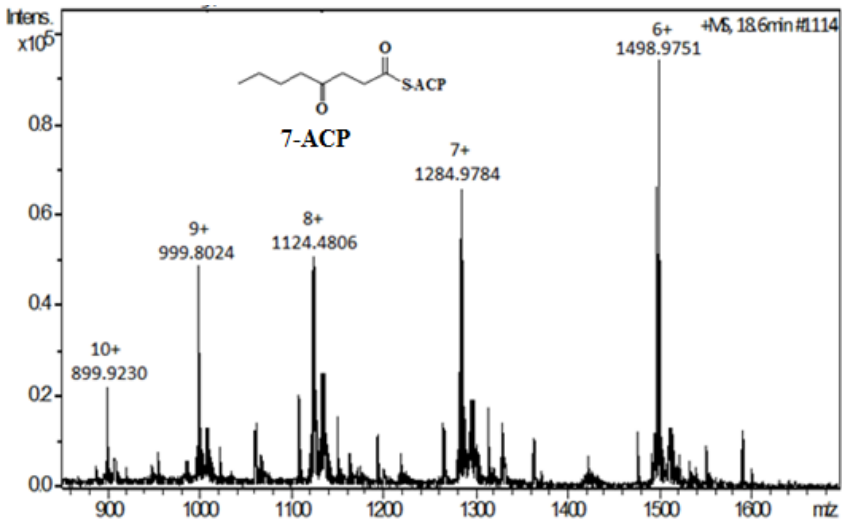

Fig. S65 HRMS spectrum of **7-ACP**.

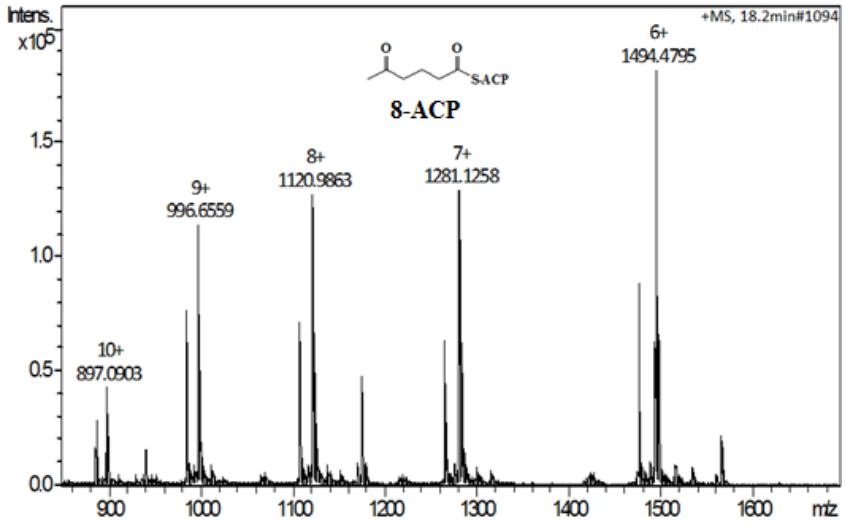

Fig. S66 HRMS spectrum of **8-ACP**.

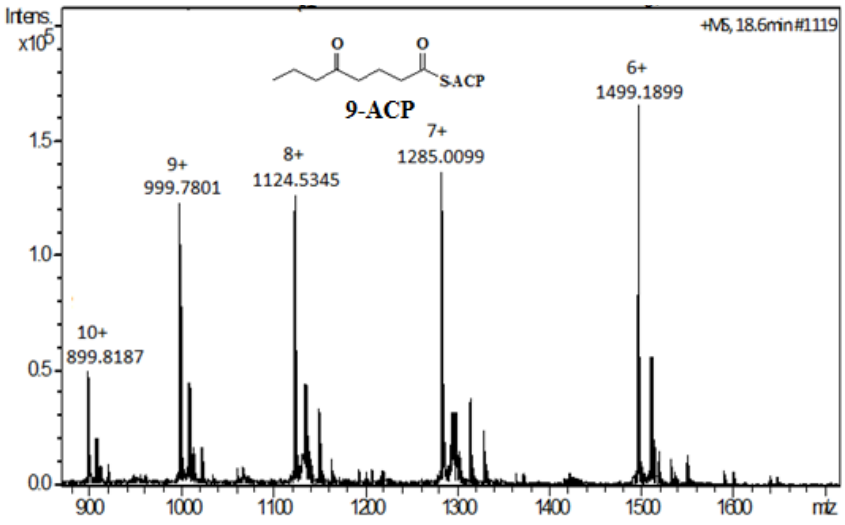

Fig. S67 HRMS spectrum of **9-ACP**.

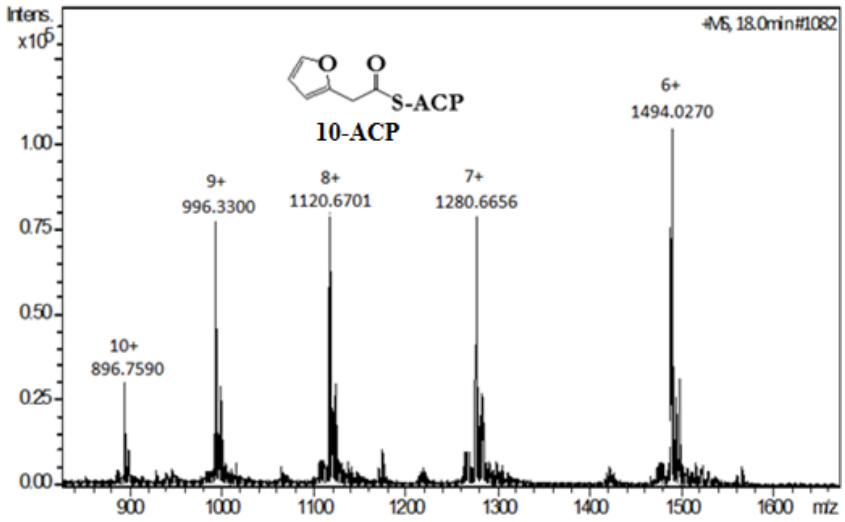

Fig. S68 HRMS spectrum of **10-ACP**.

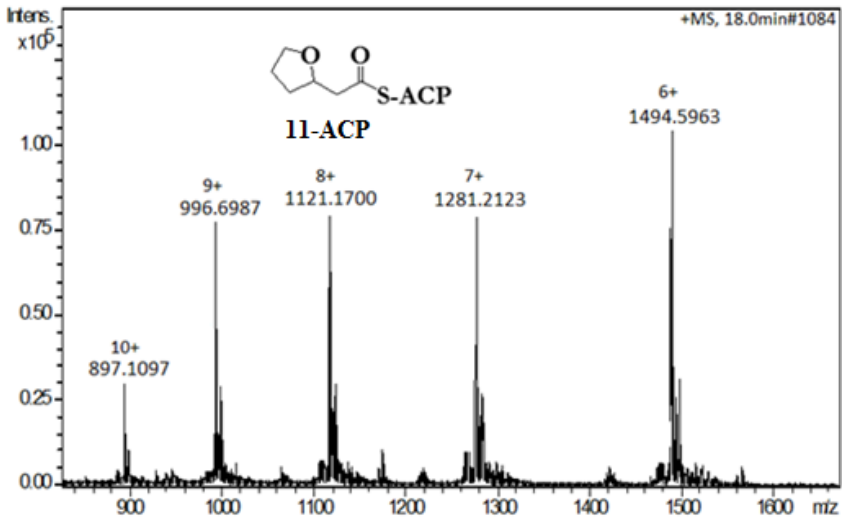

Fig. S69 HRMS spectrum of **11-ACP**.

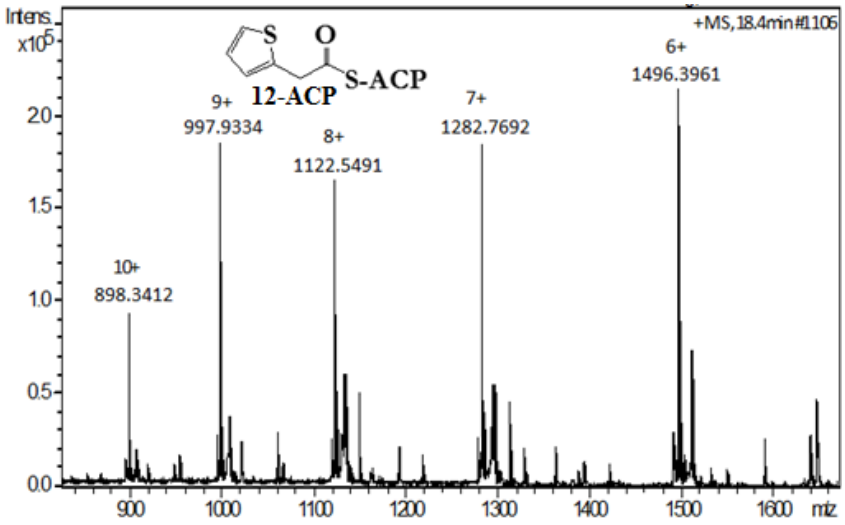

Fig. S70 HRMS spectrum of **12-ACP**.

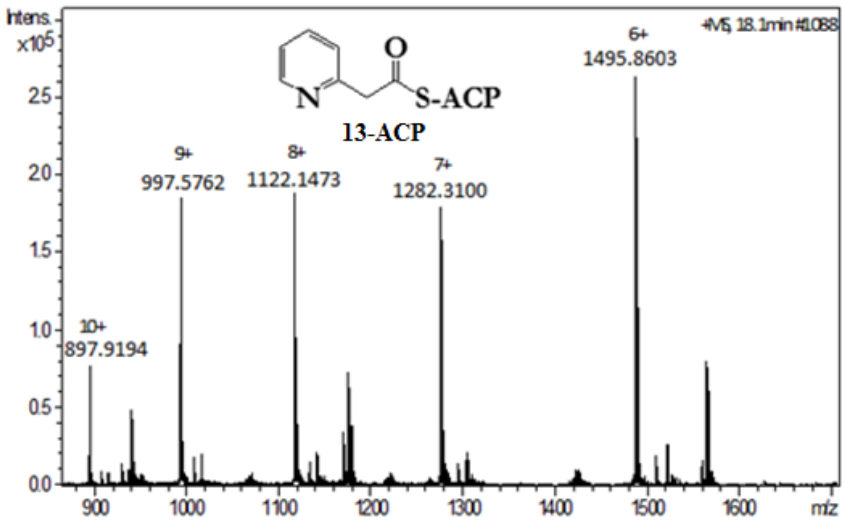

Fig. S71 HRMS spectrum of **13-ACP**.

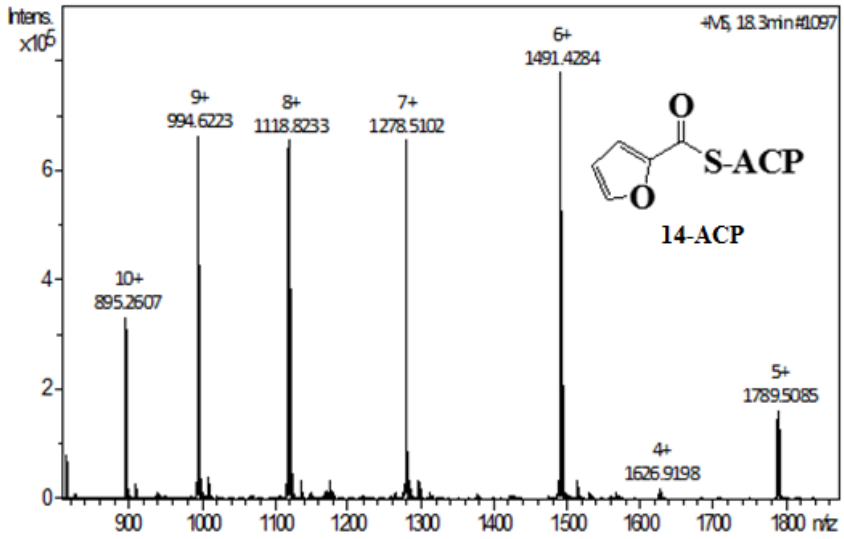

Fig. S72 HRMS spectrum of **14-ACP**.

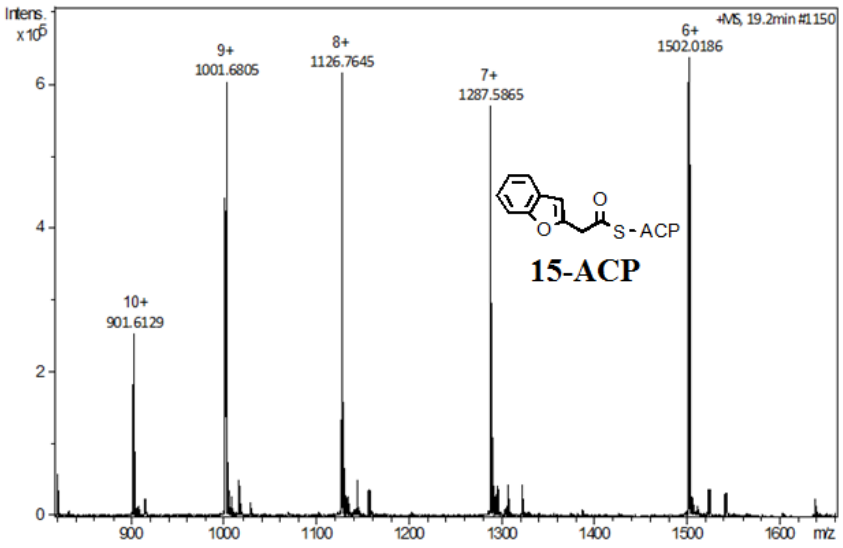

Fig. S73 HRMS spectrum of **15-ACP**.

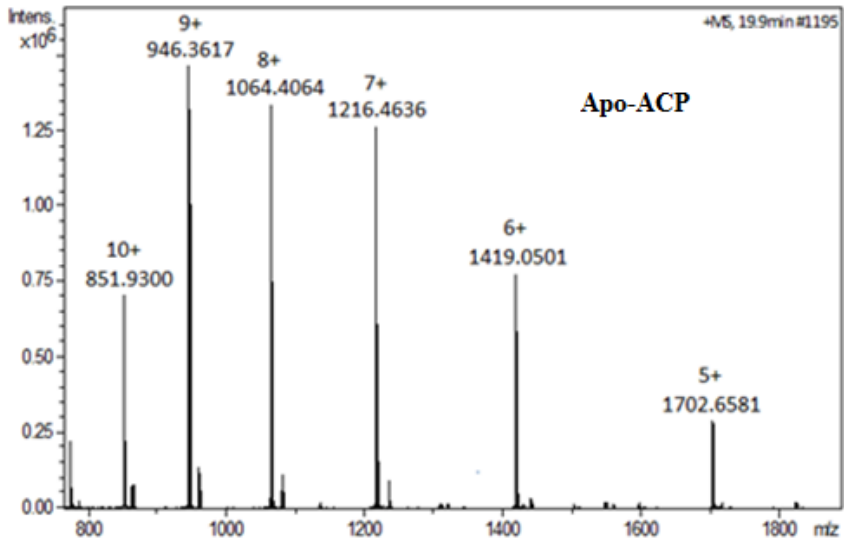

Fig. S74 HRMS spectrum of **Apo-ACP**.

EsaI wild-type and T140A mutant Growth, Expression, and Purification

Recombinant EsaI wild-type and T140A mutant in *E. coli* were grown in Luria-Bertani (LB) media containing 100 μg/mL ampicillin at 37 °C to an OD_{600} of 0.6-0.8. Expression was induced by addition of 0.5 mM isopropyl-β-D-1-thiogalactopyranoside (IPTG) at room temperature. After 4 hours, the growth cultures were then centrifuged to pellet at 5000 xg at 4 °C for 10 minutes and stored at -20 °C prior to lysis. The cell pellets were thawed on ice for 30-60 minutes before lysis. The cell pellets were suspended in 3 mL B-PER reagent per gram pellet, 1 mL of lysozyme, 40 μL of 4 mg/mL DNAse per gram pellet, 40 μL of 4 mg/mL RNAse per gram pellet, and 60 μL of (13 μg/ 750 μL isopropanol) phenylmethylsulfonyl fluoride (PMSF) per gram pellet. Lysate was incubated at room temperature with gentle shaking for 15 minutes and then centrifuged to collect supernatant at 20,000 xg at 4 °C for 30 minutes. A Ni^{2+}-NTA affinity chromatography column was used to purify the protein. The Ni^{2+}-NTA column was first equilibrated with 10X bed volumes of 0.5 M NaCl in 50 mM Tris/HCl, pH 7.5 buffer (Buffer A). The clear supernatant was loaded onto the column to allow the protein of interest to bind to the resin. The column was then washed with 10X bed volumes of 40 mM imidazole in Buffer A. The EsaI protein was eluted using 15 mL of 200 mM imidazole in Buffer A. The purity of EsaI was confirmed by SDS-PAGE gel analysis (MW = 24,667.2 Da). Concentration of EsaI was determined via UV-Vis (ε_{280} = 34,170 M^{-1} cm^{-1}).

Apo-ACP Growth, Expression, and Purification

Purification of apo-ACP was accomplished by minor modification of a previously published protocol.[4] Apo-ACP in BL21 *E. coli* competent cell was grown in LB broth containing 25 μg/mL kanamycin, 50 μg/mL streptomycin, 50 μg/mL spectinomycin, and 25 μg/mL chloramphenicol at 37 °C to an OD_{600} of 0.6-0.8. An addition of 0.1 mM IPTG was added to induce expression. The growth culture was incubated for another 3 hours and then centrifuged to pellets at 5000 xg at 4 °C for 10 minutes. The cell pellets were suspended in 3 mL B-PER reagent per gram pellet, 1 mL of lysozyme, 40 μL of 4 mg/mL DNAse per gram pellet, 40 μL of 4 mg/mL RNAse per gram pellet, and 60 μL of (13 μg/ 750 μL isopropanol) PMSF per gram pellet. The lysate was incubated at room temperature with gentle shaking for 20 minutes and then centrifuged to collect a clear supernatant at 20,000 xg at 4 °C for 60 minutes. Then $MnSO_4$ (1.2 mM) and $MgCl_2$ (25 mM) were added to the clear supernatant and the mixture was incubated at 37 °C for 4 hours to convert all holo-ACP to the apo-ACP form. Cellular protein was precipitated by adding isopropanol slowly to 50% volume with gentle shaking on ice for 1 hour. The precipitated protein was removed by centrifugation at 20,000 xg for 45 minutes. The clear supernatant was then stirred with DEAE-sepharose resin overnight at 4 °C. The media was packed into a column and washed with 10X bed volumes of 0.25 mM LiCl in 10 mM lithium 4-morpholineethane-sulfonate (MES), pH 6.1 buffer. The protein of interest was eluted with 10X bed volumes of 0.5 M LiCl in 10 mM MES, pH 6.1 buffer. Using SDS-PAGE analysis, fractions containing pure protein (MW = 9573.4 Da) were pooled and precipitated using 0.02% (0.2 mg/mL) sodium deoxycholate and 5% (50 mg/mL) trichloroacetate (w/v). The

mixture was incubated for 60 minutes with gentle shaking at 37 °C and centrifuged to pellet at 20,000 xg for 30 minutes. The apo-ACP pellet was resuspended in 0.5 M Tris-HCl, pH 8.0 buffer and concentrated using 3 kD molecular weight cutoff spin filter column. Concentration of apo-ACP was determined using UV-Vis (ε_{280} = 1490 $M^{-1}cm^{-1}$).

Sfp Growth, Expression, and Purification

Bacillus subtilis Sfp was expressed in BL21 *E. coli* competent cells. Sfp was grown in LB media containing 100 μg/mL kanamycin at 37 °C to an OD_{600} of 0.6-0.8. Expression was induced by addition of 0.5 mM IPTG and continued at 37 °C for another 3 hours. The growth cultures were then centrifuged to pellet at 5000 xg at 4 °C for 10 minutes and stored at -20 °C prior to lysis. The cell pellets were thawed on ice for 30-60 minutes before lysis. The cell pellets were suspended in 3 mL B-PER reagent per gram pellet, 1 mL of lysozyme, 40 μL of 4 mg/mL DNAse per gram pellet, 40 μL of 4 mg/mL RNAse per gram pellet, and 60 μL of (13 μg/ 750 μL isopropanol) PMSF per gram pellet. Lysate was incubated at room temperature with gentle shaking for 15 minutes and then centrifuged to collect the supernatant at 20,000 xg at 4 °C for 30 minutes. Ni^{2+}-NTA affinity chromatography column was used to purify the protein. The Ni^{2+}-NTA column was first equilibrated with 10X bed volumes of 0.5 M NaCl in 50 mM Tris/HCl, pH 7.5 buffer (Buffer A). The clear supernatant was loaded onto the column to allow the protein of interest to bind to the resin. The column was then washed with 10X bed volumes of 10 mM imidazole in Buffer A. The Sfp protein was eluted using 15 mL of 200 mM imidazole in Buffer A. The purity of Sfp was confirmed

by SDS-PAGE gel analysis (MW = 26,990.5 Da). Concentration of Sfp was determined using UV-Vis (ε_{280} = 29,130 $M^{-1}cm^{-1}$).

YspI Growth, Expression, and Purification

YspI strain was expressed in *E. coli* strain BL21 (DE3) competent cells. The recombinant YspI was grown in LB media containing 50 μg/mL streptomycin and 50 μg/mL spectinomycin at 37 °C to an OD_{600} of 0.6-0.8. Expression was induced by addition of 0.5 mM isopropyl-β-D-1-thiogalactopyranoside (IPTG) at room temperature. After overnight, the growth cultures were centrifuged to pellet at 5000 xg at 4 °C for 10 minutes and stored at -20 °C prior to lysis. The cell pellets were thawed on ice for 30-60 minutes before lysis. The cell pellets were suspended in chilled lysis buffer, containing 50 mM Tris-HCl pH 7.5, 200 mM NaCl, 5 mM DTT, and 1 mM PMSF, with ratio of cell wet weight to buffer volume of 1:1. The cell suspension was cooled on ice for 10 minutes and then sonicated with 10 short bursts of 10 seconds followed by intervals of 30 seconds for cooling. Cell debris was then removed by centrifugation at 4 °C for 30 minutes at 20,000 xg. Amylose affinity chromatography column was used to purify the protein. The amylose column was first equilibrated with 10X bed volumes of YspI Buffer A (50 mM Tris-HCl pH 7.5, 0.2 M NaCl, 0.1 mM EDTA, 0.1 mM PMSF, 0.1 mM tosyl-L-lysinechloromethyl ketone hydrochloride, 0.4 M sucrose, and 2.5% (v/v) glycerol). The clear supernatant was loaded onto the equilibrated column to allow the protein of interest to bind to the resin. The column was then washed with 10X bed volumes of YspI Buffer A. The YspI protein was eluted using 35 mL of YspI Buffer A containing 10 mM maltose. The purity of YspI with maltose

binding protein (MBP) was confirmed by SDS-PAGE gel analysis (MW = 67.99 kDa). Concentration of YspI was determined via UV-Vis (ε_{280} = 103,710 $M^{-1}cm^{-1}$).

HPLC assay

Two chemical steps, lactonization and acylation, could be resolved independently using analytical C-18 reverse-phase UHPLC. MTA peak from SAM lactonization was monitored using a gradient beginning at 100% A (99.9% water, 0.1% formic acid): 0% B (99.9% acetonitrile, 0.1% formic acid) and ending at 70% A: 30% B over a period of 10 minutes at flow rate of 500 μL/min. Holo-ACP from acylation half-reaction was monitored using a gradient beginning at 75% A: 25% B and ending at 25% A: 75% B over a period of 10 minutes at flow rate of 600 μL/min. Standard calibration curves for MTA and holo-ACP were generated by serial dilution of known analyte concentrations in buffer with quench solution, 6 M HCl (lactonization) or 4 M acetate buffer, pH 3.7 (acylation). Peak areas at each MTA and holo-ACP concentration were determined from HPLC chromatograms at 260 nm (SAM and MTA) or 220 nm (acyl-ACP and holo-ACP). A typical enzyme-catalyzed reaction (100 μL) contained nanopure water, 100 mM HEPES pH 7.3 buffer, fixed SAM concentration at 500 μM, varied acyl-ACP concentrations. The mixture was split into two equal portions for background and reaction. After incubation at room temperature for 5 minutes, the reaction and background aliquots were initiated, respectively, with 1 μM EsaI enzyme (2 μM EsaI for 2-benzofuranacetyl-ACP, 4-oxo-C8-ACP, 5-oxo-C8-ACP, and C8-ACP) and nanopure water. The reaction and background aliquots in YspI kinetic assays were initiated, respectively, with 1 μM YspI (1.5 μM for 2-

pyridylacetyl-ACP; 2 μM for C6-ACP, C8-ACP, C10-ACP and 2-furanacetyl-ACP) and nanopure water. Since the progress curves for several enzyme-substrate pairs used in this study were linear, at least until 6 minutes, we therefore decided to follow a single time point quench at 4 min. Both aliquots were quenched after 4 minutes of initiation using 6 M HCl (lactonization) or 4 M acetate buffer pH 3.7 (acylation) with final concentrations of 0.4 M HCl or 0.4 M acetate buffer, respectively. Peak areas of MTA and holo-ACP at each acyl-ACP concentration were determined from HPLC chromatograms. The initial rates were determined by dividing analyte concentration over time (4 minutes). The difference between background and reaction in peak area per minute was converted to an initial reaction rate in μM/min using standard calibration curves. The MTA standard curve had a linear fit equation of y = 0.198x; the holo-ACP standard curve had a linear fit equation of y = 0.4058x, where y = peak area of analyte, and x = known concentration of analyte. The initial rate was fitted to the Michaelis-Menten equation (Equation 1) or substrate inhibition equation (Equation 2) using GraphPad Prism 7.00. All experiments were repeated in duplicate to check for reproducibility and to estimate errors.

$$v_0 = \frac{k_{cat}[E_t][S]}{K_m + [S]} \qquad \text{(Equation 1)}$$

$$v_0 = \frac{k_{cat}[E_t][S]}{K_m + [S]\left(1 + \frac{[S]}{K_i}\right)} \qquad \text{(Equation 2)}$$

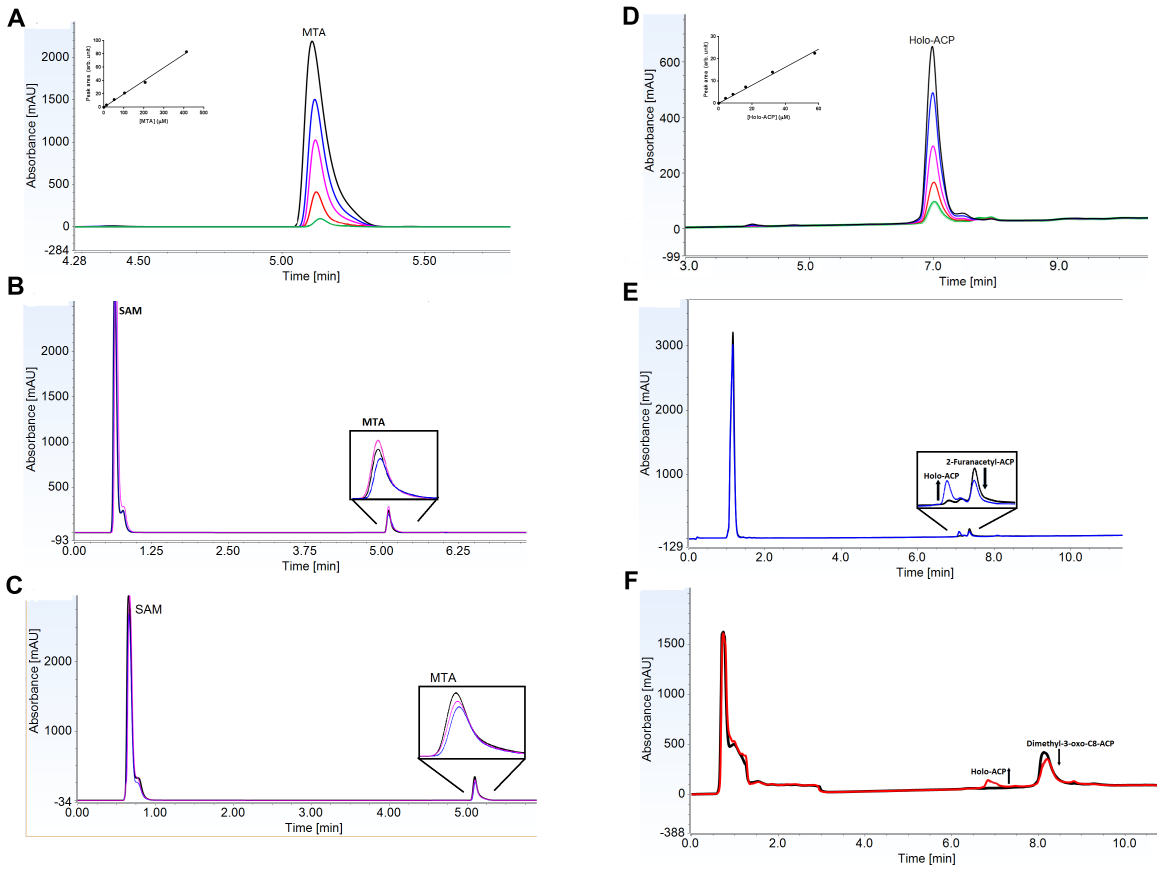

Fig. S75 HPLC Assay for EsaI and YspI. A) MTA standard curve. The concentrations of MTA used in the standard curve are 13 μM (green), 52 μM (red), 103 μM (purple), 206 μM (blue) and 412 μM (black). B) Lactonization Assay for EsaI. The chromatogram shows representative data for lactonization induced MTA release in EsaI catalyzed AHL synthesis. The blue, black and pink traces correspond to reactions containing 0 μM, 7 μM, and 15 μM 2-furanacetyl-ACP (**10-ACP**). The concentration of SAM and EsaI used in the assay, respectively, are 500 μM and 1 μM. Presence of MTA at 5 minutes in the 0 μM 2-furanacetyl-ACP (**10-ACP**) trace is attributed to MTA impurity in the commercial SAM sample. The background MTA peak from SAM was always subtracted from the MTA peak formed due to EsaI induced lactonization to determine initial rate. All reactions were stopped at 4 min using 6 M HCl quench. Standard curve data shown in Panel 'a' was used to convert MTA peak areas to concentration units for initial rate calculations. C) Lactonization Assay for YspI. The concentration of YspI and SAM used in the assay, respectively, are 1 μM and 500 μM. The blue, pink and black traces correspond to reactions containing 0 μM, 10 μM, and 20 μM 2,2-dimethyl-3-oxooctanoyl-ACP (**5-ACP**) acyl-substrate in the assay. The increase in MTA peak area at 5 minutes due to incubation of SAM with increasing concentrations of the acyl-substrate reflects the rate of YspI catalyzed AHL synthesis. D) Holo-ACP standard curve. The concentrations of holo-ACP used in the standard curve are 4 μM (green), 9 μM (red), 16 μM (purple), 32 μM (blue) and 58 μM

(black). E) Acylation Assay for EsaI. Holo-ACP and 2-furanacetyl-ACP (**10-ACP**) elutes at 6.8 minutes and 7.4 minutes, respectively. Black and blue traces, respectively, represent reaction products from incubation of 80 μM 2-furanacetyl-ACP (**10-ACP**) and 500 μM SAM with nanopure water and 1 μM EsaI. For the background (black trace), nanopure water is used in lieu of enzyme. Both reactions are quenched at 4 min using 4M acetate buffer at pH 3.6. F) Acylation Assay for YspI. Representative acylation chromatograms for 1 μM YspI catalyzed AHL synthesis. The black and red traces represent background and enzymatic reaction for the reaction of 70 μM 2,2-dimethyl-3-oxooctanoyl-ACP (**5-ACP**) and 500 μM SAM, as mentioned in 'e'. The substrate elutes at 8 minutes. Reaction mixtures were quenched at 4 min with 4M acetate buffer at pH 3.6.

Substrate-Velocity Curves

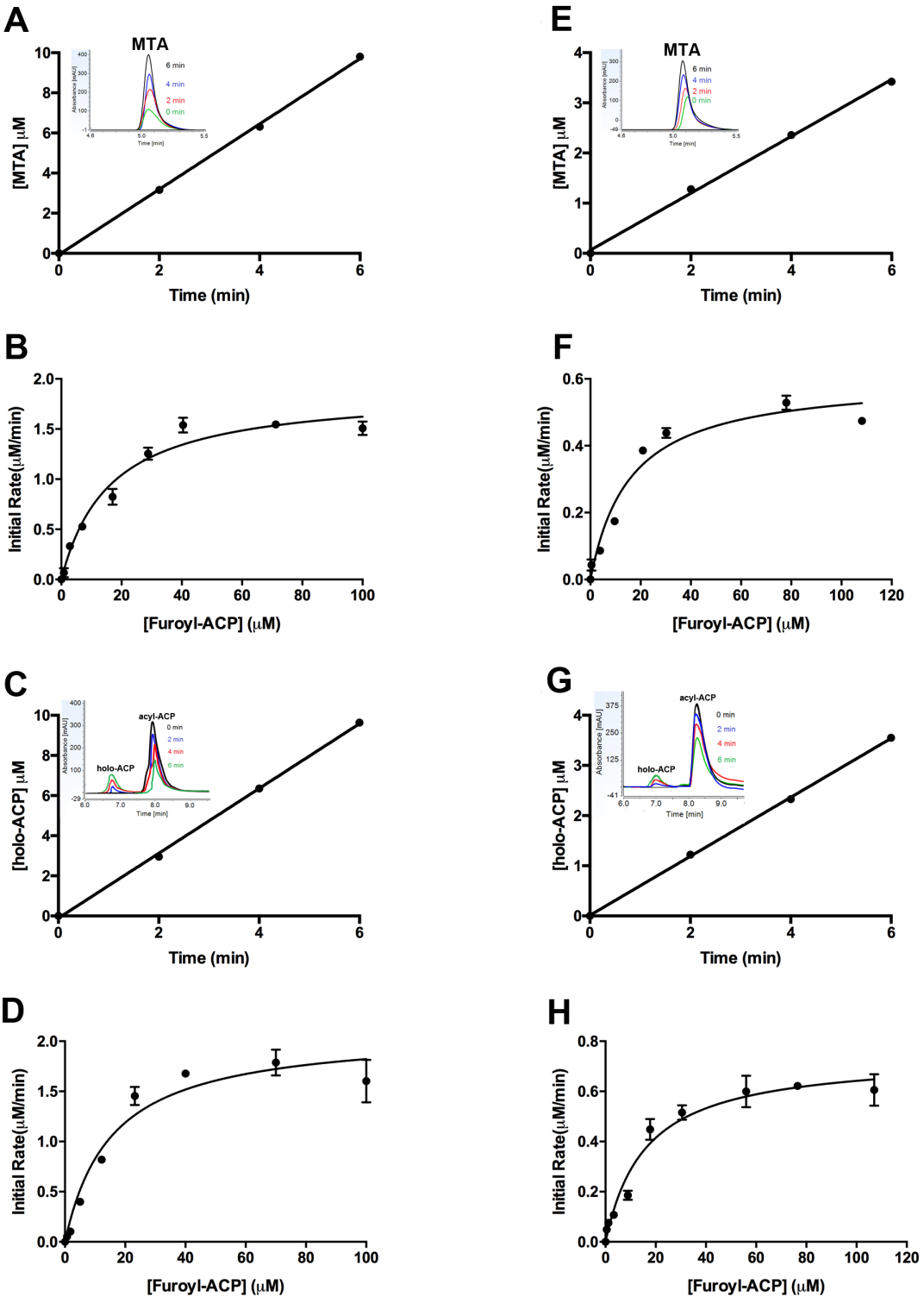

Fig. S76 Substrate-velocity curves for EsaI and YspI. A) EsaI Lactonization Progress Curve. The concentrations of 2-furoyl-ACP (**14-ACP**), SAM and EsaI, respectively, were 112 μM, 500 μM and 1.3 μM. The progress curve was linear at least until 6 minutes. The peak at 0 min is due to MTA contamination in commercial SAM sample. This peak was subtracted from the peak at 2, 4 and 6 min to determine the amount of MTA released from enzyme-catalyzed SAM lactonization. B) EsaI Lactonization Rate Curve. Initial rate was plotted as a function of substrate concentration for 1.3 μM EsaI catalyzed MTA release in 500 μM SAM chloride (fixed) and varying 2-furoyl-ACP (**14-ACP**). The standard curve shown in Figure S75, panel 'A', was used to convert MTA peak area to concentration units. Initial rate data as a function of substrate concentration was fitted to Michaelis-Menten equation (Equation 1; Page S63) using Graphpad Prism 7.0 to determine kinetic constants. C) EsaI Acylation Progress Curve. The concentrations of 2-furoyl-ACP (**14-ACP**), SAM and EsaI were identical to substrate and enzyme concentrations used for the progress curve shown in Panel 'A'. D) EsaI Acylation Rate Curve. Holo-ACP peak areas were converted to concentration units using standard curve shown in Panel 'D' (Figure S75). Initial rate was plotted as a function of substrate concentration for 1.3 μM EsaI catalyzed holo-ACP release in 500 μM SAM chloride (fixed) and varying 2-furoyl-ACP (**14-ACP**). Initial rate data as a function of substrate concentration was fitted to Michaelis-Menten equation (Equation 1; Page S63) using Graphpad Prism 7.0 to determine kinetic constants. E) YspI Lactonization Progress Curve. The concentrations of 2-furoyl-ACP (**14-ACP**), SAM and YspI, respectively, were 112 μM, 500 μM and 1.3 μM. The peak at 0 min is due to MTA contamination in the commercial SAM sample. This peak was subtracted from the peak at 2, 4 and 6 min to determine the amount of MTA released from enzyme-catalyzed SAM lactonization. F) YspI Lactonization Rate Curve. Initial rate was plotted as a function of substrate concentration for 1.3 μM YspI induced lactonization in 500 μM SAM chloride (fixed) and varying 2-furoyl-ACP (**14-ACP**). Initial rate data as a function of substrate concentration was fitted to Michaelis-Menten equation (Equation 1; Page S63) using Graphpad Prism 7.0 to determine kinetic constants. G) YspI Acylation Progress Curve. The substrate and enzyme concentrations in the progress curve were identical to conditions stated in panel 'E'. H) YspI Acylation Rate Curve. Initial rate was plotted as a function of substrate concentration for 1.3 μM YspI induced acylation in 500 μM SAM chloride (fixed) and varying 2-furoyl-ACP (**14-ACP**)**.** Initial rate data as a function of substrate concentration was fitted to Michaelis-Menten equation (Equation 1; Page S63) using Graphpad Prism 7.0 to determine kinetic constants.

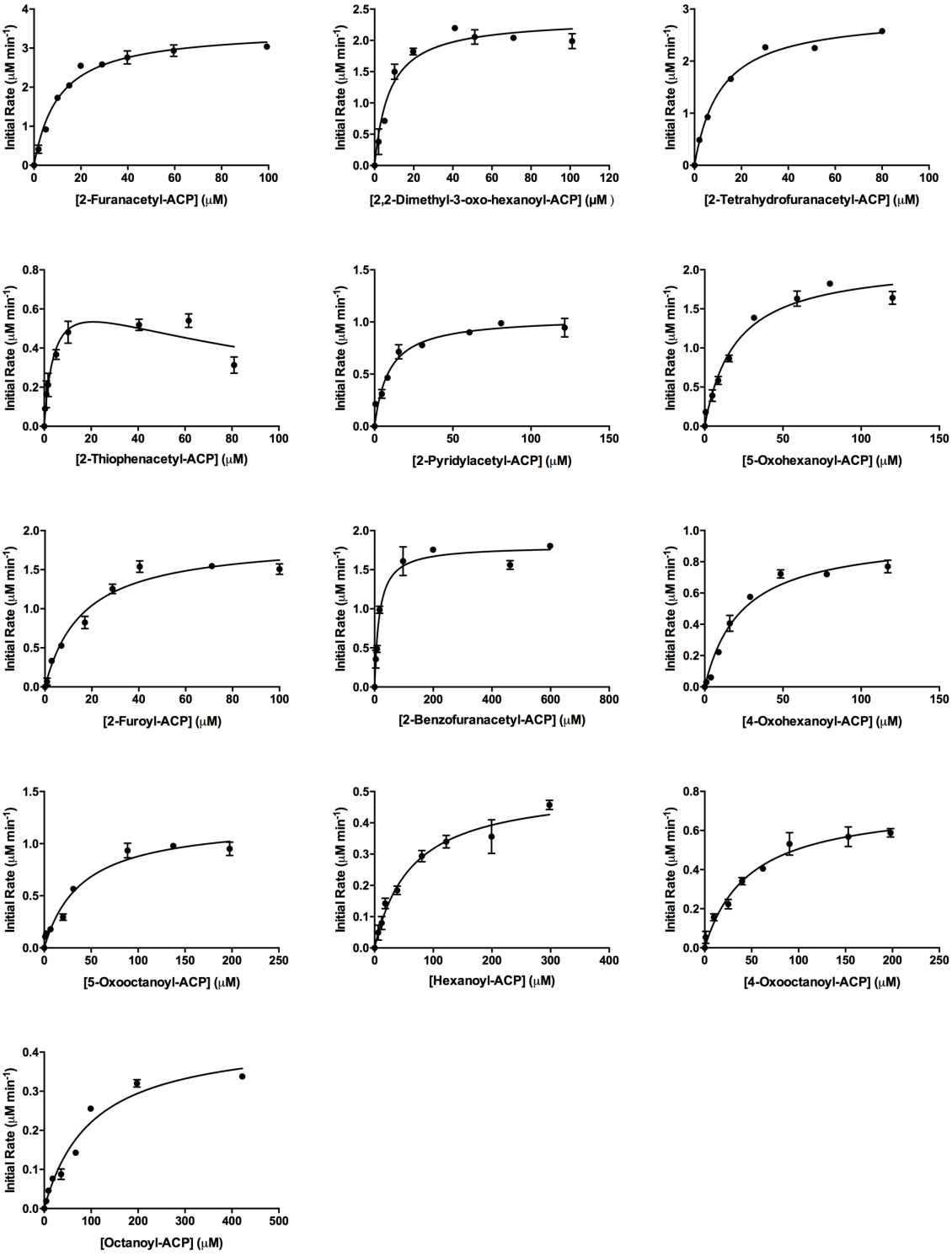

Fig. S77 Substrate-velocity curves for 3-oxoacyl-ACP substrate analogs with EsaI by lactonization assay. In general, the initial rate data for all substrates except the 2-thiopheneacetyl-ACP was fitted to Michaelis-Menten Equation (Equation 1; Page S63) using Graphpad Prism 7.0 to determine kinetic constants. The substrate-velocity data for

2-thiopheneacetyl-ACP was fitted to substrate inhibition equation (Equation 2; Page S63). The substrate inhibition constant for 2-thiopheneacetyl-ACP is 100 ± 50 μM. Substrate inhibition observed for 2-thiopheneacetyl-ACP could arise due to a combination of one or more of the following possibilities: a) two acyl-ACP substrate molecules binding to the enzyme to form an ES_2 complex, b) the free enzyme form E exists in a slow equilibrium with E′ where the affinities and reactivities of the acyl-substrate towards the two enzyme forms are noticeably different, and c) random addition of acyl-ACP and SAM to the enzyme where one addition pathway is kinetically preferred over the other (also called preferred random order addition mechanism).[4a],[5] A comprehensive investigation using structural (NMR) and enzymological tools to distinguish between these mechanistic possibilities is currently underway.

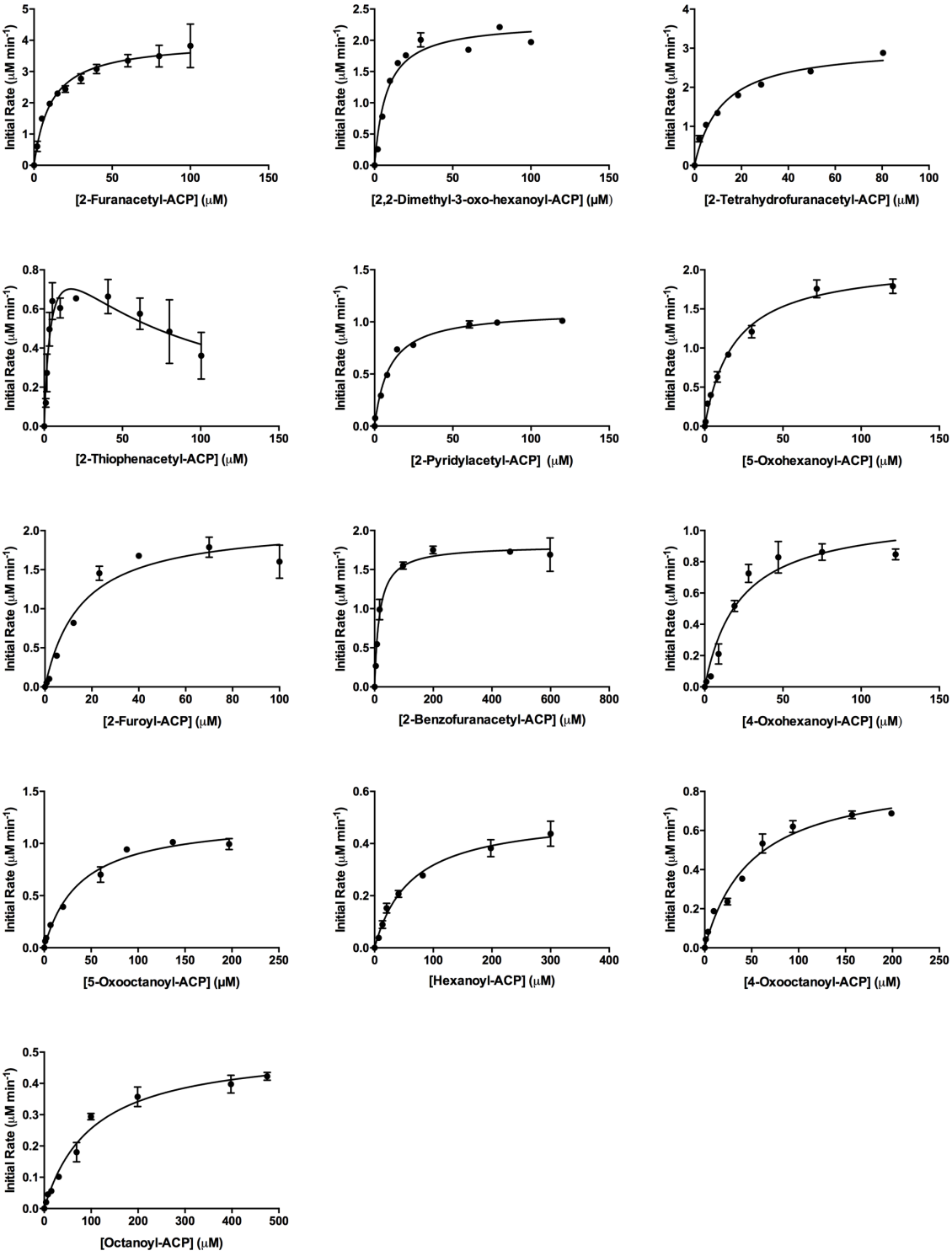

Fig. S78 Substrate-velocity curves for 3-oxoacyl-ACP substrate analogs with EsaI by acylation assay. In general, the initial rate data for all substrates except the 2-thiopheneacetyl-ACP was fitted to Michaelis-Menten Equation (Equation 1; Page S63) using Graphpad Prism 7.0 to determine kinetic constants. The substrate-velocity data for

2-thiopheneacetyl-ACP was fitted to substrate inhibition equation (Equation 2; Page S63). The substrate inhibition constant for 2-thiopheneacetyl-ACP is 68 ± 25 μM.

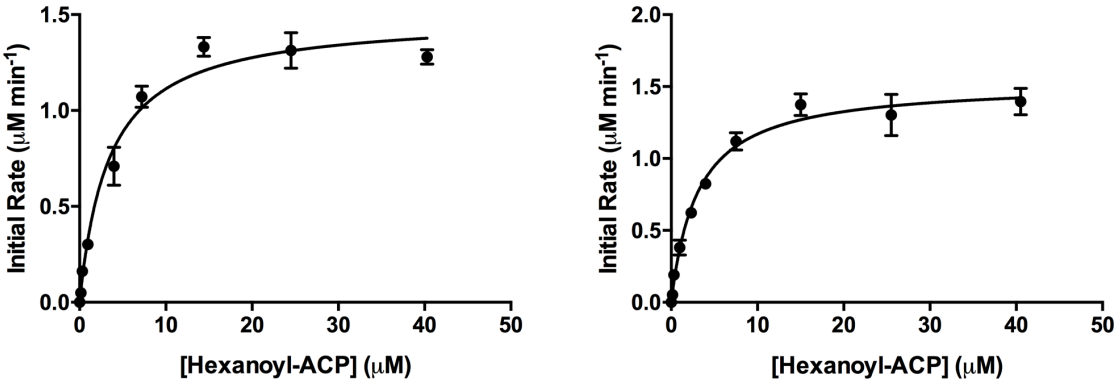

Fig. S79 Substrate-velocity curve for EsaI T140A with hexanoyl-ACP following (left) lactonization and (right) acylation. (Left) Lactonization Assay: The value of K_m was 3.43 ± 0.52 μM and k_{cat} was 1.52 ± 0.06 min^{-1}. k_{cat}/ K_m for EsaI T140A and EsaI WT, respectively, with hexanoyl-ACP are 0.45 ± 0.07 μM^{-1} min^{-1} and 0.0082 ± 0.0014 μM^{-1} min^{-1}. (Right) Acylation Assay: The value of K_m was 3.08 ± 0.33 μM and k_{cat} was 1.56 ± 0.04 min^{-1}. k_{cat}/ K_m for EsaI T140A and EsaI WT, respectively, with hexanoyl-ACP are 0.51 ± 0.06 μM^{-1} min^{-1} and 0.0083 ± 0.0011 μM^{-1} min^{-1}. The k_{cat} and K_m values for hexanoyl-ACP with wild-type EsaI are reported in Table S1. Initial rate data was fitted to Michaelis-Menten Equation (Equation 1; Page S63) using Graphpad Prism 7.0 to determine kinetic constants.

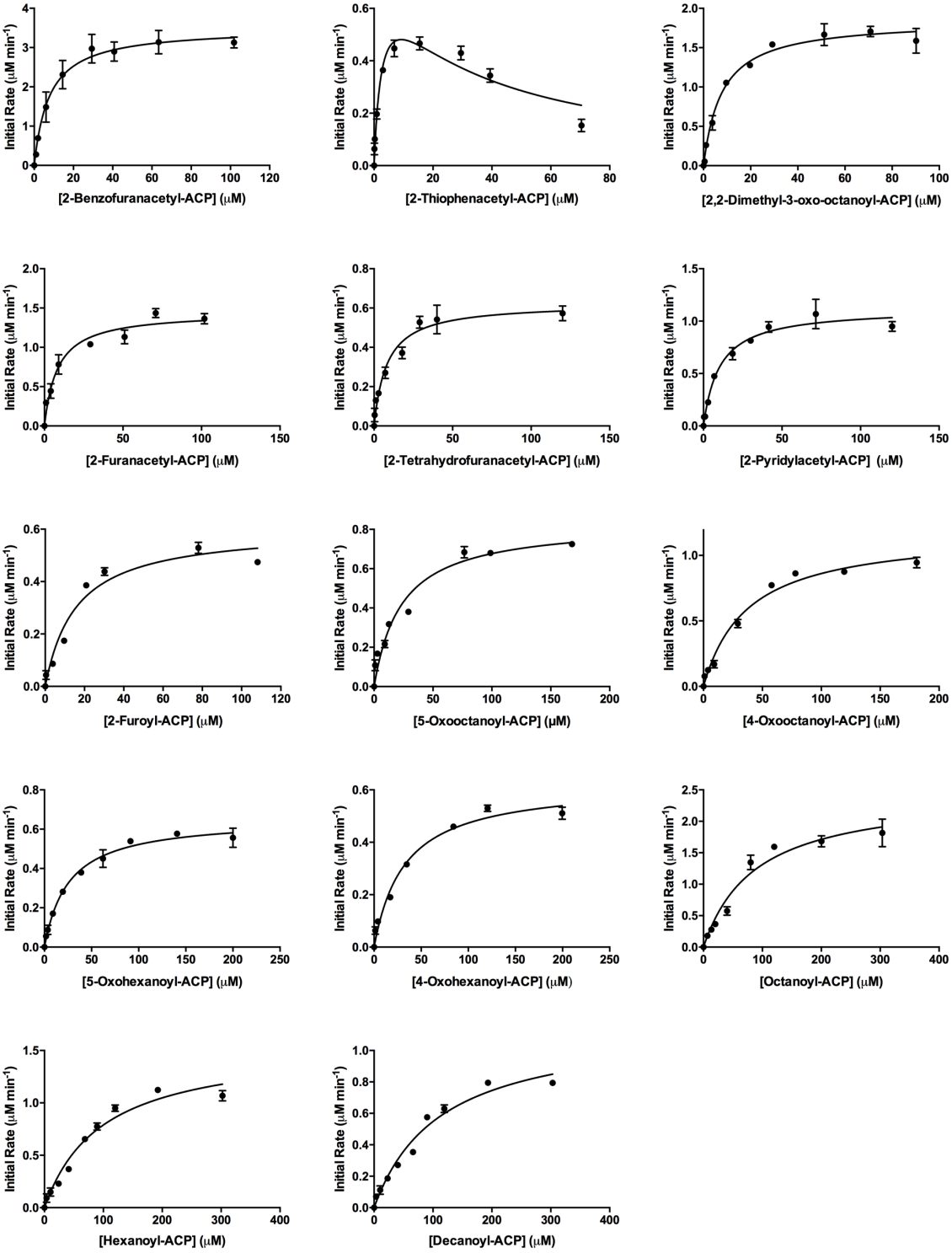

Fig. S80 Substrate-velocity curves for 3-oxoacyl-ACP substrate analogs with YspI by lactonization assay. In general, the initial rate data for all substrates except the 2-thiopheneacetyl-ACP was fitted to Michaelis-Menten Equation (Equation 1; Page S63) using Graphpad Prism 7.0 to determine kinetic constants. The substrate-velocity data for

2-thiopheneacetyl-ACP was fitted to substrate inhibition equation (Equation 2; Page S63). The substrate inhibition constant for 2-thiopheneacetyl-ACP is 30 ± 9 μM.

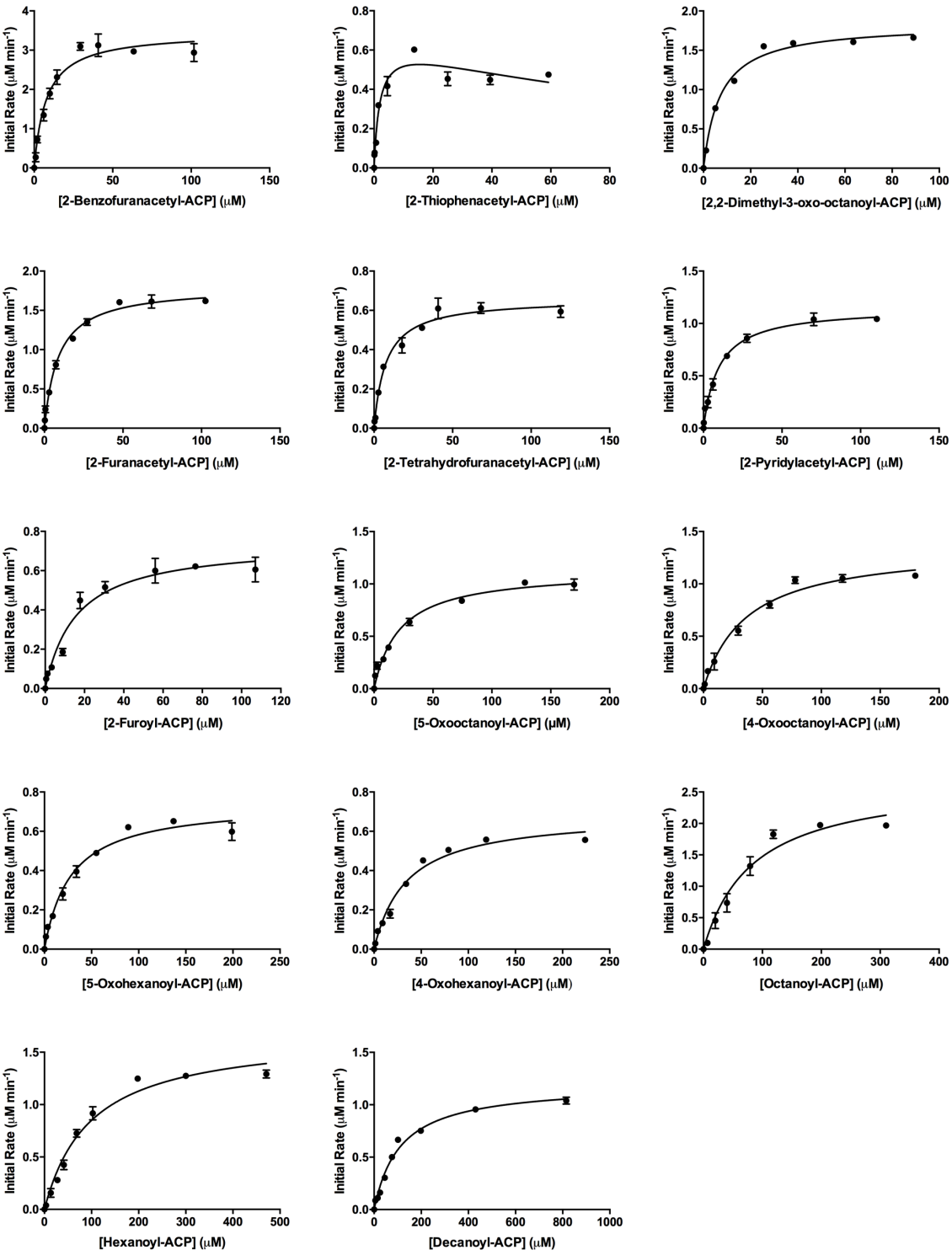

Fig. S81 Substrate-velocity curves for 3-oxoacyl-ACP substrate analogs with YspI by acylation assay. In general, for all of the substrates except the 2-thiopheneacetyl-ACP, initial rate data was fitted to Michaelis-Menten Equation (Equation 1; Page S63) using Graphpad Prism 7.0 to determine kinetic constants. The substrate-velocity data for

2-thiopheneacetyl-ACP was fitted to substrate inhibition equation (Equation 2; Page S63).

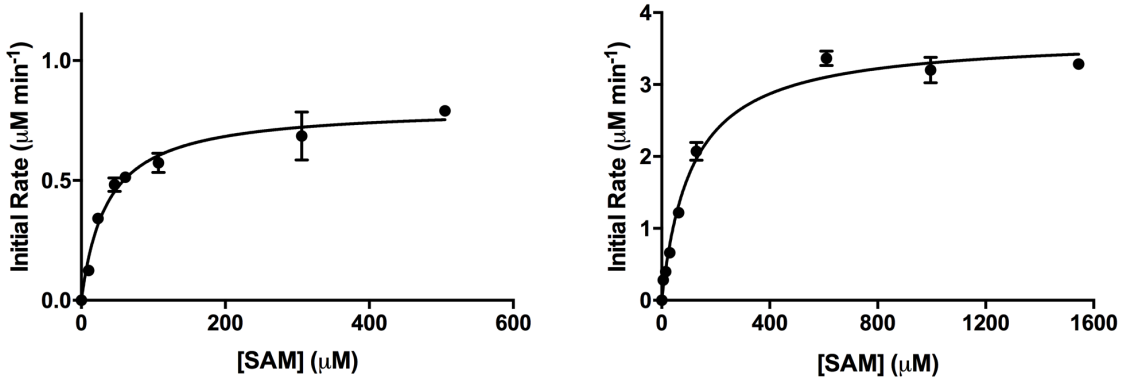

Fig. S82 Determination of K_m^{SAM} in EsaI-catalyzed reaction. (Left) 2-Thiopheneacetyl-ACP (**12-ACP**) and EsaI concentrations were fixed at 40 μM and 1.01 μM, respectively. The value of K_m^{SAM} was 36.09 ± 4.69 μM, k_{cat} was 0.796 ± 0.029 min^{-1}, and k_{cat}/K_m was 0.0221 ± 0.0029 $\mu M^{-1}min^{-1}$. (Right) 2-Furanacetyl-ACP (**14-ACP**) and EsaI concentrations were fixed at 103 μM and 1.01 μM, respectively. The value of K_m^{SAM} was 111.3 ± 10.7 μM, k_{cat} was 3.64 ± 0.09 min^{-1}, k_{cat}/K_m was 0.0327 ± 0.0032 $\mu M^{-1}min^{-1}$. Initial rate data was fitted to Michaelis-Menten Equation (Equation 1; Page S63) using Graphpad Prism 7.0 to determine kinetic constants.

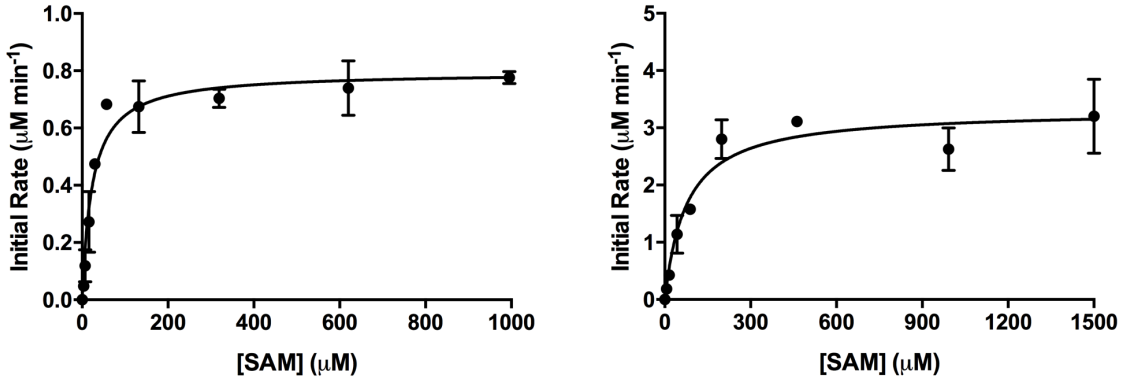

Fig. S83 Determination of K_m^{SAM} in YspI-catalyzed reaction. (Left) 2-Thiopheneacetyl-ACP (**12-ACP**) and YspI concentrations were fixed at 40 μM and 1.04 μM, respectively. The value of K_m^{SAM} was 23.52 ± 4.03 μM, k_{cat} was 0.764 ± 0.029 min^{-1}, k_{cat}/K_m was 0.0325 ± 0.0057 $\mu M^{-1}min^{-1}$. (Right) 2-Benzofuranacetyl-ACP (**15-ACP**) and YspI concentrations were fixed at 80 μM and 1.03 μM, respectively. The value of K_m^{SAM} was 75.98 ± 17.49 μM, k_{cat} was 3.21 ± 0.18 min^{-1}, k_{cat}/K_m was 0.0423 ± 0.0100 $\mu M^{-1}min^{-1}$. Initial rate data was fitted to Michaelis-Menten Equation (Equation 1; Page S63) using Graphpad Prism 7.0 to determine kinetic constants.

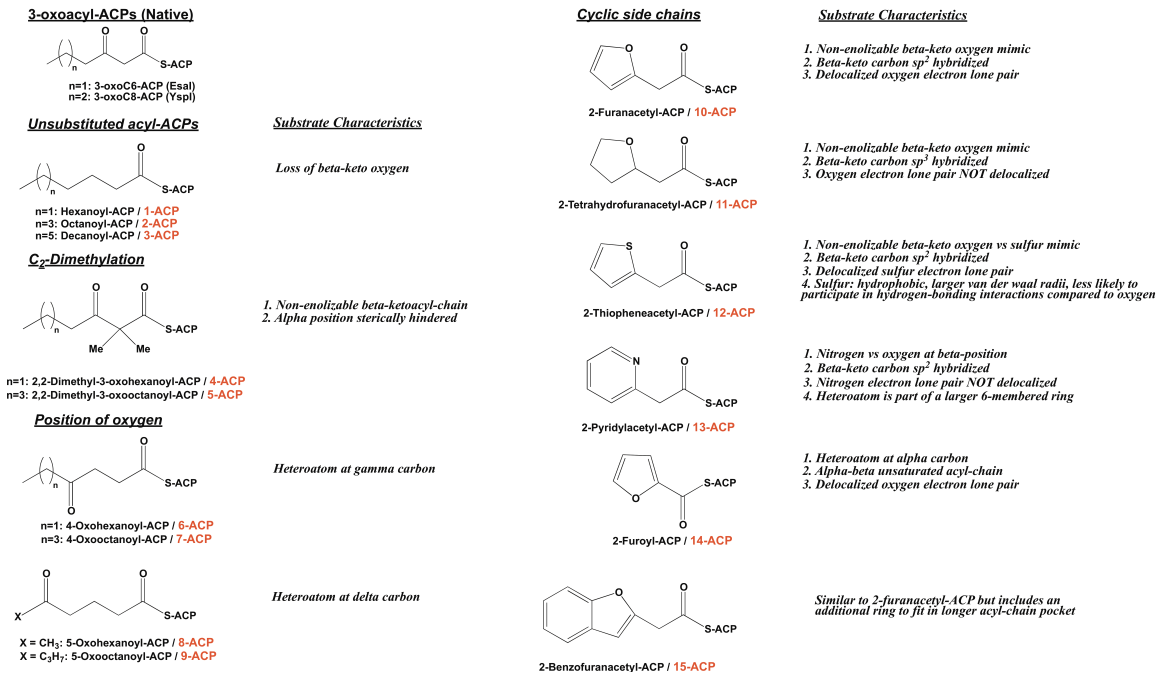

Fig. S84. Structural attributes of molecular probes used in this study. ACP refers to *E.coli* acyl carrier protein. Substrate characteristics describe the chemical functionalities probed in each acyl-chain.

Table S1. Substrate Activity with EsaI

Substrate	Lactonization				Acylation			
	K_m (μM)	k_{cat} (min^{-1})	k_{cat}/K_m x 10^{-2} (μM^{-1} min^{-1})	k_{cat}/K_m^{rel}	K_m (μM)	k_{cat} (min^{-1})	k_{cat}/K_m x 10^{-2} (μM^{-1} min^{-1})	k_{cat}/K_m^{rel}
2-Furanacetyl-ACP (10-ACP)	10.6 ± 1.03	3.49 ± 0.10	33.0 ± 3.40	100.00	10.8 ± 1.42	3.99 ± 0.14	36.8 ± 5.00	100.00
2,2-Dimethyl-3-oxoC6-ACP (4-ACP)	7.63 ± 1.34	2.35 ± 0.10	30.8 ± 5.50	93.33	7.65 ± 1.12	2.30 ± 0.08	30.1 ± 4.50	81.79
2-Tetrahydrofuranylacetyl-ACP (11-ACP)	11.1 ± 1.00	2.90 ± 0.07	26.1 ± 2.40	79.09	11.6 ± 1.51	3.07 ± 0.12	26.6 ± 3.60	72.28
2-Thiophenacetyl-ACP (12-ACP)	4.34 ± 1.82	0.76 ± 0.15	17.4 ± 8.00	52.73	4.33 ± 1.52	1.06 ± 0.17	24.4 ± 9.50	66.30
2-Pyridylacetyl-ACP (13-ACP)	9.15 ± 1.54	1.02 ± 0.04	11.2 ± 1.90	33.94	9.42 ± 0.67	1.08 ± 0.02	11.5 ± 0.80	31.25
5-Oxohexanoyl-ACP (8-ACP)	19.6 ± 2.74	2.11 ± 0.09	10.7 ± 1.60	32.42	18.7 ± 1.89	2.10 ± 0.07	11.2 ± 1.20	30.43
2-Furoyl-ACP (14-ACP)	16.1 ± 2.64	1.43 ± 0.03	8.80 ± 1.50	26.66	15.4 ± 3.24	1.51 ± 0.10	9.80 ± 2.20	26.63
2-Benzofuranacetyl-ACP (15-ACP)	16.2 ± 2.24	0.84 ± 0.02	5.16 ± 0.73	15.64	16.6 ± 1.88	0.84 ± 0.02	5.05 ± 0.58	13.73
4-Oxohexanoyl-ACP (6-ACP)	23.6 ± 3.55	0.97 ± 0.05	4.10 ± 0.70	12.42	22.2 ± 5.02	1.11 ± 0.09	4.90 ± 1.20	13.32
5-Oxooctanoyl-ACP (9-ACP)	39.8 ± 7.56	0.61 ± 0.04	1.50 ± 0.30	4.54	38.3 ± 5.52	0.62 ± 0.03	1.60 ± 0.20	4.35
Hexanoyl-ACP (1-ACP)	62.7 ± 9.86	0.52 ± 0.03	0.82 ± 0.14	2.48	61.9 ± 7.69	0.51± 0.02	0.83 ± 0.11	2.26
4-Oxooctanoyl-ACP (7-ACP)	47.2 ± 7.06	0.37 ± 0.02	0.78 ± 0.12	2.36	50.2 ± 6.88	0.44 ± 0.02	0.88 ± 0.13	2.39
Octanoyl-ACP (2-ACP)	102 ± 17.5	0.22 ± 0.02	0.21 ± 0.04	0.64	102 ± 13.1	0.25 ± 0.01	0.25 ± 0.03	0.68

Table S2. Substrate Activity with YspI

Substrate	Lactonization				Acylation			
	K_m (μM)	k_{cat} (min^{-1})	k_{cat}/K_m x 10^{-2} μM^{-1} min^{-1}	k_{cat}/K_m^{rel}	K_m (μM)	k_{cat} (min^{-1})	k_{cat}/K_m x 10^{-2} μM^{-1} min^{-1}	k_{cat}/K_m^{rel}
2-Benzofuranacetyl-ACP (15-ACP)	7.71 ± 1.19	3.28 ± 0.12	42.5 ± 6.78	100.0	7.68 ± 1.11	3.24 ± 0.12	42.2 ± 6.32	100.00
2,2-Dimethyl-3-oxoC8-ACP (5-ACP)	7.78 ± 0.89	1.85 ± 0.05	23.8 ± 2.81	56.0	7.09 ± 0.97	1.79 ± 0.04	25.3 ± 2.32	59.91
2-Furanacetyl-ACP (10-ACP)	8.35 ± 1.64	0.70 ± 0.03	8.39 ± 1.69	19.76	8.86 ± 0.85	0.86 ± 0.02	9.76 ± 0.96	23.12
2-Pyridylacetyl-ACP (13-ACP)	10.2 ± 1.50	0.74 ± 0.03	7.27 ± 1.09	17.12	9.64 ± 0.95	0.77 ± 0.02	7.96 ± 0.81	18.88
2-Furoyl-ACP (14-ACP)	15.8 ± 3.12	0.57 ± 0.03	3.64 ± 0.75	8.56	15.9 ± 2.78	0.71 ± 0.04	4.44 ± 0.81	10.54
2-Tetrahydrofuranylacetyl-ACP (11-ACP)	8.19 ± 1.46	0.61 ± 0.03	7.44 ± 1.37	17.52	7.49 ± 0.93	0.64 ± 0.02	8.58 ± 1.10	20.34
4-Oxooctanoyl-ACP (7-ACP)	37.4 ± 5.19	1.12 ± 0.05	3.00 ± 0.44	7.06	36.6 ± 5.25	1.29 ± 0.06	3.53 ± 0.53	8.37
5-Oxooctanoyl-ACP (9-ACP)	23.4 ± 3.98	0.79 ± 0.04	3.36 ± 0.59	7.92	21.8 ± 2.81	1.07 ± 0.04	4.89 ± 0.66	11.59
Octanoyl-ACP (2-ACP)	87.9 ± 16.8	1.22 ± 0.09	1.38 ± 0.28	3.26	83.9 ± 16.1	1.34 ± 0.10	1.59 ± 0.33	5.95
4-Oxohexanoyl-ACP (6-ACP)	32.3 ± 4.67	0.59 ± 0.03	1.83 ± 0.28	4.32	34.2 ± 3.91	0.65 ± 0.02	1.90 ± 0.23	4.50
5-Oxohexanoyl-ACP (8-ACP)	25.7 ± 2.44	0.62 ± 0.02	2.40 ± 0.24	5.67	28.1 ± 3.49	0.70 ± 0.03	2.51 ± 0.33	5.95
Hexanoyl-ACP (1-ACP)	97.7 ± 15.9	0.78 ± 0.05	0.80 ± 0.14	1.88	97.7 ± 12.1	0.84 ± 0.04	0.86 ± 0.11	2.04
Decanoyl-ACP (3-ACP)	113 ± 16.9	0.56 ± 0.04	0.50 ± 0.08	1.18	111 ± 10.1	0.58 ± 0.02	0.52 ± 0.05	1.24
2-Thiophenacetyl-ACP (12-ACP)	2.81 ± 0.89	0.77 ± 0.12	27.5 ± 9.66	64.8	1.94 ± 0.51	0.66 ± 0.07	33.9 ± 9.46	80.31

Table S3. Effect of acyl-substrate on the kinetic constants for SAM.

Fixed S [a]	Enzyme[b]	K_m (μM)	k_{cat} (min^{-1})	k_{cat}/K_m μM^{-1} min^{-1}
2-Furanacetyl-ACP (103 μM)	EsaI	111.3 ± 10.7	3.64 ± 0.09	0.033 ± 0.003
2-Thiopheneacetyl-ACP (40 μM)	EsaI	36.10 ± 4.69	0.80 ± 0.03	0.022 ± 0.003
2-Benzofuranacetyl-ACP (80 μM)	YspI	75.98 ± 17.49	3.21 ± 0.18	0.042 ± 0.010
2-Thiopheneacetyl-ACP (40 μM)	YspI	23.52 ± 4.03	0.76 ± 0.03	0.033 ± 0.006

[a] The concentration of acyl-ACP substrates were maintained at $10K_m$ values (approx) to ensure the fixed substrate was approaching saturation under the conditions of this experiment.
[b] The concentration of EsaI and YspI was maintained at 1 μM.

References

[1] R. C. Brinkerhoff, H. F. Tarazona, P. M. de Oliveira, D. C. Flores, C. R. M. D'Oca, D. Russowsky, M.G.M. D'Oca, *RSC Adv.* 2014, **4**, 49556.

[2] Y. Nishimoto, A. Okita, M. Yasuda, A. Baba, *Angew. Chem. Int. Ed.* 2011, **50**, 8623.

[3] M. D'Ambrosio, A. Guerriero, *J. Chem. Research* 2002, **12**, 631.

[4] a) A. N. Montebello, R. M. Brecht, R. D. Turner, M. Ghali, X. Pu, R. Nagarajan, *Biochemistry* 2014, **53**, 6231; b) Q. H. Christensen, T. L. Grove, S. J. Booker, E. P. Greenberg, *PNAS* 2013, **110**, 13815.

[5] a) P. M. Kaiser, *Journal of Molecular Catalysis* 1980, **8**, 431; b) C. M. Porter, B. G. Miller, *Bioorganic Chemistry* 2012, **43**, 44.